Comparison of DigSILENT, Matlab PST and PSAT for Steady State and Stability Studies on HVAC-HVDC Systems

PREPARED BY:
ALBINO VIRGÍLIO UBISSE

This dissertation is submitted to the University of Cape Town in full fulfilment of the academic requirements for the Master of Science Degree in Electrical Engineering

SUPERVISOR:
ASSOCIATE PROF. K.A FOLLY

UNIVERSITY OF CAPE TOWN
IDYUNIVESITHI YASEKAPA • UNIVERSITEIT VAN KAAPSTAD

DEPARTMENT OF ELECTRICAL ENGINEERING
UNIVERSITY OF CAPE TOWN
CAPE TOWN

Date: May 2012

Dedication

I dedicate this research work to my late father, Reginaldo Armando Ubisse, "MAJOR", for his guidance, love and perseverance. You shall forever live within us and your legacy shall flourish.

"OURO MAJOR"

Declaration

I hereby declare that this is my own work. All alternative sources used have been identified and referenced. This dissertation has not been submitted before for any degree at this or any other institution for any degree or examination.

Signature:
Mr. Albino Virgilio Ubisse
Signed at the University of Cape Town
28 May 2012.

Acknowledgements

First and foremost, my gratitude goes to the Almighty for giving me the strength and the courage to finish my dissertation, and for keeping me safe and clear of any difficulties that could have hindered me from finishing my research.

Secondly, I would like to express my special appreciation to my supervisor, Prof K. Folly. You have been an inspiration, a person whom I have always relied on for help when things were not going well. Thank you for having the trust in me to allow me to do my dissertation under your supervision. A Special thanks to my co-supervisor, Mrs K. Awodele as well for her guidance when it was needed.

Thirdly I would like to thank my mom Arminda Novela, my brothers Mandito and Neto, my grandmother "Vo Regina", as well as my family for their constant support.

I cannot forget my colleagues from the Power Engineering Research Group, as well as my friends both at UCT and at home; you have been supportive and helpful in whatever difficulties that I faced. Last, but not least, I want to thank Philip and Chris from the power and machines laboratory for your help during my stay at UCT.

"The more time you spend thinking about the problem, the less time you spend thinking about the solution"

Synopsis

It is said that the electric power system is the most complex system ever built by mankind. Over the past few decades, many software packages focusing on the study of this complex system have been developed. These software packages range from academic/ research based to industrial/commercial based software. Before any component/ device is installed in the power system, it undergoes rigorous research, simulation and testing. Once the component/ devices are connected to the power system, it is very difficult, if not impossible, to do any experiment on the actual system without compromising the system's security. The software simulation tool can help to predict the behaviour of the whole system and individual components under steady-state and transient condition quickly.

High Voltage Alternating Current (HVAC) systems have been used to transmit power for many years; however for long distance they have become impractical, as they incur higher losses when compared to High Voltage Direct Current (HVDC) systems. The terminal reactive power on the transmission lines increases as a function of the power transmitted along the lines, where it can cause overvoltages in the system if the line supplies too much reactive power or undervoltages if the line consumes too much reactive power. HVDC has become the preferred choice for bulk power transmission because of its efficiency, high controllability and the ability to interconnect two systems operating at different frequencies. Moreover, it is seen in literature that HVDC transmission systems increase the stability of power systems, as the power angle reduces when an HVDC system is used in parallel to the HVAC system, thereby reducing the voltage difference between the sending and receiving ends of a transmission system, hence helping the system recover from transient instability after a fault.

Several academic and industrial simulation tools are used to study HVAC systems, but only a few of these are applied to HVDC systems. These simulation tools differ in their component modelling and hence different results might be obtained for the same power system model. In this dissertation, three simulation tools, namely DigSILENT (industrial-

grade tool) and Matlab PST and PSAT (academic-based tools) are investigated. Their features and capabilities are compared based on component modelling and tool flexibility in terms of data input, modelling, ease of use and graphical representation.

In this dissertation the HVDC system used was the modified form of the Cigre Benchmark. The system is modified in terms of the power and current ratings. Two power system models are investigated, a Single Machine Infinite Bus system and a Two-Area Multi Machine system. Under normal operating conditions, the rectifier station is set to use Current Control (CC) and the inverter station is set to use Constant Extinction Angle (CEA).

Two transmission schemes have been investigated, HVAC and HVAC-HVDC for the SMIB and TAMM systems.

The load flow of the SMIB HVAC system indicates that the system transmits close to 1000 MW of power from the external grid to the load connected close to the generator. The small signal stability study was performed under three control scenarios: Generator in manual control, generator with Automatic Voltage Regulator (AVR) only and generator with AVR and Power System Stabilizer (PSS) installed on the generator. Both the HVAC and HVAC-HVDC systems were stable for all three scenarios. The small signal stability of the system improved when only AVR was used and improved further when the PSS was used with the AVR. The transient stability on the SMIB system was performed for the scenario where AVR and PSS were used. The disturbance applied was a three-phase fault lasting for 50 ms. This fault was cleared by removing the faulted line. For all the software packages investigated both the schemes with HVAC and HVAC-HVDC were stable. Overall the results in DigSILENT and PST were very similar, whereas PSAT gave different results for the HVAC system. For the HVAC-HVDC system, PST gave higher values for the voltage and active power responses owing to the interaction of the HVAC system with the HVDC system in this specific software package for the Singe Machine Infinite Bus system.

When the studies were performed using the TAMM systems, the load flow for the HVAC system showed that approximately 380 MW were transferred from area 1 with two generators to area 2 with two generators, one of which is the swing bus, and that this power was split equally between the two HVAC transmission lines. The small signal stability analysis for the HVAC scheme was performed under the three control scenarios previously described (generators with manual control, generators with AVR only and generators with AVR and PSS). Under manual control, the inter-area and local modes were stable across all packages. When only the AVR was used in all generators, the damping ratio for the inter-area mode became unstable in DigSILENT and PST and remained stable in PSAT with a slight reduction. On the other hand, the local modes were stable across all packages. When the PSS was added to the AVR, the inter-area modes became stable in DigSILENT and PST. In PSAT the inter-area mode remained stable. The performance of the HVAC-HVDC system was similar to that of the HVAC system. The transient stability of the system was performed by applying a three-phase fault that lasted for 50 ms and was cleared by removing the faulted line. The HVAC system showed similar behaviour across all packages; however in PSAT the results obtained had a smaller range than in DigSILENT and PST than observed in the SMIB cases. The system stabilized more quickly in PSAT than in DigSILENT and PST; however it had more oscillations in PSAT.

It has been observed that different results are obtained in different software packages when using the same system to perform studies such as small-signal and transient stability. From the results obtained in this dissertation DigSILENT is the only software package for all studies (considered in this dissertation) that can be presented as standard software to use on HVAC or HVAC-HVDC systems, since it is the only software package that behaves as expected for all scenarios on the different systems. PST can be fully trusted when performing HVAC studies alone, as the results agree with the examples used in literature. When considering the HVAC-HVDC systems, the SMIB system has very high oscillations on the transient stability studies due to the HVDC system, which disagree with the expectations. However, the Two Area Multi-Machine system behaves quite as expected for all studies. PSAT has to be investigated in more detail as it has large inconsistencies with the other two software packages and literature

on the HVAC system, introducing serious doubt about it accuracy. Further work is necessary to determine the causes of these inconsistencies.

Table of Contents

List of Figures

List of Tables

Chapter 1

Introduction

With the increase in power demand over the past few years, HVDC has become the preferred alternative to the conventional AC transmission system in the transmission of bulk power over long distances [1 - 3]. This is due to its economic and technical advantages in long distance power transfer. HVDC transmission systems offer suitable solutions for interconnecting HVAC systems with different frequencies and HVDC systems can deliver more power over longer distances with fewer losses. HVDC systems also offer high controllability of the power transmitted [1].

When compared to HVAC transmission system, the HVDC transmission system is considered a new type of technology, because it has not been in use for as long as the HVAC system for bulk power transmission. Many software packages can study the performance/behaviour of power systems that use HVAC transmission lines, but not many cater for HVDC system studies. Only a limited number of software packages allow HVDC systems to be studied, and from these, three were selected and were investigated in this dissertation.

1.1 Background to dissertation

The demand for stable electric power is increasing in Southern Africa and across the word. Many of the existing transmission systems are connected with HVAC transmission lines. However, because of controllability, low losses and the ability to interconnect systems with different frequencies, HVDC systems are now being widely used across the globe. Before any device is installed, it needs to be studied in order to detect and correct any possible flaws. Not many software packages allow HVDC systems modelling and not many have been studied in detail when it comes to HVDC systems. This dissertation is a stepping stone on studies of some of the software packages that allow HVDC system modelling, as this dissertation contributes to the literature that is already available on HVAC-HVDC system modelling and on the comparison of these software packages.

In this dissertation, three software packages are investigated; namely DigSILENT, Matlab PST and Matlab PSAT. The differences among them in terms of their modelling capabilities, power flow studies and stability analyses are described.

1.2 Objectives of the dissertation

The objectives of this dissertation are to:

- Investigate the HVAC and HVDC modelling capabilities of the different software packages used
- Investigate the steady state of the HVAC and HVDC systems across all three software packages
- Study the small signal and transient stability for the HVDC system when interconnected to an HVAC system
- Compare the performance of the three software packages in terms of the steady state performance, small-signal stability performance and transient stability performance

1.3 Methodology

A literature review was conducted in order to increase the researcher's knowledge on the topic covered in this dissertation and to know what has already been done in this field. Two base systems where studied: a Single Machine Infinite Bus system (SMIB) and a Two-Area Multi-Machine system (TAMM). Both HVAC and HVAC-HVDC systems were studied for each base system and the results were compared across the three packages. The steady state results were validated in [4] and for stability studies, the results were compared among the software packages used. Email communications with the software technical support were exchanged to clarify any queries encountered during the research, (see Appendix E). Since the developer of PSAT could not be reached the researcher made use of the PSAT forum available from Yahoo but with little help from the forum.

1.4 Limitations and Scope

The dissertation only covers HVAC and hybrid HVAC-HVDC systems for the base systems discussed above because of the inability of Matlab PST and PSAT to model the HVDC system without a HVAC system connected in parallel to the HVDC system. When studying transient stability, only three-phase HVAC line faults are considered. This is to maintain the uniformity of the applied faults across all three software packages, as PSAT only models three-phase faults on the HVAC system. No modelling was done from base level, where the user built the components by connecting the different controllers that make up the component, as the software packages do not allow changes to be made. Although DigSILENT has the ability to model from base level, the licence used does not cater for DigSILENT Simulator Language (DSL). The results presented are from simulations performed across the three software packages used in this dissertation.

1.5 Outline of the Dissertation

The dissertation is summarized as follows:

Chapter 1 Gives an introduction to the dissertation and briefly hints at what is discussed further.

Chapter 2 Discusses HVDC systems with regard to the advantages, systems configurations, HVDC transmission line modelling and the conversion process for AC to DC and the control of the HVDC system.

Chapter 3 Describes the different AC components such as generators, transmission lines, Automatic Voltage Regulator (AVR), Power System Stabilizer (PSS), transformers, loads and bus classification on the systems and how they are modelled.

Chapter 4 Presents the features and capabilities of the three software packages used and how they are used to model the HVAC and HVDC components.

Chapter 5 Presents the results for the Single Machine Infinite Bus (SMIB) HVAC and HVAC-HVDC systems for the steady state, small signal stability and transient stability. It further compares the results obtained across the three packages.

Chapter 6 Presents results for the Two-Area Multi-Machine (TAMM) HVAC and HVAC-HVDC systems for the steady state, small-signal stability and transient stability. It further compares the results obtained across the three packages.

Chapter 7 Summarises the results of the simulations, draws conclusions based the simulation results and makes recommendations and suggestions for further work.

Chapter 2

HVDC System Configurations and Modelling of Components

2.1 Introduction

High-Voltage Direct Current (HVDC) was first used by Marcel Deprez in 1881. He designed a system that could transmit 1.5 kW at 2 kV over a distance of 56 km, and since then many HVDC transmission systems have been widely used around the world [4]. The first HVDC transmission systems used mercury-arc valve systems, but with the advent of thyristor valves for converter stations, HVDC became much more attractive to use. HVDC systems have the ability of controlling the power transmitted, and when used in parallel with HVAC transmission lines can improve the stability of the system [1 – 3, 5 - 6].

2.2 Advantages of HVDC transmission systems

HVDC has the following advantages:

- Bulk power can be transmitted across the HVDC system - for underground and submarine cables - at above 30-50 km (break-even distance); the HVDC system becomes more economical as no reactive power compensation is needed as in the case of HVAC lines/ cables. For overhead lines, the system becomes more economical above 500-800 km (break-even distance). If the distance is less than the break-even distance stated above for overhead lines and cables, the AC transmission system is more economical than the DC system.
- HVAC systems that cannot be interconnected because they have different nominal frequencies can be interconnected using an HVDC system.
- Corona loss and radio interference are reduced in HVDC systems.

- No reactive power compensation is needed for HVDC lines; however the converter stations require 50-60% of the active power transmitted as reactive power in order to operate
- The length of the line is not restricted by stability.
- The HVDC transmission system has lower losses when compared to the AC transmission system.

2.3 HVDC system configurations

2.3.1 Monopolar HVDC link

The Monopolar link has one conductor, usually of negative polarity and for the return uses ground or water. A metallic conductor is used where the resistivity of the soil is too high or where interference with underground/underwater structures is possible. Figure 2.1 shows a Monopolar system using earth as a return path [1, 5 - 7].

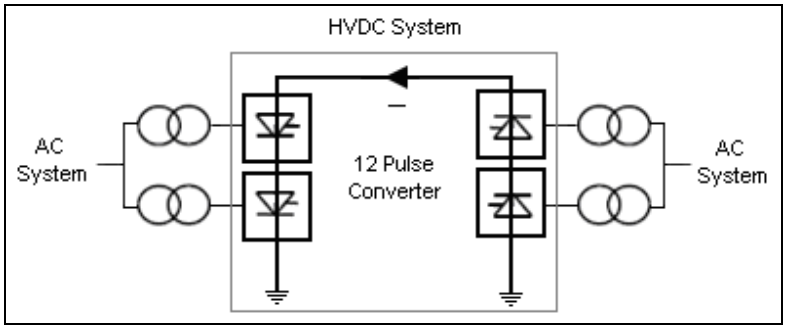

Figure 2.1: Monopolar HVDC link

2.3.2 Bipolar HVDC link

The Bipolar link, shown in figure 2.2, has two conductors, one of positive and the other of negative polarity. Each terminal has two converters of the same rated voltage and the junctions between the converters are grounded. In the event of a fault occurring in one of the conductors, the other can still operate by carrying half of its rated capacity or more by using the overload capacities, making this system more reliable than the Monopolar system [1, 5 - 7].

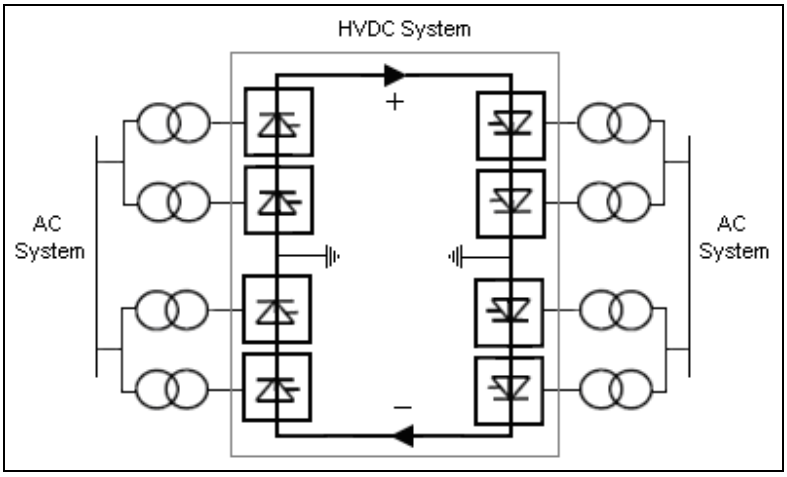

Figure 2.2: Bipolar HVDC link

2.3.3 Homopolar HVDC Link

The configuration for a homopolar link is shown in figure 2.3. It comprises two or more conductors, all of the same polarity, and it uses ground as the return path. It usually uses negative polarity, as it causes less radio interference due to corona [1].

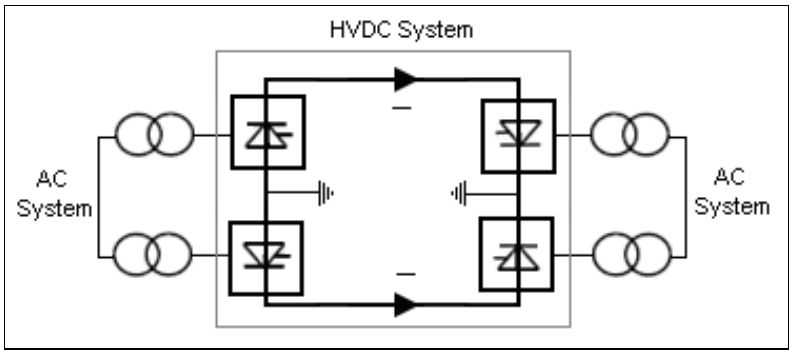

Figure 2.3: Homopolar HVDC link

2.3.4 Back-to-back HVDC Link

The Back-to-back link, shown in figure 2.4, is normally used where two AC systems of different frequencies need to be interconnected in the same location. It is generally used to interconnect asynchronous systems. An example of such a system can be found in Japan, where half the country operates at 50 Hz and the other half at 60 Hz and a back-to-back Shin-Shinano HVDC system is used to connect these two systems [2, 5].

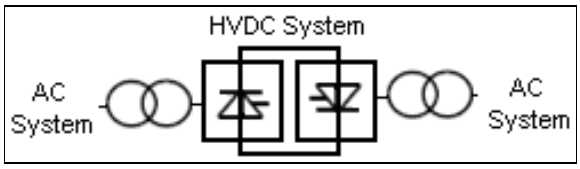

Figure 2.4: Back-to-back HVDC Link

2.3.5 Multi-terminal HVDC link

Multi-terminal HVDC links are found when two or more HVDC converter stations are interconnected with HVDC transmission lines or cables. If the system is connected to the same voltage it is called a parallel Multi-terminal system, shown in figure 2.5. If one or more converter stations are connected in series in at least one pole, it is called a series Multi-terminal system, shown in figure 2.6. When the parallel system is combined with a series system, the system is called a hybrid Multi-terminal system. Multi-terminal links are not economically viable owing to the additional cost of substations [7].

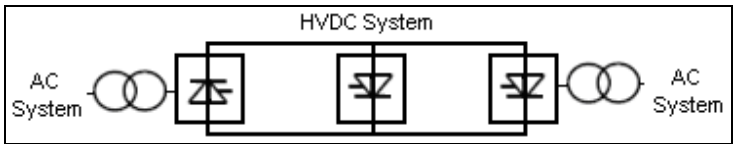

Figure 2.5: Parallel Multi-terminal HVDC link

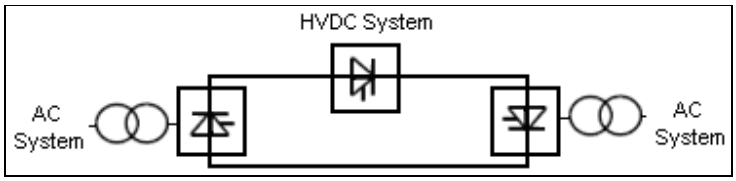

Figure 2.6: Series Multi-terminal HVDC link

2.4 HVDC Transmission lines

On HVAC systems, HVAC cables require compensation stations to counter the effect of the high capacitance on distances above 50 km. HVDC cables become convenient and economical for distances longer than 30-50 km as they do not absorb or produce any reactive power. HVDC overhead lines become more economical for bulk power transmission when used for distances above 500-800 km, as fewer conductors are used to transmit the same quantity of power at three-phase than an AC system would need.

The HVDC transmission lines are modelled using π equivalent circuit, as shown in figure 2.7. The modelling of the line is similar to the one employed in HVAC transmission lines, with the HVDC lines operating at a steady-state frequency of 5 Hz and during transient ranging between 90-100 Hz [7 - 10].

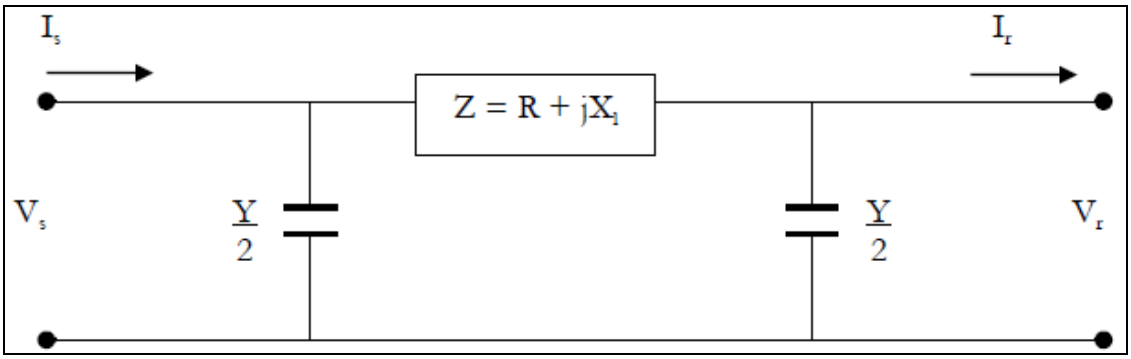

Figure 2.7: Equivalent π circuit of a transmission line

From the above π equivalent circuit, the sending end voltage and current are derived:

$$V_S = \left(1 + \frac{Y}{2}Z\right)V_R + ZI_R \tag{2.1}$$

$$I_S = Y\left(1 + \frac{Y}{4}Z\right)V_R + \left(1 + \frac{Y}{2}Z\right)I_R \tag{2.2}$$

where:
V_s and I_s are the sending end voltage and current, respectively
V_r and I_r are the receiving end voltage and current, respectively
$Z = R + jX_l$ is the series impedance of the line
Y is the shunt admittance of the line

The transmission line modelling is similar to the one used for the HVAC system.

2.5 AC to DC conversion

To convert the power to DC power and vice-versa, converter stations are used. To convert from AC into DC, a rectifier station is used and to convert from DC into AC, an

inverter station is used. In what follows, a two-terminal DC link is assumed, with the control in the multi-terminal DC systems being similar.

HVDC converters are connected to the AC system by means of converter transformers. A 12-pulse converter bridge is normally built by connecting two 6-pulse bridges in series. The bridges are then connected separately to the AC system by means of converter transformers; normally one transformer has a Y-Y winding structure and the other has a Y-Δ winding structure, as shown in Figure 2.4 [7, 11].

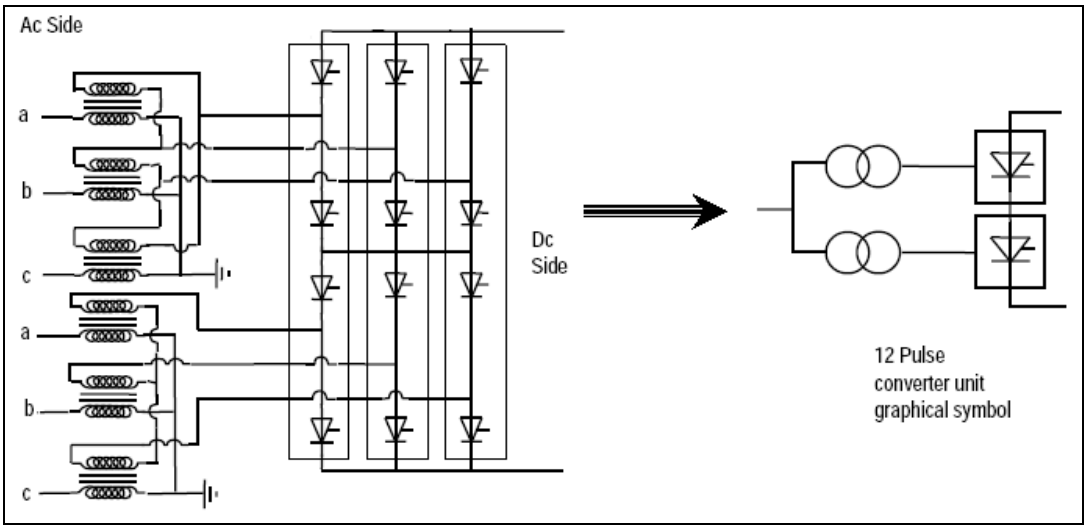

Figure 2.8: 12- pulse valve bridge circuit with two converter transformers, with one transformer in star-star and the other in star-delta configuration [7]

Assuming that the AC system as well as the converter transformer can be represented as ideal systems, the line-to-neutral voltages would be:

$$\begin{cases} V_A = V\cos(\omega t + 60°) \\ V_B = V\cos(\omega t - 60°) \\ V_C = V\cos(\omega t - 180°) \end{cases} \tag{2.3}$$

Denoting ωt by θ, the line-to-line voltages are then given by:

$$\begin{cases} V_{AC} = V_A - V_C = \sqrt{3}V\cos(\theta + 30°) \\ V_{BA} = V_B - V_A = \sqrt{3}V\cos(\theta - 90°) \\ V_{CB} = V_C - V_B = \sqrt{3}V\cos(\theta + 150°) \end{cases} \tag{2.4}$$

where:

V_A, V_B, V_C – instantaneous line-to-neutral voltages

V_{AC}, V_{BA}, V_{CB} – instantaneous line-to-line voltages

V – peak line-to-neutral voltage

The power transfer on a DC system is a function of the voltage magnitude between the sending and receiving end. The power flows from high to low voltage magnitudes.

Each pulse in the 6-pulse bridge has a segment of 60º over the full cycle of 360º. The average DC voltage is obtained by integrating the AC voltage over a period of 60º, taking into account the delay angle α.

$$V_{DC} = \frac{3}{\pi} \int_{-(60-\alpha)}^{\alpha} V_{AC} d\theta \tag{2.5}$$

The voltages at the rectifier and inverter stations are given by:

$$V_{DC(R)} = \frac{3\sqrt{2}}{\pi} BTV_{REC} \cos\alpha \tag{2.6}$$

$$V_{DC(I)} = \frac{3\sqrt{2}}{\pi} BTV_{INV} \cos\gamma \tag{2.7}$$

The current flowing through the DC link is given as:

$$I_{DC} = \frac{V_{DC(R)} - V_{DC(I)}}{R_R + R_{DC} - R_I} \tag{2.8}$$

where:

V_{DC} – average DC voltage

$V_{DC(R)}$, $V_{DC(I)}$ – rectifier and inverter DC voltages

V_{REC}, V_{INV} – rectifier and inverter rms line-to-line AC voltages

R_{DC} – HVDC line resistance

R_R, R_I – rectifier and inverter resistances

B – number of converter bridges in series

T – transformer turns ratio

α – delay/firing angle

γ – extinction angle

From equations 2.6 and 2.8, the output power at the rectifier station ($P_{DC(R)}$) is given by:

$$P_{DC(R)} = V_{DC(R)} I_{DC} \tag{2.9}$$

Under steady-state conditions, the conversion of power from AC into DC and vice versa, the reactive power required by the converter stations is 50-60 % of the active power being converted [1, 2]. A reduction in the voltage leads to an increase in the reactive power consumed by the converter station [2, 5].

During the conversion process, harmonics are generated on the AC and DC sides of the converter stations. These harmonics affect the quality of power that is supplied by interfering with other telecommunication systems, overheating capacitors and generators in the vicinities of the converter stations.

The harmonics present on the AC side are of the order:

$$h = np \pm 1 \tag{2.10}$$

The harmonics present on the DC side are of the order:

$$h = np \tag{2.11}$$

Because these harmonics are harmful to the system, filters are used on both the AC and DC sides to mitigate the effect of the harmonics. These filters also serve as sources of reactive power to the system.

2.6 HVDC systems control

HVDC systems offer very high levels of controllability by maximizing the flexibility of the power controlled while maintaining stable and safe operations of the HVDC system. Adequate control strategies must be employed on the rectifier and inverter stations to achieve this state of operation.

From equations 2.8 and 2.9, the voltage, current or power at any point on the DC line can be controlled by controlling the internal voltages: ($V_{DC(R)}$) and ($V_{DC(I)}$). Power reversal can be obtained through the reversal of polarity of the direct voltages at both ends of the line. To ensure that the voltage on the line remains close to the rated voltage, the firing angle α at the rectifier is limited to a minimum of 5º but α is normally in the range of 15 – 20º. The extinction angle γ at the inverter is normally operated at 15º for 50Hz systems and 18º for 60Hz systems. Under normal operating conditions, the rectifier operates at Constant Current (CC) while the inverter operates with Constant Extinction Angle (CEA) [1, 22].

Figure 2.5 shows the actual characteristic of an HVDC rectifier that has two segments (FA and AB) - where FA corresponds to minimum ignition angle and is a representation of the constant ignition angle (CIA) control and segment AB represents the normal CC control mode. FAB shows the complete characteristic of the rectifier at normal voltage and when the voltage is reduced, the segments then shift to F'A'B. The characteristics of the inverter are given by DGH, where segment DG represents CEA and segment GH represents CC.

Under normal operating conditions, the rectifier controls the direct current and the inverter controls the direct voltage. This operating condition is shown as point E in figure 2.5. If there is a nearby fault, causing the rectifier voltage to drop, a new operating (E') condition is established. In this operating condition, the roles of rectifier and inverter are reversed; in other words, the inverter takes over the current control and the rectifier establishes the voltage. This is known as *mode shift*.

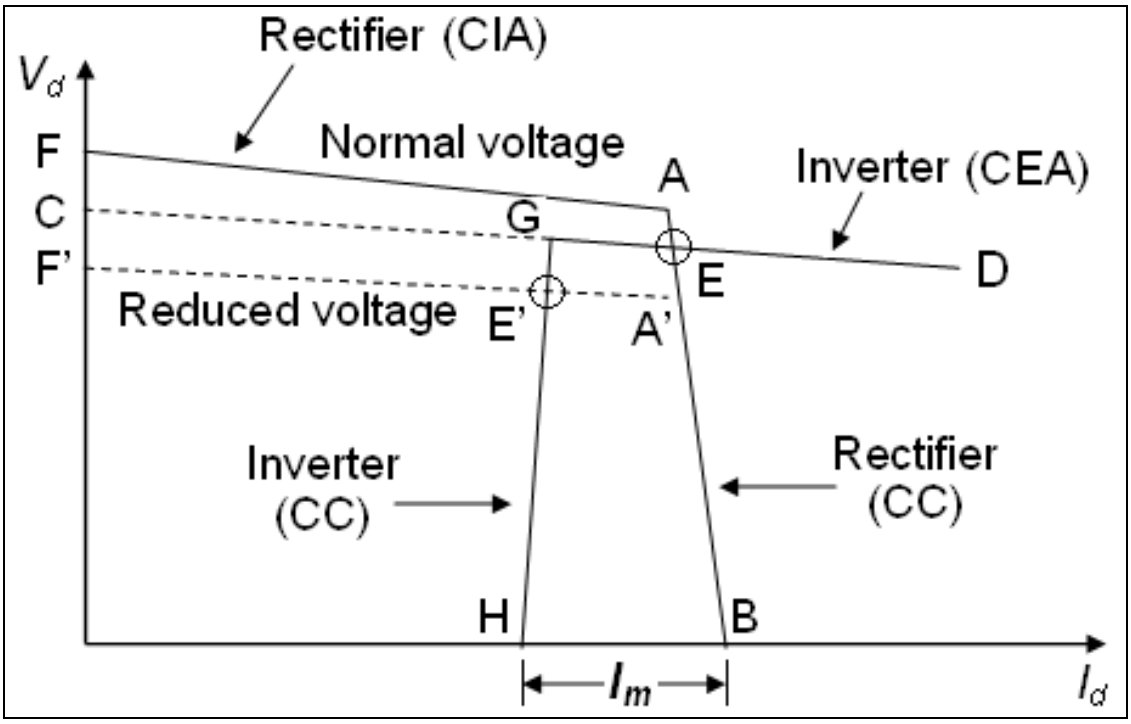

Figure 2.9: Actual V-I characteristics of HVDC converters under steady state [2]

2.7 Summary

This chapter discussed the modelling of HVDC systems. The different types of HVDC configurations such as Monopolar, Bipolar, Back-to-back and Multiterminal were described. The HVDC transmission line modelling was discussed. The process of conversion from AC to DC was explained with the help of mathematical equations. The different types of HVDC system controls such as Constant Current (CC) and Constant Extinction Angle (CEA) used in this thesis were explained.

The modelling of HVDC systems using the three software packages are discussed in chapter 4.

Chapter 3

Power System Component Modelling

3.1 Introduction

Electric power generation, transmission and distribution are interconnected by a network of transmission lines linking generators and loads, some of which cross entire continents. The supply of electric power presents a variety of challenges as the systems become more and more complex [1, 12, 13]. To be able to predict the correct behaviour and performance of such systems, engineers must equip themselves with powerful tools that can analyse these systems.

A model is a set of equations that describes the relationship between the inputs and outputs of a system. Simple models of components are not adequate or reliable for accurate description of power system dynamics. As dynamic and complex as systems may be, they can be simplified into smaller subsystems on which the dynamic characteristics can be modelled and analysed easily [14].

When generating electric power, it must always match the load demand and the losses on the system. If subjected to a disturbance, protection systems must be able to detect and eliminate a minimal number of faulted components on the power system, in order to enhance the stability and recovery of the power system [13].

In this chapter, the modelling of different components of the power system is discussed. In Fig 3.1, an example of a modified model of a Single Machine Infinite Bus (SMIB) system is shown, to illustrate the different components used across all systems. These components are applicable to both the Single Machine Infinite Bus system and the Two-Area Multi-machine system which have been used as test cases in this research project.

The components are:

- Synchronous generator equipped with an excitation system comprising an Automatic Voltage Regulator (AVR) and a Power System Stabilizer (PSS)
- Two winding transformer
- Transmission line(s)
- Load
- Infinite bus

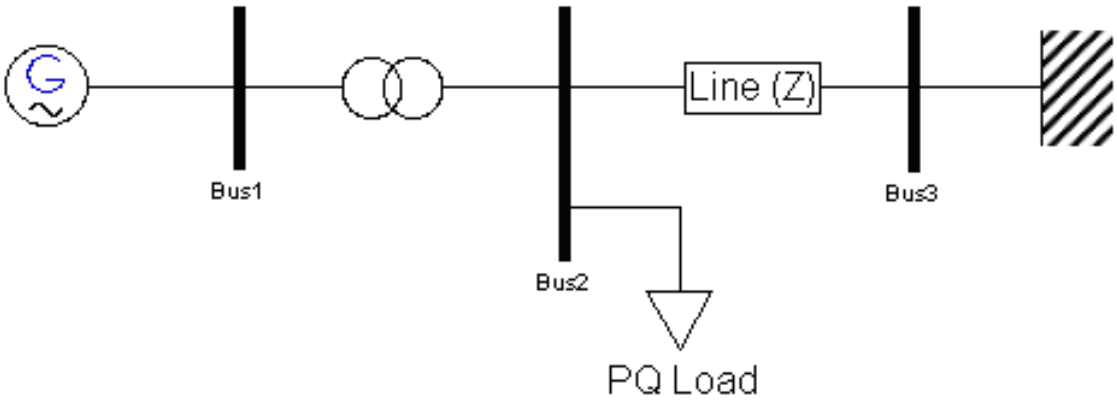

Figure 3.1: Example of a Single Machine Infinite Bus System

3.2 Synchronous generator

Synchronous generators form the most important source of electric power generation in power systems. Understanding generator characteristics and their accurate modelling is very important to the study of power system stability since maintaining synchronous generators in synchronism is very important to power stability [1]. Modelling of synchronous generators is therefore very important for reliable power system stability analysis.

3.2.1 d-q representations

To perform power system studies, synchronous generators are used. These generator models range from the simplest classical (2^{nd} order) to the more detailed 8^{th} order generator models [1, 13 - 16], depending on the stability studies that need to be performed on the system. For the classical model, the voltage behind the transient is

assumed to be constant [1, 12, 15, 17, 18] where flux decay and damper windings are neglected. For the 3rd order and higher models, rotor characteristics are represented by a field winding and amortisseur on the direct axis (*d*-axis) and/or quadrature axis (*q*- axis) for a more complete synchronous machine model as the order increases.

Table 3.1 shows the number of rotor circuits in each model, with the model order indicating the number of state variables associated with each machine model. The 6th order machine model is preferred for representing the round rotor in stability analysis [1, 15, 17] and this machine model is used in this research. The variables commonly used to represent the 6th order generator model are rotor angle, rotor angular velocity, field flux linkage, *d*-axis amortisseur flux linkage, two *q*-axis amortisseur flux linkages (δ, ω_m, ψ_{fd}, ψ_{1d}, ψ_{1q}, ψ_{2q}).

Table 3.1: Number of rotor circuits in generator models [15]

Machine model	No. of windings	
	d-axis	*q*-axis
3rd	1	0
4th	1	1
5th	2	1
6th	2	2
7th	3	2
8th	3	3

From [15], the linearized generator equations of motion and rotor circuit equations for a 6th order generator model are given as:

$$
\begin{aligned}
\Delta\dot{\delta} &= \omega_0 \Delta\omega_m \\
\Delta\dot{\omega} &= \frac{1}{2H}\left(\Delta T_m - \Delta T_e - K_D \Delta\omega_m\right) \\
\Delta\dot{\psi}_{fd} &= \frac{\omega_0 R_{fd}}{L_{fd}}\Delta\psi_{ad} - \frac{\omega_0 R_{fd}}{L_{fd}}\Delta\psi_{fd} + \omega_0 \Delta e_{fd} \\
\Delta\dot{\psi}_{1d} &= \frac{\omega_0 R_{1d}}{L_{1d}}\Delta\psi_{ad} - \frac{\omega_0 R_{1d}}{L_{1d}}\Delta\psi_{1d} \\
\Delta\dot{\psi}_{1q} &= \frac{\omega_0 R_{1q}}{L_{1q}}\left(\Delta\psi_{1q} - \Delta\psi_{aq}\right) \\
\Delta\dot{\psi}_{2q} &= \frac{\omega_0 R_{2q}}{L_{2q}}\left(\Delta\psi_{2q} - \Delta\psi_{aq}\right)
\end{aligned}
\tag{3.1}
$$

where:

ω_0 – base angular velocity

H – onertia constant

T_m – mechanical torque

T_e – electrical torque

K_D – damping torque coefficient

L_{fd} – field winding leakage inductance

L_{1d} – d-axis amortisseur reactance

L_{1q}, L_{2q} – 1st and 2nd q-axis amortisseur reactances

e_{fd} – field voltage

R_{1d} – d-axis amortisseur resistance

R_{1q}, R_{2q} – 1st and 2nd q-axis amortisseur resistance

ψ_{ad}, ψ_{aq} –d and q-axis mutual flux linkages

ψ_{1d} – d-axis amortisseur flux linkage

ψ_{1q}, ψ_{2q} – 1st and 2nd q-axis amortisseur flux linkage

In power systems analysis, synchronous machine models are usually represented using operational-impedance and coupled-circuit methods [15]. Synchronous machine data are usually specified in terms of standard parameters, also known as derived parameters (transient and sub-transient inductances and time constants) and can be obtained from manufacturers data and/or field tests. Models represented by the operational-impedance

method use data specified in standard parameter format, whereas models represented by the coupled-circuit method use data specified in basic parameter format, also known as fundamental parameter format (resistances and inductances). If a machine is modelled using the coupled circuit method, standard parameters are converted to basic parameters. Fig. 3.2 shows the operational-impedance of a 6th order machine.

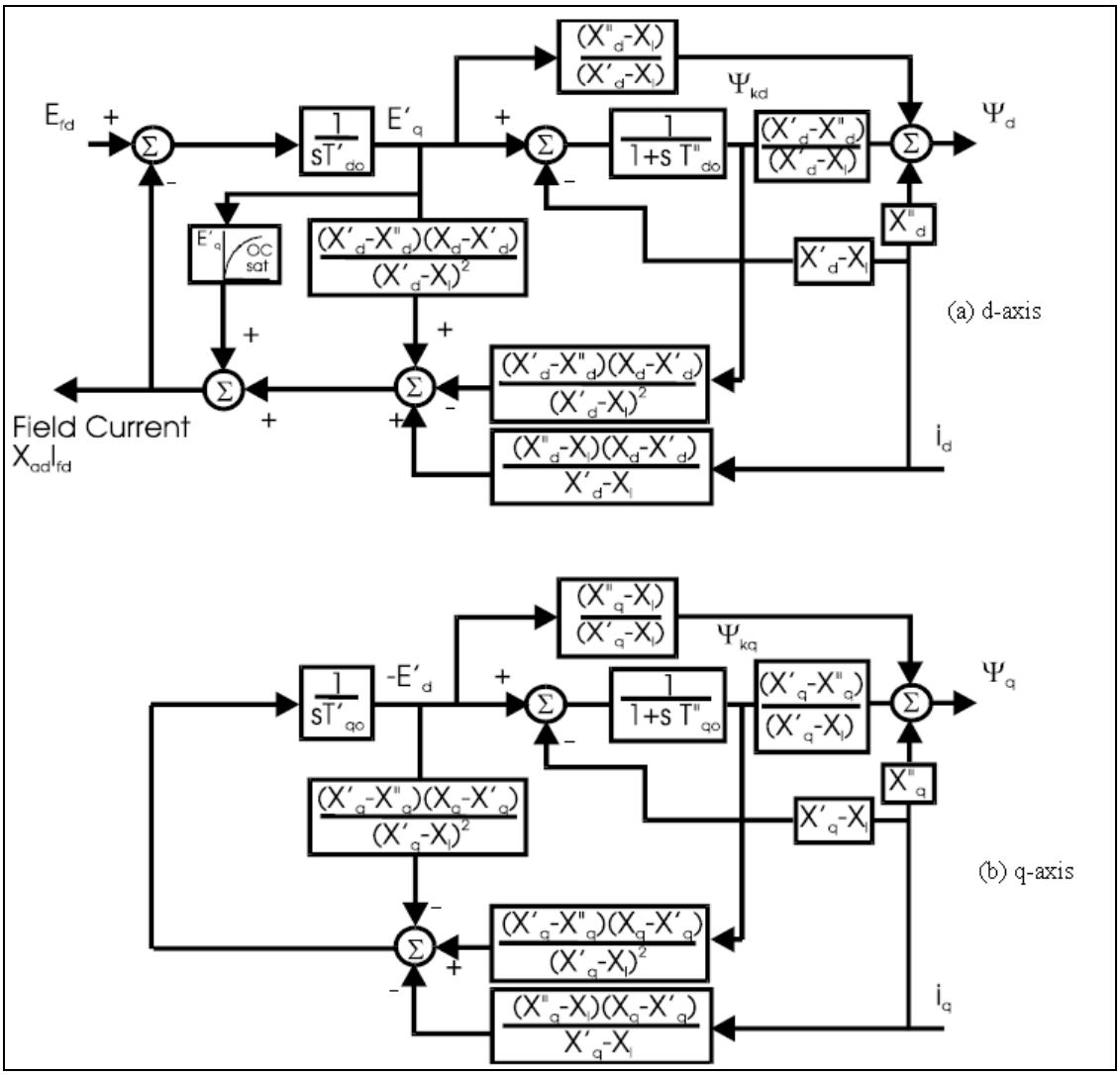

Figure 3.2: Representation of *d*-axis and *q*-axis of the 6th order generator model using operational-impedance method [25]

In Fig. 3.3, a coupled-circuit method representation of the direct axis and the quadrature axis of a 6th order machine is shown.

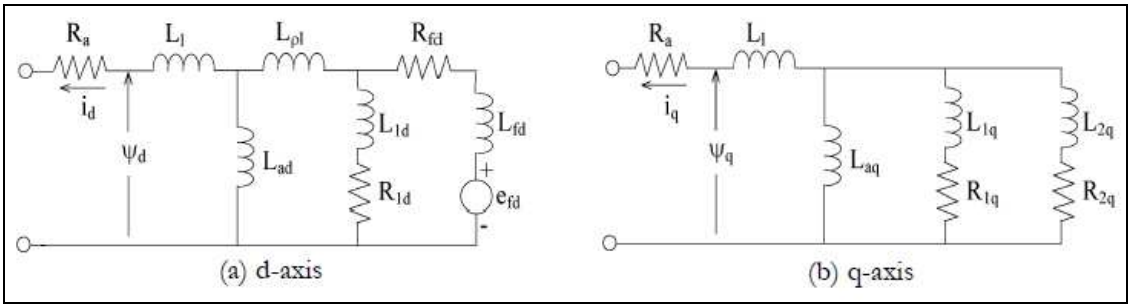

Figure 3.3: Representation of *d*-axis and *q*-axis of the 6th order generator model using coupled-circuit method [1]

3.2.2 Saturation modelling

Figure 3.4 depicts the open circuit curve used to represent the saturation characteristic of a loaded generator. The air gap line shows the Open Circuit Characteristic (OCC) if magnetic saturation is neglected.

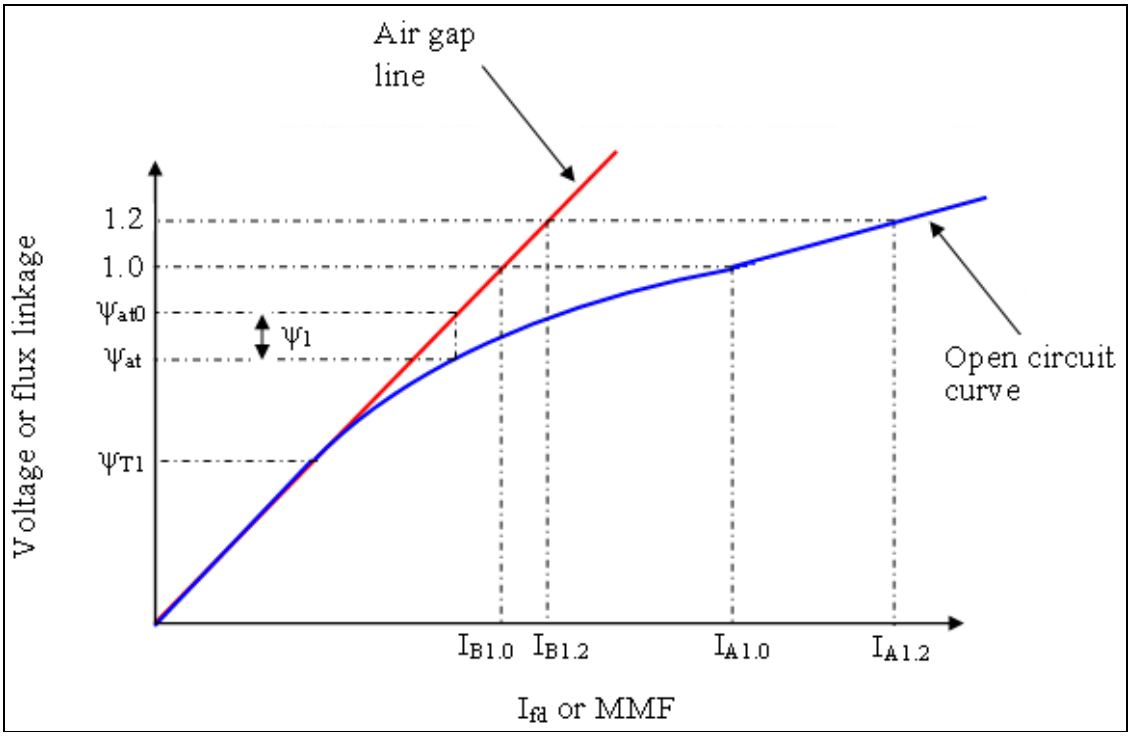

Figure 3.4: Open circuit saturation curve [1, 25]

Saturation representation is considered an important factor when modelling a synchronous generator. Nevertheless, no standard method is used when modelling the saturation of a generator for small signal stability studies [15, 19]. Most software

packages represent saturation with the total saturation method. It uses the $S_{1.0}$ and $S_{1.2}$ parameters, which correspond to the 1.0 pu and 1.2 pu flux linkage (terminal voltage) respectively [15]. The field currents $I_{A1.0}$, $I_{B1.0}$, $I_{A1.2}$ and $I_{B1.2}$ shown in figure 3.4 contribute to the saturation parameters in the form:

$$S_{1.0} = \frac{I_{A1.0} - I_{B1.0}}{I_{B1.0}} \tag{3.2}$$

$$S_{1.2} = \frac{I_{A1.2} - I_{B1.2}}{I_{B1.2}} = \frac{I_{A1.2} - 1.2I_{B1.0}}{1.2I_{B1.0}} \tag{3.3}$$

3.3 Excitation system

The AVR performs control and protective functions that are essential to a satisfactory performance of the generator. Excitation systems have as a basic requirement - the supply and automatic adjustment of the field current of the synchronous machine generator. This is in order to maintain the terminal voltage, as the output varies within the continuous capability of the generator. In addition, it must be able to respond rapidly to a disturbance in order to enhance the transient stability of the system, and to modulate the generator field to enhance the small-signal stability [1, 18].

There are three different types of excitation systems, namely DC excitation systems (which utilise a DC generator with commutator), AC excitation systems (which use alternators and either stationary or rotating rectifiers to produce the direct current needed) and Static excitation systems (in which the power is supplied through transformers and rectifiers) [1, 13, 15, 18, 20].

The excitation system employed in this dissertation, shown in Fig. 3.5, is the AC4A excitation system model. The excitation system for this model is provided in the form of a series lag-lead network with transient gain reduction [1]. From left to right, the first block is a lead-lag block (excitation system stabilization) which is similar to a single time constant block, followed by a high value gain, which takes the highest value from the inputs as the output and the last block represents an amplifier.

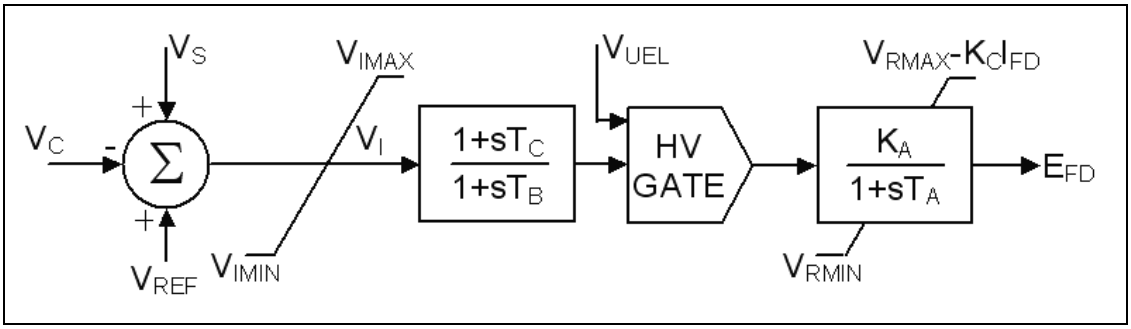

Figure 3.5: Type AC4A excitation system model [1, 20, 25]

3.4 Power System Stabilizer (PSS)

Power system stabilizers are used to damp power system oscillations. They use auxiliary stabilizing signals to control the excitation system in order to improve power system dynamic performance. Commonly used signals are the shaft speed, terminal frequency and power [1, 18, 20]. An example of a PSS is shown below in figure 3.6. From left to right, the first block represents a stabilizing circuit for the PSS and the last two blocks allow two stages of lead-lag compensation, as set by constants T_1 to T_4.

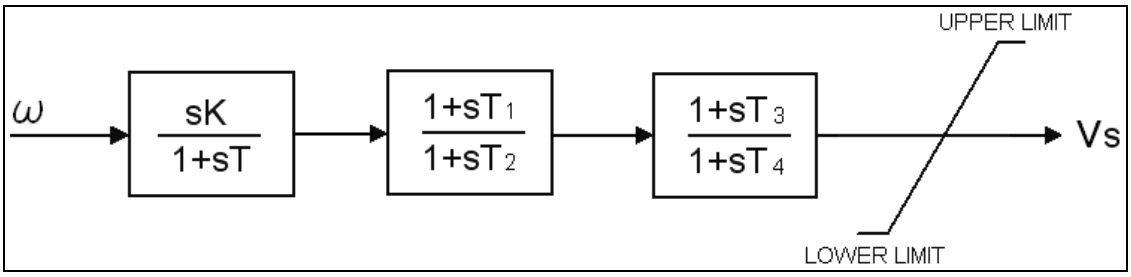

Figure 3.6: Power System Stabilizer (PSS) [1, 20, 25]

3.5 AC Transmission lines

There are different models of transmission lines. They can be modelled using T or π nominal circuits; however the representation by the π equivalent circuit is normally used when modelling AC transmission lines (see section 2.4). For 60 Hz AC lines, the transmission lines may be classified according to their length:

- Short lines: lines normally shorter than 80 km, represented by the nominal π circuit where the shunt admittances are neglected
- Medium lines: lines whose length range from 80 km to approximately 250 km, represented by the nominal π circuit
- Long lines: lines longer than 250 km are represented by the nominal π circuit [1, 21]

3.6 Transformers

Transformers are used because of their capability to either step up or step down the voltage across the power system. Since it is not feasible to generate and consume power at high voltages, it is normally stepped up for power transmission after generation and stepped down for consumption. Figure 3.7 below shows a standard equivalent circuit for a two-winding transformer,

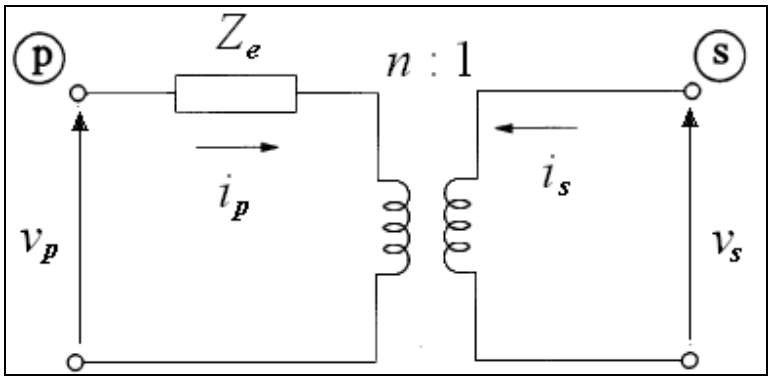

Figure 3-7: Standard equivalent circuit for an ideal two-winding transformer [1, 13]

where:

v_p and i_p are the primary voltage and current, respectively

v_s and i_s are the secondary voltage and current, respectively

Z_e is the transformer impedance

n is the turns ratio

The representation shown in figure 3.7 is widely used for power flow and stability analysis, but in digital computer analysis a more realistic representation must account for winding parameters as well as exciter current [22].

3.7 Loads

The stable operation of a power system relies on the ability of a continuous match between the electrical power generated and the electrical load. For power system studies, load representation is simplified owing to its complexity, and load models are classified as static or dynamic models. With dynamic loads, they vary rapidly with changing voltage and frequency and are given by differential functions of bus voltage magnitudes dependent on the past instant [1, 23]. When performing stability studies on a power system, it is often advised to use dynamic modelling [1, 13, 23]. However, dynamic load models will not be discussed in detail, as they are not used in this dissertation. Static load models are not dependent on time and the relation of the active and reactive power is given as algebraic functions of the voltage and/or frequency at any instant of time.

Static load models, which are used for active and reactive power, are expressed in a polynomial or exponential form, and a brief description of these models excluding frequency dependence follows below.

***ZIP* or polynomial model**

The characteristics of this load model can be classified into constant impedance (Z), constant current (I) and constant power (P) in accordance with their relationship to the voltage. For constant impedance the power dependence on the voltage is quadratic, for constant current it is linear, and for constant power, the power is independent of changes in voltage. The coefficients p_1 to p_3 and q_1 to q_3 are the parameters of the model, which define the proportion of each component, and V_0, P_0 and Q_0 are the initial condition of the system.

$$P = P_0\left[p_1\left(\frac{V}{V_0}\right)^2 + p_2\left(\frac{V}{V_0}\right) + p_3 \right] \tag{3.5}$$

$$Q = Q_0 \left[q_1 \left(\frac{V}{V_0} \right)^2 + q_2 \left(\frac{V}{V_0} \right) + q_3 \right] \tag{3.6}$$

Exponential model

Equations 3.7 and 3.8 express the power relationship to the voltage as an exponential function.

$$P = P_0 \left(\frac{V}{V_0} \right)^a \tag{3.7}$$

$$Q = Q_0 \left(\frac{V}{V_0} \right)^b \tag{3.8}$$

The parameters for this model are *a* and *b*, which are the exponent values for different load model behaviour. The values for the initial voltage, active and reactive power are V_0, P_0 and Q_0 respectively. To represent constant power, constant current or constant impedance the exponents *a* and/ or *b* are set to 0, 1 and 2 respectively.

3.8 Summary

This chapter illustrated the modelling of the different components of a power system with the help of mathematical equations and diagrams. The components discussed are synchronous generators, AVRs, PSSs, AC transmission lines, transformers and loads. The modelling of these components in the packages used in this dissertation is discussed in the next chapter.

Chapter 4

Features and Capabilities of DigSILENT, Matlab PST and PSAT

4.1 Introduction

Since the beginning of electrical engineering, modelling and simulations have been the basic means of investigating important phenomena in power systems. Since power systems are the backbone of industry, power system simulation is becoming more important than ever before, as the demand for electrical power is continuously increasing and more power systems need to be built to cater for this increase in demand. A better understanding of systems prior to their manufacture leads to optimally designed devices, and an analysis of the impact of the introduction of new devices prior to their installation into the electrical network results in optimized power systems and fewer surprises. All this is possible by applying modern power system simulation tools that have been developed and improved over time.

Power systems software packages for power system analysis can be divided into two classes, industrial-grade commercial software packages and educational or research based software packages. Commercial software packages available on the market are usually well tested and computationally efficient. However, educational or research based software packages can prove to be quite difficult to run and their accuracy and efficiency are not as good as those of the commercial packages.

In the following section, an overview of the different software packages used in this dissertation is given.

4.2 DigSILENT Power Factory

DigSILENT stands for Digital Simulation and Electrical Network calculation program and it was developed by DigSILENT Power Factory. It is an industrial based software package that has been in operation for more than 25 years [24].

DigSILENT has the ability to simulate load flow, fault analysis, harmonic analysis and stability analysis for AC, DC and AC-DC systems. To model components, DigSILENT makes use of a graphical user interface (GUI), where the components are dragged from the library available and dropped onto the main screen. New components could not be developed from scratch using DigSILENT simulator language (DSL). However, this was not pursued in this dissertation as the licence used does not include DSL. This limits the flexibility of the user on this software package.

The load flow in DigSILENT is performed using the Newton Raphson method. HVDC systems (converter stations) can be modelled in detail and it also allows the converter stations to be modelled using voltage, active power, reactive power, current, Gamma and external control. DigSILENT can model AC systems, DC systems and AC-DC systems. Different types of AC and DC faults can be simulated in DigSILENT.

AC faults can be applied to the transmission lines and buses, as well as on synchronous machines. These faults can range from single-phase faults to three-phase faults. DC faults are single-phase faults and can be performed on the converter stations and on the DC lines. The action of circuit breakers is performed by removing a specific line or generator after a fault.

4.3 Power System Toolbox

The Power System Toolbox (PST) is Matlab run research software that was developed by Joe Chow. It allows users to model components and performs AC and AC-DC system analysis in a Matlab environment. It consists of Matlab m-files, data files and power system application files. These files are easily accessible for system and component

modifications. PST provides dynamic models of machines and controls for performing damping controller designs, transient and small-signal stability simulations [25].

PST models HVDC systems and it allows the user to modify the systems, but the user must know the software in detail in order to make full use of this option. Power flow analysis is performed using the Newton Raphson method. The system converter stations are modelled using voltage, power and inverter controls. PST can only model AC faults - the faults range from single-phase faults to three-phase faults. However, faults can only be applied on transmission lines. The action of circuit breakers is performed by removing a line - whenever a fault is applied a line must be removed to clear the fault, in other words, if a fault is applied on a line, the fault cannot be cleared while the line on which the fault occurred remains operational.

Some of the data, such as the frequency and base MVA, are input whenever small signal and transient stability studies are performed.

4.4 Power System Analysis Toolbox (PSAT 2.1.4)

Power System Analysis Toolbox (PSAT) is an academic Matlab toolbox used for static and dynamic analysis of electric power systems. It was developed by Federico Milano and is open-source software. PSAT includes power flow, continuation power flow, optimal power flow, small-signal stability analysis and transient stability that can be used on AC and AC-DC systems. It uses Newton Raphson algorithm to perform power flow analysis.

All operations can be assessed by means of graphical user interfaces (GUIs) and a Simulink-based library provides a user-friendly tool for network design [26]. PSAT can only model three-phase AC faults. These faults can be modelled on transmission lines and buses. Faults can be cleared by removing the fault applied or disconnecting the line to which it has been applied in the case of transmission lines. To disconnect a line, circuit breakers are used. If the fault is applied on a bus it is removed by clearing the fault.

4.5 Components and data format in DigSILENT, PST and PSAT

Table 4.1 shows the components used in DigSILENT, PST and PSAT. Each component modelling is described for each software package.

Table 4.1: Components and data format in DigSILENT, PST and PSAT

Component	DigSILENT	PST	PSAT
HVDC system	In DigSILENT, the converter stations are already modelled and the user cannot modify the converter type. The rectifier/inverter model is handled internally like a current source. The dynamic comes from the HVDC controller (modelled in DSL) and not from the rectifier/inverter model itself. No HVDC modes are displayed when the small-signal stability analysis is performed. The parameters (rated DC voltage and current, nominal turns ratio and firing angle, minimum and maximum turns ratio for the converter transformer, minimum and maximum firing angle, minimum extinction angle, actual winding ration and firing angle for the converter transformer, commutation reactance and phase shift for the converter transformer) are entered by inserting their values in the spaces provided.	PST models a HVDC system using three different matrix files. The first matrix file is **dcsp_con**, which models the rectifier and inverter converter stations. The data file is given as: dcsp_con = [… A1 B1 C1 D1 E1 F1 G1 H1 A2 B2 C2 D2 E2 F2 G2 H2]; where: A1/A2 – HVDC converter number B1/B2 – AC bus number connected to HVDC converter station C1/C2 – converter type: 1 – rectifier 2 – inverter D1/D2 – HVDC rated voltage (kV) E1/E2 – commutating reactance (Ohms/bridge)	PSAT models the HVDC system using **Hvdc.con** given in the matrix form: Hvdc.con = [… From bus (i) To bus (j) MVA kV (i) kV (j) Freq kV (DC) kA (DC) X_{tR} X_{tI} $Tapratio_R$ $Tapratio_I$ K_I K_P R_{DC} L_{DC} α_{Rmax} α_{Rmin} γ_{Imax} γ_{Imin} I_{R0max} I_{R0min} I_{I0max} I_{I0min}]; where: buses *i* and *j* are the AC buses to which the HVDC system is connected. The MVA is the system's power rating and Freq is the power system's frequency. The transformer reactances (X_{tR}, X_{tI}), the tap ratios for the rectifier and inverter transformers ($Tapratio_R$ and $Tapratio_I$), integral gain (K_I) proportional gain (K_P) and the maximum and minimum

	Rectifiers and inverters are modelled separately by choosing orientation *R* for rectifiers and *I* for inverters. Rectifiers and inverters have some input parameters that are present on both converters and are displayed/ input in the following form: • Converter type (DC voltage rating, DC current rating, nominal turns ratio and nominal firing angle (α)) • Activation of the *Thyristor* option on the Diode/Thyristor converter type • Activation of the *built-in converter station transformer* The remaining rectifier parameters are input as follows: • Firing angle control is set by choosing current control from a menu that contains DC voltage (Vdc), AC voltage (Vac), active power (P), reactive power (Q), current (I), Gamma angle or extinction angle. The values for the parameters min α, max α and min γ are then input in the spaces provided	F1/F2 – number of bridges in series G1/G2 – rectifier min and max firing angle α H1/H2 – inverter min and max extinction angle γ The second matrix file is **dcl_con** which models the HVDC line, and is given as : dcl_con = [… A1 A2 I J K L M N O]; where: I – HVDC line resistance (Ohms) J – HVDC line inductance (mH) K – HVDC line capacitance (μF) L – rectifier smoothing reactance (mH) M – inverter smoothing reactance (mH) N – HVDC line rating (MW) O – current margin for inverter current control The third matrix file is **dcc_con**, which models the controls for the HVDC converter stations, and is given as: dcc_con = [… A1 P1 Q1 R1 S1 T1 U1 V1 W1 A2 P2 Q2 R2 S2 T2 U2 V2 W2];	reference currents for the rectifier and inverter (I_{R0max}, I_{R0min}, I_{I0max} and I_{I0min} respectively) are given in pu. The values for R_{DC} and L_{DC} are entered as the resistance and reactance for the entire length of the line. The HVDC system in PSAT has three modes which are given as: I_{dc}, x_R, x_I (state variables for the DC current, rectifier and inverter reactance respectively).

	• The converter transformer is represented by the following data: tap-changer (set to fixed tap-changer), actual winding ratio, commutation reactance and transformer phase shift • DC power set point The DC line is modelled similarly to the AC line (see AC transmission line); however, under the line type, DC is used instead of AC. This removes the three-phase and zero sequence impedance from the modelling of the line. The parameters for the HVDC system can be found in Appendix B.	where: P1/P2 – proportional gain Q1/Q2 – integral gain R1/R2 – output gain S1/S2 – max integral limit T1/T2 – min integral gain U1/U2 – max output limit V1/V2 – min output limit W1/W2 – control type: 0 – inverter control 1 – rectifier current control 2 – rectifier power control Note that A1, B1 … is used to represent the rectifier parameters and A2, B2 … is used to represent the inverter parameters. The HVDC system in PST has five modes given as: *v_conr, v_coni, i_dcr, i_dci, v_dcc*.	
Synchronous generator	DigSILENT has two synchronous generator models - salient pole (5^{th} order) and round rotor (6^{th} order). The 6^{th} order machine uses δ, ω, ψ_d, ψ_q, ψ''_d and ψ''_q as state variables and P_m as turbine output. The machine is set as a generator from the generator/ motor option. To model the synchronous generator, the following data must be input into the *type* data window: • S, V, power factor, type of connection (D,	The generators can be modelled from the simplest model (classical model with two-state variables) to the most complex (sixth order model which uses δ, ω, E'_d, E'_q, ψ_{kd} *and* ψ_{kq} as the state variables for the machines), except the third order model. The turbine output in PST obtained as mechanical torque T_m. *The* sixth order machine was used in this dissertation.	PSAT models generators from the classical model (with two state variables) to the most complex (eighth order model which uses δ, ω, E'_d, E'_q, E''_d, E''_q ψ_{kd} *and* ψ_{kq} as the state variables for the machines) and the turbine output is represented as mechanical torque T_m. The sixth order machine (without the two last variables from the eight order model) is the only model considered for the studies

	Y, YN) • d-axis and q-axis synchronous, transient and subtransient reactances (X_d, X_q, X'_d, X'_q, X''_d, X''_q) • d-axis and q-axis open-circuit time constants and open-circuit subtransient time constants (T_{d0}', T_{q0}', T_{d0}'', T_{q0}'') • Zero and negative sequence impedance (X_0, R_0, X_2, R_2) • Stator resistance (rstr), leakage reactance (Xl, Xrl) • Saturation parameters (SG_{10}, SG_{12}) • Round rotor (activated from the rotor type menu) • Inertia (H) and mechanical damping coefficient (D) Bus modelling for the generator is done on the synchronous generator load flow window. To set a slack bus, the reference machine option must be selected from the load flow window. The external grid uses a generator model with high inertia and high power internally. The model is slightly different from the standard synchronous generator therefore it has one more state variable than the synchronous	The machine data are implemented in a row vector matrix in the file **mac_con**. Only the data for one machine is presented below. In order to add more machines the data needs to be repeated for the number of machines added. The synchronous machine data are in the form: mac_con = [… Mac# Bus# MVA X_l R_a X_d X'_d X''_d T'_{d0} T''_{d0} X_q X'_q X''_q T'_{q0} T''_{q0} d0 d1 $S_{1.0}$ $S_{1.2}$]; where: Mac# and Bus # are the machine and bus numbers respectively MVA – the base MVA X_l – leakage reactance R_a – resistance X_d – d-axis synchronous reactance X'_d – d-axis transient reactance X''_d – d-axis subtransient reactance T'_{d0} – d-axis open-circuit time constant T''_{d0} – d-axis open-circuit subtransient time constant X_q – q-axis synchronous reactance X'_q – q-axis transient reactance X''_q – q-axis subtransient reactance T'_{q0} – q-axis open-circuit time constant	performed in this dissertation. The (Model#) allowed to be input in the synchronous generator modelling window are 2, 3, 4, 5.1, 5.2, 5.2, 6 and 8 where they are related to the different generator models. In PSAT, the 5^{th} order model has three different types, hence 5.1, 5.2 and 5.3. Type 5.1 uses δ, ω, e'_q, e'_d, e''_d, type 5.2 uses δ, ω, e'_q, e''_q, e''_d and type 5.3 uses where δ, ω, ψ_f, ψ_q, ψ_d as the state variables. The machine data given in the row vector matrix is **Syn.con**. Only the data for one machine are presented below. To add more machines, the data need to be repeated for the number of machines added. The synchronous machine data are in the form: Syn.con = [… Bus# MVA kV Freq Model# X_l R_a X_d X'_d X''_d T'_{d0} T''_{d0} X_q X'_q X''_q T'_{q0} T''_{q0} M(2H) D K_W K_P γ_P γ_Q T_{AA} $S_{1.0}$ $S_{1.2}$]; where: bus # - bus number to which the machine is connected

generator (sat_filt). See also the screenshot below in figure 4.1:

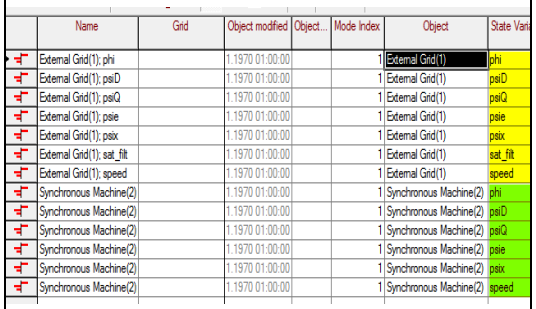

	Name	Grid	Object modified	Object...	Mode Index	Object	State Vari
	External Grid(1); phi		1.1970 01:00:00		1	External Grid(1)	phi
	External Grid(1); psiD		1.1970 01:00:00		1	External Grid(1)	psiD
	External Grid(1); psiQ		1.1970 01:00:00		1	External Grid(1)	psiQ
	External Grid(1); psie		1.1970 01:00:00		1	External Grid(1)	psie
	External Grid(1); psix		1.1970 01:00:00		1	External Grid(1)	psix
	External Grid(1); sat_filt		1.1970 01:00:00		1	External Grid(1)	sat_filt
	External Grid(1); speed		1.1970 01:00:00		1	External Grid(1)	speed
	Synchronous Machine(2)		1.1970 01:00:00		1	Synchronous Machine(2)	phi
	Synchronous Machine(2)		1.1970 01:00:00		1	Synchronous Machine(2)	psiD
	Synchronous Machine(2)		1.1970 01:00:00		1	Synchronous Machine(2)	psiQ
	Synchronous Machine(2)		1.1970 01:00:00		1	Synchronous Machine(2)	psie
	Synchronous Machine(2)		1.1970 01:00:00		1	Synchronous Machine(2)	psix
	Synchronous Machine(2)		1.1970 01:00:00		1	Synchronous Machine(2)	speed

Figure 4.1: Slack bus state variable snapshot

PV and PQ buses are set by selecting the voltage and power factor options respectively from the mode of local voltage controller section. The values for the active power, voltage and reactive power are later input in the spaces provided. The external grid is used as an infinite bus in DigSILENT for the SMIB simulations.

Under the dispatch section on the synchronous generator menu, the input mode (default, PQ, Pcosφ, Scosφ, Qcosφ, SP and SQ) is selected. The values for active power, reactive power, voltage, angle and frequency are also input under the dispatch section. Reactive and active

T''_{q0} – q-axis open-circuit subtransient time constant

d0 and d1 are the damping coefficients

$S_{1.0}$ and $S_{1.2}$ are the saturation parameters

The data can be found in Appendix B.

The machines can be modelled as slack, PV and PQ. The matrix used is **bus** and is given in the form:

Bus = […

Bus# V(pu) angle(degrees) P_{gen}(pu) Q_{gen}(pu) P_{load}(pu) Q_{load}(pu) G_{shunt}(pu) B_{shunt}(pu) A Q_{genmax} Q_{genmin} V_{rated}(kV) V_{max}(pu) V_{min}(pu)];

where:

V(pu) - voltage magnitude in pu

angle(degrees) - voltage angle in degrees

P_{gen}(pu) – generator active power in pu

Q_{gen}(pu) - generator reactive power in pu

P_{load}(pu) - load active power in pu

Q_{load}(pu) – load reactive power in pu

G_{shunt}(pu) – shunt conductance

B_{shunt}(pu) – shunt susceptance

A – bus type:

1 – swing/ slack bus

MVA – base MVA

kV – voltage rating

Freq – frequency rating

Model # - machine model number

M(2H) – mechanical starting time (2 x inertia constant)

D – damping coefficient

K_W and K_P - speed and active power feedback gain respectively

γ_P, γ_Q - percentage of active and reactive power ratios respectively. The input are either 0 or 1

T_{AA} - *d*-axis additional leakage time constant

The description for all other parameters is the same as in PST.

The data can be found in Appendix B.

The generators are modelled as slack/swing bus, PV bus and PQ machines. They are modelled separately in **SW.con** (used for slack bus in the case of a multi-machine system and used as external grid in the case of a single machine infinite bus system, as seen on the m files) for the swing/slack bus, **PV.con** for the PV bus and **PQ.con** for the PQ

	power limits, as well as active power ratings, are required. The parameters can be found in Appendix B.	2 – PV bus 3 – PQ bus Q_{genmax} – generator maximum reactive power Q_{genmin} generator minimum reactive power V_{rated}(kV) – rated voltage V_{max}(pu) – maximum voltage V_{min}(pu) – minimum voltage To model an infinite bus, the vector **ib_con** is used. This vector has the length of the number of machines installed in the system, and only the machine with a 1 represents the infinite bus while the others are represented by 0. For example, if six machines are installed in a specific system, but the 4^{th} machine on **mac_con** is to be modelled as an infinite bus, **ib_con** will be: Ib_con = [0 0 0 1 0 0];	bus. They are given as: SW.con = [… Bus# MVA kV V δ Q_{max} Q_{min} V_{max} V_{min} P_0 γ Refbus status]; where: Bus # - bus number MVA – base MVA kV – rated voltage V – voltage in pu δ – voltage angle Q_{max} – maximum reactive power in pu Q_{min} – maximum reactive power in pu V_{max} - maximum voltage in pu V_{min} – minimum voltage in pu P_0 – active power guess (supply) in pu γ – loss participation factor If Refbus and status are set to zero then it means that it is not set as the reference bus and disconnected. If set to 1, it is set as the reference bus and is connected. PV.con = [… Bus# MVA kV P_G V_0 Q_{max} Q_{min} V_{max} V_{min} γ status]

			The parameters are the same as in SW.con. PQ.con = [… Bus# MVA kV P_L Q_L V_{max} V_{min} u] The parameters are the same as in SW.con.
AVR excitation system	DigSILENT has 60 different types of AVR in its library of which 15 are IEEE-based models. The AVR used in DigSILENT is the ESAC4A, shown in figure 4.2. The shaded block represents the voltage transducer, used to filter and rectify the synchronous generator terminal voltage. The voltage transducer is given in DigSILENT as part of the AVR system, 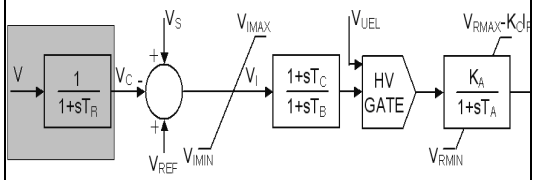 **Figure 4.2: ESAC4A AVR block diagram** where: T_r – input filter time constant T_b, T_c – voltage regulator time constants K_a – amplifier gain	PST has four types of AVR models, namely the simple AVR, DC1, DC2 and ST3. All these AVRs are IEEE models. The simple AVR is used in PST and the modelling is done with the matrix **exc_con**, described below: exc_con = [… A Mac# T_r K_a T_a T_b T_c V_{rmax} V_{rmin}]; where: A – AVR type: 0 – simple AVR 1 – DC1 2 – DC2 3 – ST3 Mac # - machine number T_r – input filter time constant T_b, T_c – voltage regulator time constants K_a – amplifier gain T_a – amplifier time constant V_{rmax}, V_{rmin} – maximum and minimum voltage	PSAT has three types of AVR models: AVR types I, II and III. All these AVRs are IEEE models; the AVR Type II is used in this dissertation as it can easily be simplified into the IEEE AC4A AVR when compared to the other types. The modelling is done with the matrix **Exc.con**, described below and shown in figure 4.4: Exc.con = [… Mac# AVRtype V_{rmax} V_{rmin} K_a T_a K_f T_f 0 T_e T_r A_e B_e status]; where: Mac # - machine number AVR type: 1 – Type I 2 – Type II 3 – Type III V_{rmax}, V_{rmin} – maximum and minimum voltage regulator output

	T_a – amplifier time constant V_{rmax}, V_{rmin} – maximum and minimum voltage regulator output V_{imax}, V_{imin} – maximum and minimum internal signal Time constants T_B and T_C are normally small and hence can be neglected [20] and K_C is set to zero. The values for other parameters can be found in Appendix B.	regulator output V_{imax}, V_{imin} – maximum and minimum internal signal **The diagram for the AVR in PST is similar to the one used in DigSILENT, figure 4.2.** The data used can be found in Appendix B.	K_a – stabilizer gain T_a – amplifier time constant T_f – stabilizer time constant K_f – amplifier gain T_e – field circuit time constant T_r – input filter time constant A_e, B_e – 1st and 2nd ceiling coefficients The coefficients A_e and B_e shown in Exc.con are the saturation coefficients, and status (0 or 1) is used to show if the AVR is disconnected or connected respectively. A_e and B_e are not used in this dissertation as they are the ceiling coefficients for the limiter, which has been eliminated in the simplification. 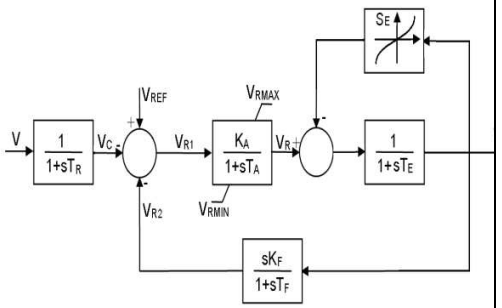 **Figure 4.3: Type II AVR block diagram** The data used can be found in Appendix B.
Power System	DigSILENT has 19 different types of PSS that	Two types of PSSs are available in PST. Type	Five types of PSSs are available in PSAT.

<table>
<tr>
<td>Stabilizer</td>
<td>can be used to damp power systems oscillation(s) on the systems' modelled. The PSS used in DigSILENT is the STAB1 shown in figure 4.3,
 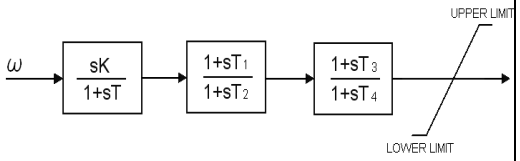

Figure 4.4: STAB1 PSS block diagram

where:
K – washout gain
T – washout time constant
T_1, T_2, T_3, T_4 – stabilizer lead-lag time constants

The parameters used can be found in A appendix B.</td>
<td>1 uses the generator speed as the input and type 2 uses the generator electric power as the input. Only type 1 is used and discussed in this dissertation. The PSS is modelled using pss_con and is given by:
pss_con = […
A Mac# K T T_1 T_2 T_3 T_4 Upper limit Lower limit];

where:
A – PSS type:
1 – speed input
2 – power input
Mac # - machine number
K – washout gain
T – washout time constant
T_1, T_2, T_3, T_4 – stabilizer lead-lag time constants

The diagram is similar to the one shown used in DigSILENT, figure 4.4.

The data for the PSS can be found in Appendix B.</td>
<td>Each type supports three types of input: the rotor speed, the generator active power and the generator terminal voltage. The PSS used in this dissertation is Type II (because it is the one that is closest to the ones used in the other software packages and does not require much simplifications as the other types require) and the input used is the speed. The PSS is modelled using Pss.con and is given by:

Pss.con = […
AVR# PSSmodel# PSSsignal V_{smax} V_{smin} K_w T_w T_1 T_2 T_3 T_4];

The PSSmodel# is the model number of the PSS (1, 2, 3, 4 or 5) that specifies the type of model used. PSS signal indicates the input signal to the PSS. Figure 4.5, depicts PSS type II which is used in this dissertation.
 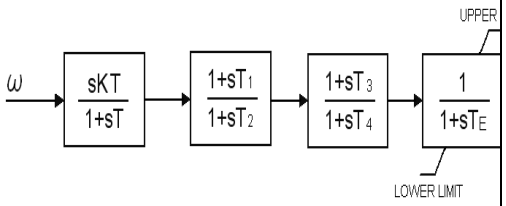

Figure4.5: Type II PSS block diagram
where:
K – washout gain</td>
</tr>
</table>

			T – washout time constant T_1, T_2, T_3, T_4 – stabilizer lead-lag time constants T_E – field circuit time constant By setting T_E to zero the block diagram now becomes similar to the one used in DigSILENT and PST. The parameters can be found in Appendix B.
AC Transmission lines	Transmission lines can be modelled using a nominal π circuit model with lumped parameters, or can be modelled as a distributed parameter line. The distributed parameter line is almost equivalent to using an infinite number of π sections with lumped resistance. This model is a single-frequency model and produces constant surge impedance [27, 28]. The transmission line model used in this dissertation is the lumped parameters model. The data input is in the following order: • Number of parallel lines • Length of line (km) • Rated voltage (kV) • Rated current (kA) • Nominal frequency (Hz)	In PST, the AC transmission line is modelled using a nominal π equivalent with lumped parameters. The modelling is done using **line** data matrix given by: Line = [… From bus (i) To bus (j) R(pu) X(pu) B(pu) tap ratio tap phase tapmax tapmin tapsize]; where: R – resistance X – reactance B – susceptance Tap ratio – transformer tap ratio Tap phase – transformer tap phase Tapmax, tapmin – maximum and minimum transformer tap ratios Tapsize – transformer tap size	PSAT models AC transmission line(s) using a nominal π equivalent with lumped parameters. The modelling is done using **Line.con** data matrix, which is given by: Line.con = [… From bus# To bus# MVA kV Freq linelength 0 R X B 0 0 I_{max} P_{max} S_{max}]; where: R – resistance X – reactance B – susceptance I_{max} – maximum current P_{max} – maximum real power S_{max} – maximum apparent power If the length of the line is specified R, X and

	• Overhead line (activated from a drop down menu) • System type (AC with 3 phases) • Parameters for negative and positive sequence per length. Ohm/km for R, X and μS/km for B. • Short-circuit location for faults under the RMS simulation menu The parameters can be found in Appendix B.	The data format above represents a single line between two buses, hence for each line added to the system the format must be repeated. The data used for the systems studied can be found in Appendix B.	B must be in Ω/km; however if the length is set to zero R, X and B must be in pu for the entire length of the line. I_{max}, P_{max} and S_{max} are the current, active power and apparent power limits for the line respectively. The value 0 denotes that those values are not applicable in this specific modelling. The data used for the systems studied can be found in Appendix B.
Transformers	Six different types of transformers can be found in the DigSILENT component library ranging from two-winding transformers, auto-transformers to three-winding transformers. Only the two-winding transformers were discussed in this dissertation. The data is input in the following order: • Number of parallel transformers • Three-phase transformer (activated from the Technology drop-down menu) • Rated power • Nominal frequency • Rated voltage (HV and LV sides) • Transformer vector group • Negative sequence impedance (% short-	Transformers are modelled as two winding transformers. Their data representation is done in **line**, where R and B are set to zero for this dissertation and only X is used.	Transformers are modelled as two winding transformers with no iron losses. Their data representation is done in **Line.con**, and is given as: Line.con = [… FromBus# ToBus# MVA kV Freq 0 Vratio R X 0] R and X are given in pu and the value 0 denotes that those values are not applicable in the specific modelling.

	circuit voltage) • X/R ratio • Phase shift The data for the transformer can be found in Appendix B.		
Loads	Loads can be modelled as static or dynamic loads in DigSILENT. However, only static loads were considered for the studies performed in this dissertation. The data for the loads are input in the following order: • P,Q balanced load (activated from the input mode drop down menu) • Active power • Reactive power • Voltage • Load scaling factor to change the load values The load data can be found in Appendix B.	Loads can be modelled as static loads (constant power, constant current, constant impedance or a combination of the three), or as dynamic loads (induction machines, voltage-dependant loads). Only static loads were considered.	Loads can be modelled as static loads (constant power, constant current, constant impedance or a combination of the three known as ZIP), or as dynamic loads (induction machines, voltage-dependant loads). Only static ZIP loads were considered, and their modelling is done in two data matrices. The first is PQ.con, described above, and the second is **Pl.con**, which models a ZIP load, shown below: Pl.con = [… Bus# MVA kV Hz g I_P P_n b I_Q Q_n u] The conductance (g), susceptance (b), active and reactive current and power (I_P, I_Q, P_n and Q_n respectively) are given in pu percentage (% pu).

4.6 Summary

The modelling of the HVDC systems in the different software packages was discussed in this chapter. Also included was the different modelling of synchronous generators in terms of the variables used by each package. The AVR and PSS diagrams were included for each package to show the difference in the input parameters used. Load modelling was also examined.

Chapter 5

Simulation Results for the Single Machine Infinite Bus System (SMIB)

5.1 Power system descriptions

This chapter presents the simulation results for the Single Machine Infinite Bus (SMIB) system. It covers the load flow, small signal and transient stability analysis for the SMIB system.

Figure 5.1 and figure 5.2 show the single line diagram for case 1 (HVAC system) and case 2 (HVAC-HVDC system) respectively. The systems are rated at 1000 MVA, 500 kV and operate at 50 Hz.

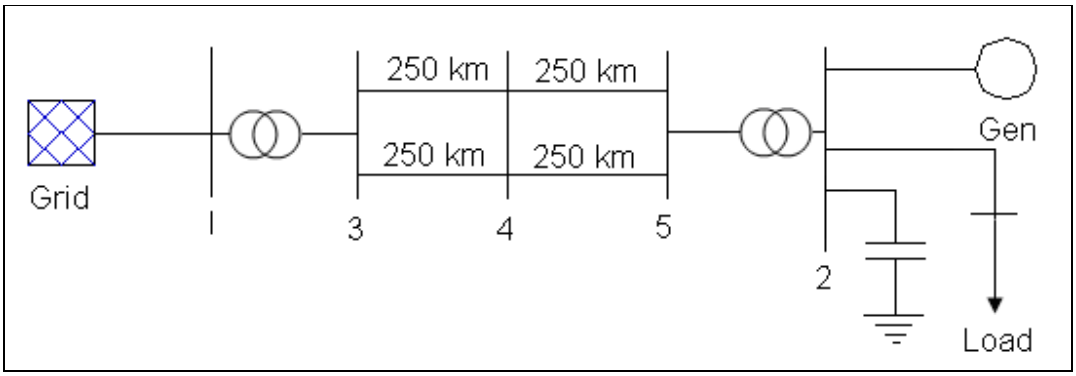

Figure 5.1: SMIB HVAC Power System Model

The HVAC system is composed of an external grid or infinite bus (Grid) with a voltage rating of 345 kV that is connected to bus 1 and a generator (Gen) with a voltage rating of 230 kV connected to bus 2. The generator was set to supply 1000 MW to the load. A load of (2000 + j 1000) Mvar is connected to bus 2; a 500 km double circuit of 500 kV HVAC transmission lines, rated at 1000 MVA, is connected between bus 3 and bus 5. These lines are modelled using the equivalent π model. Two transformers rated 1000 MVA are connected between buses 1and 3 and 2 and 5. A 700 MW capacitor was connected to bus

2 to supply some of the reactive power consumed by the load so that the generator did not supply all the reactive power that the load consumes.

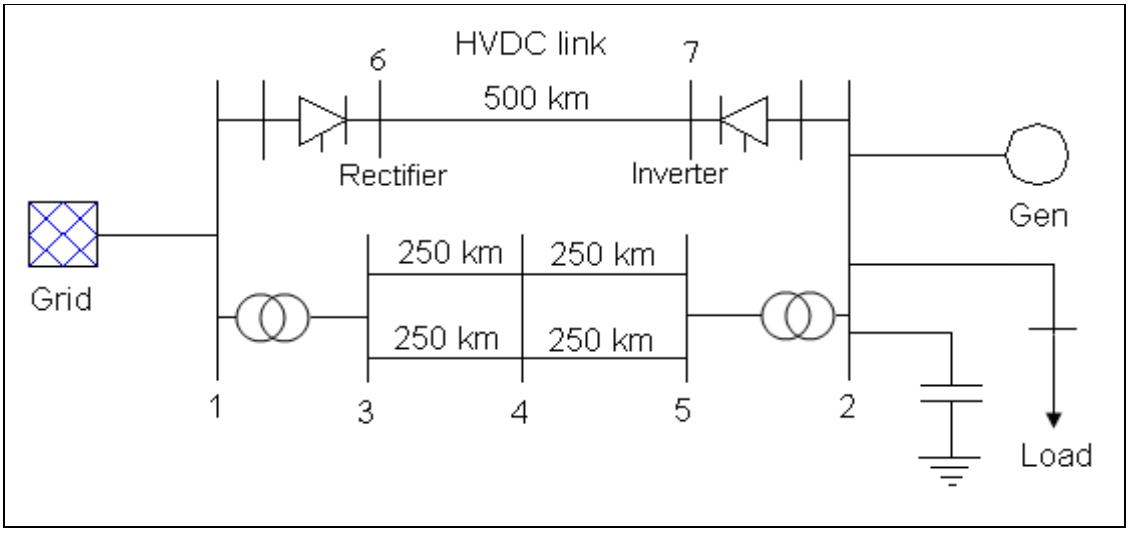

Figure 5.2: SMIB HVAC-HVDC Power System model

The HVAC-HVDC system is similar to the HVAC system; however a HVDC transmission line is added between bus 1 and bus 2 without altering the previous HVAC system. The HVDC system uses a modified CIGRE benchmark model [29]. This is a monopolar system rated 500 kV, 1000 MVA, 2 kA HVDC link with 12 pulse converters on both the rectifier and inverter sides. The HVDC line is of the same length as the HVAC lines, 500 km long. To control the power transmitted across the HVDC link, current control is used on the rectifier station, which is set to 0.5 kA and CEA is used on the inverter side. With this current setting, approximately 250 MW is expected to be transmitted through the HVDC line. No filters were used as PST and PSAT do not cater for the modelling of these components. Hence the impact of harmonics on the system as a result of the HVDC system is not discussed.

The simulations in this section are separated into three parts, namely load flow, small signal stability and transient stability.

5.2 Load flow study

The load flow results for the two cases are discussed below.

5.2.1 Case 1: HVAC

The double-circuit HVAC transmission system is used to transmit power from the external grid to the load, as the generator close to the load cannot supply all the power required by the load. Tables 5.1, 5.2 and 5.3 show the voltages and powers, both active and reactive, at all the buses in the system.

For table 5.1, the lowest voltages are observed at bus 1 (slack bus) and bus 2 (PV bus) where the voltages are fixed at 1 pu, and the highest voltage of 1.07 pu is observed at bus 4, in the middle of the HVAC transmission lines. As the load angle increases between the sending and receiving ends, the transmitted power increases accordingly and this is accompanied by a reduction of the voltage in the middle of the HVAC transmission line (bus 4) and an increase in the current. When the opposite happens, in other words, if the load angle decreases, the voltage in the middle of the HVAC line is expected to increase and the current is expected to decrease, accompanied by a reduction in the power transmitted. This can be seen in table 5.4, where the load angle decreased and the mid-point voltage increased when compared to table 5.1.

Table 5.1: Voltage magnitude and angle for HVAC SMIB system

Element	Rated voltage (kV)	Voltage (pu) and angle (deg)		
		DigSILENT	**PST**	**PSAT**
Bus 1	345	1∠0º	1∠0º	1∠0º
Bus 2	230	1∠-25.38º	1∠-25.39º	1∠-25.45º
Bus 3	500	1.05∠-5.64º	1.05∠-5.64º	1.05∠-5.65º
Bus 4	500	1.07∠-12.92º	1.07∠-12.93º	1.07∠-12.97º
Bus 5	500	1.03∠-19.83º	1.03∠-19.84º	1.03∠-19.89º

The direction of real power flow in the system is from the grid to the load; hence the negative signs seen in tables 5.2 and 5.3 mean that the power at that specific bus for a specific element is in the opposite direction. An example can be seen in table 5.2 in the column DigSILENT. Looking at the HVAC transmission, line 1 it is connected at bus 3 and bus 5. Power flows from bus 3 towards bus 5 (from grid to load), hence the positive value. At bus 5, the direction of flow of power is towards, hence the negative value at bus 5 when considering the HVAC line 1.

Table 5.2: Active power for SMIB HVAC system

Element	Bus	Active power (MW)		
		DigSILENT	PST	PSAT
Ext Grid	1	1027.51	1027.6	1030.5
Gen	2	1000	1000	1000
HVAC Line 1	3	513.75	513.8	515.3
	5	-500	-500	-500
HVAC Line 2	3	513.75	513.8	515.3
	5	-500	-500	-500
Load	2	2000	2000	2000
Cap	2	0	0	0

Table 5.3: Reactive power for SMIB HVAC system

Element	Bus	Reactive power (Mvar)		
		DigSILENT	PST	PSAT
Ext Grid	1	-396.93	-400.8	-401.68
Gen	2	14.21	14.8	13.55
HVAC Line 1	3	-264.6	-264.5	-267.45
	5	202.4	201.9	198.39
HVAC Line 2	3	-264.6	-264.5	-267.45
	5	202.4	201.9	198.39
Load	2	1000	1000	1000
Cap	2	700	700	700

The external grid supplies approximately 1027 MW in DigSILENT and PST and about 1030 MW in PSAT. In DigSILENT and PST, each of the HVAC transmission lines transmits about 513 MW from the external grid to the load located at bus 2. In PSAT about 515 MW was transmitted from the external grid to the load located at bus 2. Each HVAC line has an active power loss of approximately 1.65 %. Because the HVAC lines transmit power below their SIL (1000 MW), the reactive power generated by the capacitive reactance of the lines is much higher than the reactive power absorbed by the inductive reactance of the lines, hence the lines supply reactive power at both ends.

5.2.2 Case 2: HVAC-HVDC system

In this case, the HVDC system is used in parallel with the HVAC system and the power transfer across the systems is divided equally between the HVAC and HVDC transmission lines, in other words, 50 % of the total power is transmitted in each line. The voltage and power of the system are given in tables 5.4, 5.5 and 5.6.

Table 5.4: Voltage magnitude and angle for SMIB HVAC-HVDC system

Element	Rated voltage (kV)	Voltage (pu) and angle (deg)		
		DigSILENT	**PST**	**PSAT**
Bus 1	345	1∠0º	1∠0º	1∠0º
Bus 2	230	1∠-12.35º	1∠-12.39º	1∠-12.39º
Bus 3	500	1.06∠-2.77º	1.06∠-2.77º	1.06∠-2.77º
Bus 4	500	1.1∠-6.4º	1.1∠-6.4º	1.1∠-6.45º
Bus 5	500	1.06∠-9.61º	1.06∠-9.65º	1.06∠-9.65º
Bus 6	500	1.06	1.06	*
Bus 7	500	1.03	1.03	*

* Not displayed in PSAT

According table 5.4, the lowest voltage is observed at bus 1 (slack bus) and bus 2 (PV bus), where the voltages are fixed at 1 pu. The highest voltage in the system of 1.1 pu is at bus 4.

The direction of power flow in the system is from the grid to the load. The negative signs, in table 5.5 and table 5.6, show that the power at the bus, for a specific element, is flowing in the opposite direction (from the load to the grid).

Table 5.5: Active power for HVAC-HVDC SMIB system

Element	Bus	Active power (MW)		
		DigSILENT	**PST**	**PSAT**
Ext Grid	1	1022.72	1022.9	1022.9
Gen	2	1000	1000	1000
HVAC Line 1	3	255	255.8	255.9
	5	-250.78	-251.5	-251.22
HVAC Line 2	3	255	255.8	255.9
	5	-251.78	-251.5	-251.22
HVDC Line	6	511.69	511	511.04
	7	-498.47	-496.9	-497.52
Rectifier	1	511.69	511	511.04
Inverter	2	498.47	496.9	497.52
Load	2	2000	2000	2000

Table 5.5 shows that the external grid supplies approximately 1022 MW to the system and close to 511 MW is transmitted through the HVDC line with an active power loss of approximately 1 %. Each HVAC line transmits close to 251 MW to the load at bus 2 and experiences real power losses of approximately 1.5 % of the power.

Table 5.6: Reactive power for HVAC-HVDC SMIB system

Element	Bus	Reactive power (Mvar)		
		DigSILENT	PST	PSAT
Ext Grid	1	-303.4	-306.5	-307.8
Gen	2	55.16	50.77	48.05
HVAC Line 1	3	-304.64	-304.4	-306.04
	5	-273.53	-273.1	-271.54
HVAC Line 2	3	-304.64	-304.4	-306.04
	5	-273.53	-273.1	-271.54
HVDC Line	6	0	0	0
	7	0	0	0
Rectifier	1	239.28	235.7	236.53
Inverter	2	-242.32	-241.1	-235.77
Load	2	1000	1000	1000
Cap	2	700	700	700

From table 5.6, it can be seen that the HVAC lines supply reactive power, as they transmit active power below their SIL. The HVDC line does not produce any reactive power.

5.3 Small signal stability

The results shown in this section are for the small signal stability analysis of the SMIB system. Three control strategies are considered:

1. Manual control (no AVR and no PSS)
2. Control with AVR only
3. Control with AVR and PSS

For the simulation results presented in this dissertation, the synchronous machine is modelled using the 6^{th} order model with no turbine governor; hence six modes are expected in the results for the small signal stability analysis. The AVR and PSS used have been described in sections 3.3 and 3.4., and in the different software packages they add a different number of states as seen in Appendix C and Appendix D. This is because each software package models the grid differently, (see table C1 in Appendix C). The parameters for the AVR and PSS can be found in Appendix B. For the AVR and PSS used, it depends on the block diagram used in each software package. Taking DigSILENT as an example, for the AVR, one has to set Tb and Tc to zero and this gives an additional zero state.

HVDC links interact with the torsional modes of turbine generators and can significantly alter the stability of these modes of oscillation by providing negative damping - this interaction is a function of the HVDC control action. Current control in a DC system is the parameter that contributes to the negative damping of rotor oscillations. The HVDC converter appears as a constant power load to the AC transmission system, at least within the bandwidth of the current controller [30 - 35].

HVDC systems were not designed to damp electromechanical oscillations, but if HVDC modulation control is implemented correctly, the damping of electromechanical oscillations can be increased [1, 36]. No HVDC modulation control was used in this dissertation.

Modulation control can be implemented in DigSILENT; however DSL is needed to make use of this property. In PST, modulation control is not available but the user has the ability to use feedback controllers for HVDC systems. PSAT has no HVDC modulation control available or feedback controllers for HVDC systems. PSAT does not display the damping ratio for the modes; hence they have to be calculated manually.

5.3.1 Case 1: HVAC system

Tables 5.7, 5.8 and 5.9 show the eigenvalue results for each of the software tools. For tables 5.8 and 5.9, the values presented in bold are the percentage changes observed with respect to the values given in the previous table, and the equation used to calculate the percentage changes is given as:

$$\%\Delta f = \left(\frac{f - f_0}{f_0} \right) \times 100\% \tag{5.1}$$

$$\%\Delta \zeta = \left(\frac{\zeta - \zeta_0}{\zeta_0} \right) \times 100\% \tag{5.2}$$

where:

Δf , $\Delta\zeta$ - change in frequency and damping ratio respectively

f , ζ - current/actual values of frequency and damping ratio respectively

f_0 , ζ_0 - previous values of frequency and damping ratio respectively

The complete tables can be seen in Appendix C.

- **System with no AVR and no PSS**

The generator is modelled using a 6th order model without a speed governor.

Table 5.7: SMIB HVAC with no AVR and no PSS

Mode	Eigenvalue, frequency, damping ratio		
	DigSILENT	PST	PSAT
Local mode	-0.4394 ± 6.0672 f = 0.965; ζ = 0.0723	-0.4383 ± j6.2591 f = 0.996; ζ = 0.0699	-0.7283 ± j6.3054 f = 1.0035; ζ = 0.1147

- **System with AVR only**

The AVR used is the AC4A excitation system model. The parameters used for this model are the amplifier gain (K_a), amplifier time constant (T_a) and input filter time constant (T_r).

Table 5.8: SMIB HVAC with AVR only

Mode	Eigenvalue, frequency, damping ratio		
	DigSILENT	PST	PSAT
Local mode	-0.6734 ± j5.6603 f = 0.9; **-6.74 %** ζ = 0.1181; **63.47 %**	-0.78 ± j5.87 f = 0.93; **-6.63 %** ζ = 0.13; **85.98 %**	-0.9385 ± j6.1026 f = 0.9713; **-3.21 %** ζ = 0.152; **32.52 %**

- **System with AVR and PSS**

The AVR used remains the same and a PSS is added to the system. The parameters for this PSS are the washout gain (K), washout time constant (T) and the lead-lag time constant (T_1, T_2, T_3 and T_4). The input for the PSS is the rotor speed (ω).

Table 5.9: SMIB HVAC with AVR and PSS

Mode	Eigenvalue, frequency, damping ratio		
	DigSILENT	PST	PSAT
1 &2	-1.563 ± j5.1205 f = 0.8149; **-9.45 %** ζ = 0.2919; **147.16 %**	-1.7813 ± j5.2425 f = 0.8344; **-10.23 %** ζ = 0.3217; **147.46 %**	-1.3942 ± j5.8975 f = 0.9386; **-3.36 %** ζ = 0.2301; **51.38 %**

When no AVR or PSS is used, the system is stable, as shown in table 5.7. When only the AVR is used the system remains stable and shows improvement as the damping ratio increases (63.47 % in DigSILENT, 85.98 % in PST and 32.52 % in PSAT) and the frequency of oscillation decreases (6.74 % in DigSILENT, 6.63 % in PST and 3.21 % in PSAT). When AVR and PSS are incorporated in the generator, the system is stable. The performance of the system improves further, as seen in table 5.9; the damping ratio increases (147.16 % in DigSILENT, 147.46 % in PST and 51.38 % in PSAT) and the frequency decreases (9.45 % in DigSILENT, 10.23 % in PST and 3.36 % in PSAT). PSAT shows the smallest improvement for both for the damping ratio and the frequency of oscillation of the local mode. Parameters T_e, K_f and T_f, in PSAT are set to zero to simplify the model and make it similar to the model used in DigSILENT and PST. Note that if the direction of power flow was from the generator to the grid, the AVR would add negative damping, agreeing with the example shown in Kundur [1]. But because the direction of power flow is from the grid to the load (which is in the same location as the generator) the AVR adds positive damping to the system and not negative damping as observed in the literature.

5.3.2 Case 2: HVAC-HVDC system

Tables 5.10, 5.11 and 5.12 show the eigenvalue results for the local model HVAC-HVDC system for all the software packages for the different scenarios. For tables 5.11 and 5.12, the values presented in bold are the percentage changes observed with respect to the values given in the previous scenario. The conditions remain the same as in case 1. Complete tables can be found in Appendix C.

- **System with no AVR and no PSS**

Table 5.10: SMIB HVAC-HVDC system with no AVR and no PSS

Mode	Eigenvalue ,frequency, damping ratio		
	DigSILENT	PST	PSAT
Local area	-0.3009 ± j6.4045 f = 1.0193; ζ = 0.0469	-0.4849 ± j6.7043 f = 1.067; ζ = 0.0721	-0.7263 ± j6.4062 f = 1.0196; ζ = 0.1126

- **System with AVR only**

Table 5.11: SMIB HVAC-HVDC system with AVR only

Mode	Eigenvalue, frequency, damping ratio		
	DigSILENT	PST	PSAT
Local area	-0.6414 ± j5.6508 f = 0.899; **-11.8 %** ζ = 0.1128; **140.51 %**	-0.9900 ± j6.0500 f = 0.9600; **-10.03 %** ζ = 0.1600; **121.91 %**	-0.9058 ± j6.2434 f = 0.9937; **-2.54 %** ζ = 0.1436; **27.53 %**

- **System with AVR and PSS**

Table 5.12: SMIB HVAC-HVDC system with AVR and PSS

Mode	Eigenvalue, frequency, damping ratio		
	DigSILENT	PST	PSAT
Local area	-1.7653 ± j4.3767 f = 0.6968; **-29.02 %** ζ = 0.3741; **231.65 %**	-2.7207 ± j5.0313 f = 0.8008; **-19.88 %** ζ = 0.4757; **197.31 %**	-1.3664 ± j6.0381 f = 0.9609; **-3.41 %** ζ = 0.2207; **53.69 %**

From table 5.10 it can be seen that the system is stable when no AVR or PSS is used. From table 5.11, it can be seen that when the AVR is added to the system, the damping ratio increases (140.51 % in DigSILENT, 121.91 % in PST and 27.53 % in PSAT) and the frequency of oscillation decreases (11.8 % in DigSILENT, 10.03 % in PST and 2.54 % in PSAT). When the AVR and PSS are used in the system, the system performance improves by increasing the damping ratio of the system (231.65 % in DigSILENT, 197.31 % in PST and 53.69 % in PSAT) and decreasing the frequency of oscillation on the local area mode (29.02 % in DigSILENT, 19.88 % in PST and 3.41 % in PSAT). PSAT shows the smallest improvement in system performance when compared to the other packages.

Comparing the HVAC system to the HVAC-HVDC system, when no AVR or PSS is used, the frequency of oscillation of the local mode is higher in the HVAC-HVDC system

and the damping ratio is smaller in the HVAC-HVDC system. However, in PST and PSAT, the damping ratios are almost the same for the HVAC and HVAC-HVDC systems. When only the AVR is used, the frequency of oscillations has higher values on the HVAC-HVDC system and the damping ratio is higher in the HVAC system, with the exception of PST. When the AVR and PSS are incorporated into the systems, the HVAC system has lower frequency values on the HVAC-HVDC system and the damping ratio has higher values in the HVAC-HVDC systems with the exception of PSAT.

Literature [31, 32] suggests that HVDC links produce negative dumping at generators and this phenomenon can be observed when the HVAC system is compared to the HVAC-HVDC system. DigSILENT is the only package among the three where the damping ratio is smaller on the HVAC-HVDC system for the three different scenarios, namely when no AVR or PSS is used, when only the AVR is used and when both the AVR and PSS are used.

5.4 Transient stability

A three-phase fault is applied at one of the lines between bus 3 and bus 4. This fault is applied at t = 1s, lasts for 50 ms and is cleared by removing the faulted line. The effects of this fault on the HVAC and HVAC-HVDC systems are presented in this section. The results presented here are for the systems that incorporate the AVR and PSS. The results for the systems that do not incorporate these controls systems can be found in Appendix C.

In a system where HVDC transmission lines are operated in parallel with HVAC transmission lines, the system is prone to both transient and voltage instability and the risk increases during disturbances [37, 38]

5.4.1 Case: HVAC system with AVR and PSS

The simulation results obtained for this system are shown in figures 5.3 – 5.11. The generator terminal voltage on the different packages is shown in figures 5.3 – 5.5; the rotor angle results are shown in figures 5.6 – 5.8 and the active power results are shown in figures 5.9-5.11.

- **Generator terminal voltage**

Before the fault is applied, the terminal voltage of the generator is 1 pu, which is confirmed by the load flow. The voltage response of the machine in DigSILENT is displayed in figure 5.3. After the fault has been applied, the voltage reaches a minimum of 0.67 pu, a maximum of 1.07 pu and settles to 1 pu in about 4 seconds. The voltage response for PST is shown in figure 5.4, where the voltage reaches a minimum of 0.66 pu, a maximum of 1.12 pu and settles to 1 pu within 4 seconds. The voltage response for PSAT is shown in figure 5.5, after the fault is applied, the voltage reaches a minimum of 0.77 pu, a maximum of 1.03 pu and settles to 1 pu after about 3.5 seconds at 1 pu.

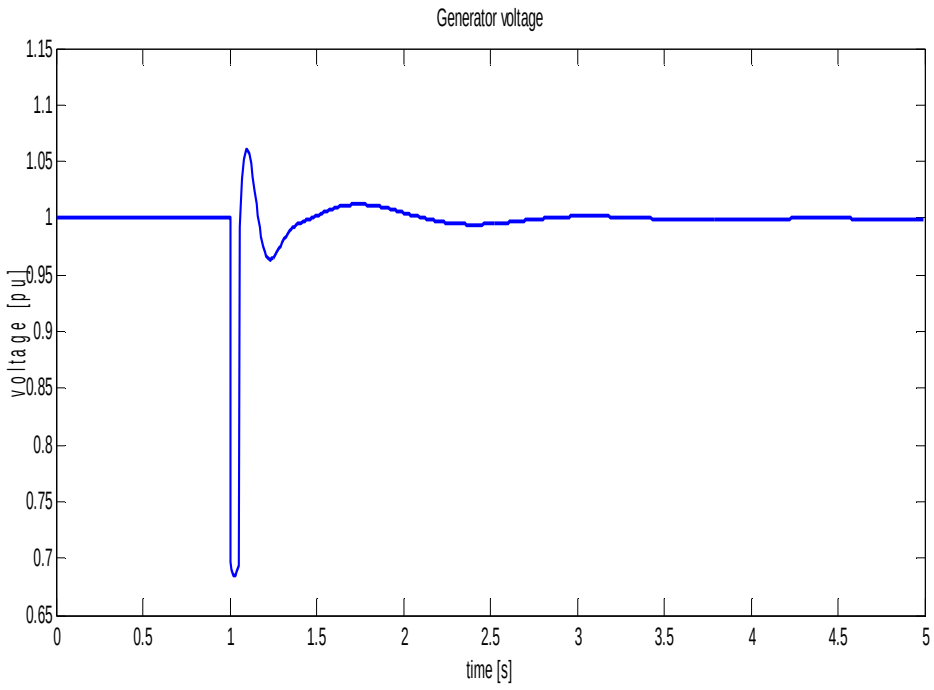

Figure 5.3: Voltage response in DigSILENT

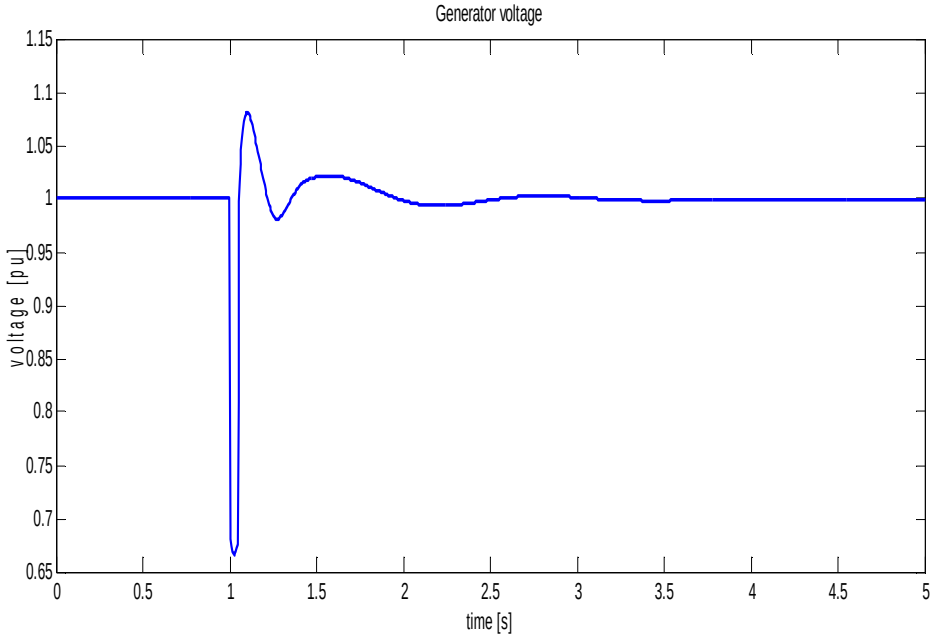

Figure 5.4: Voltage response in PST

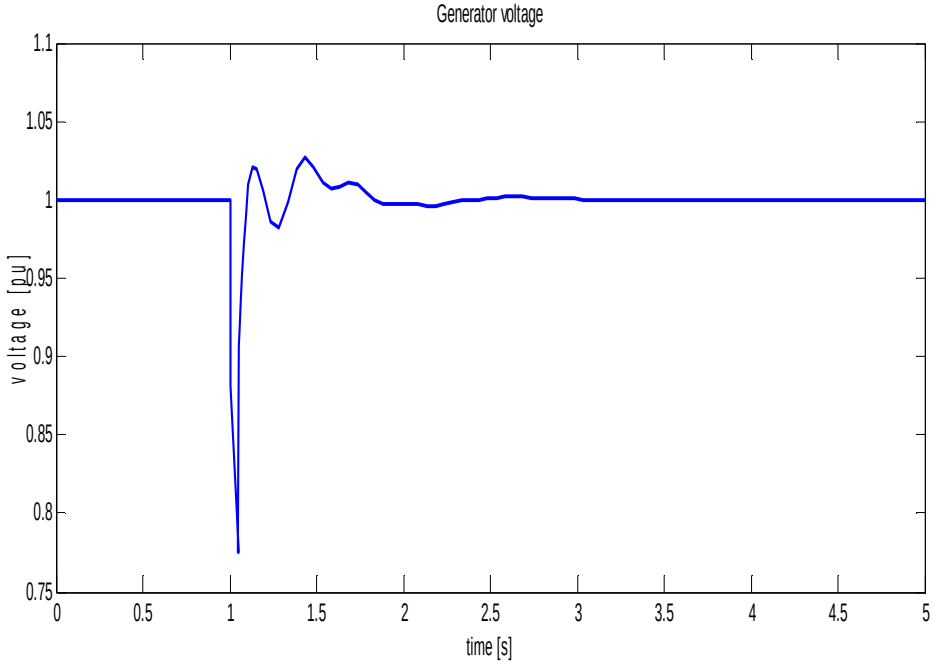

Figure 5.5: Voltage response in PSAT

- **Generator rotor angle**

The rotor angle response in DigSILENT is shown in figure 5.6. After the fault has been applied the rotor angle reduced from -75º to -88º and after the fault had been cleared it stabilized and settled at -80º after 5 seconds. The rotor angle in PST, shown in figure 5.7, reduced from 11º to 0º when the fault was applied and once it was cleared it reached a maximum of approximately 12.5º before settling at a new rotor angle of 12º within 4.5 seconds. Figure 5.8 shows the response of the rotor angle when the fault was applied in PSAT. The rotor angle reduced from 14º to approximately 8º and settled at the pre-fault value within 4 seconds. The response in DigSILENT and PST was as expected as the absolute value of the rotor angle increased after the fault had been cleared and the rotor angle settled at a higher value than the pre-fault value.

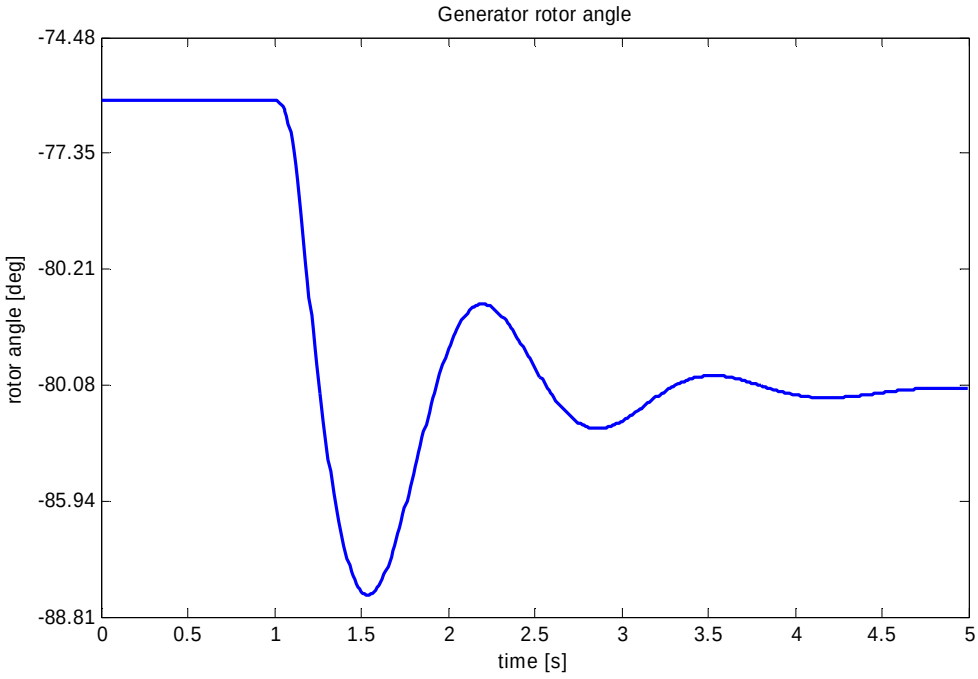

Figure 5.6: Rotor angle response in DigSILENT

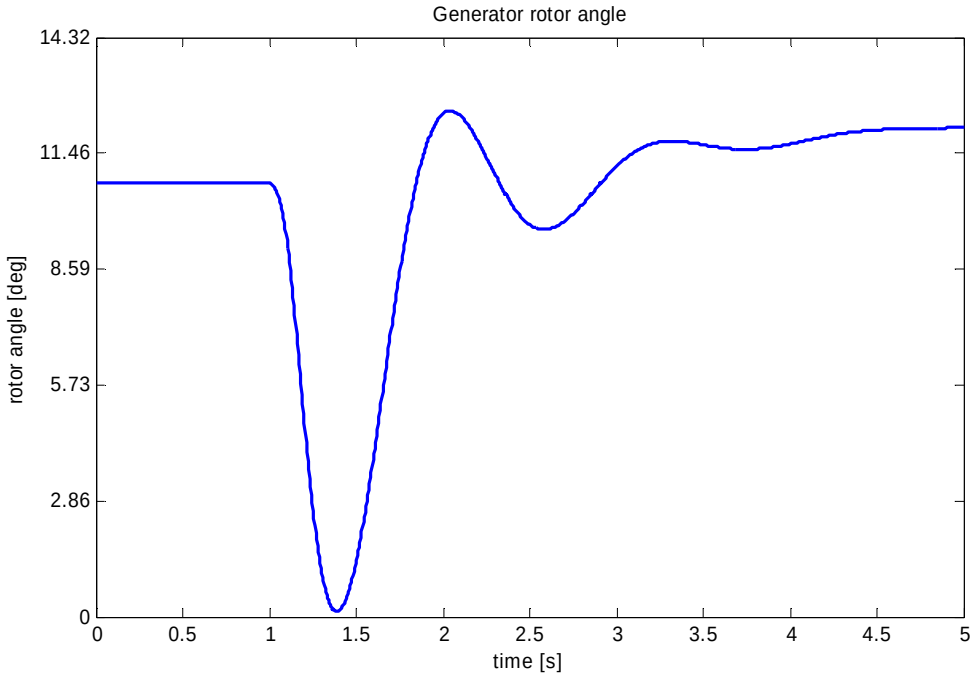

Figure 5.7: Rotor angle response in PST

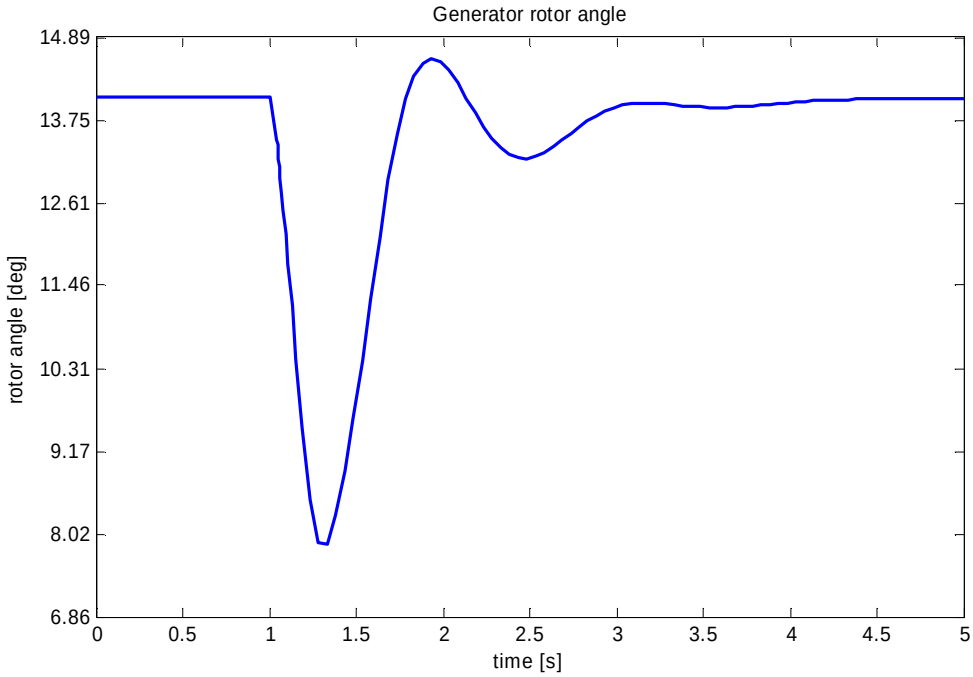

Figure 5.8: Rotor angle response in PSAT

- **Generator active power**

In figure 5.9 - 5.11, the active power obtained in DigSILENT, PST and PSAT is shown. The active power response in DigSILENT is shown in figure 5.9, where the active power reaches a maximum of 1.5 pu, a minimum of 0.8 pu and settles after 4 seconds. The response in PST is shown in figure 5.10, where it reaches a maximum of 1.56 pu, a minimum of 0.66 pu and settles after 4 seconds. The response in PSAT is shown in figure 5.11, where it reaches a maximum of 1.92 pu, a minimum of 0.68 pu and settles after 3.5 seconds. All software packages perform as expected, since the generator increases its supply to the load in response to the fault. However PSAT gives higher overshoot values when compared to the other software packages.

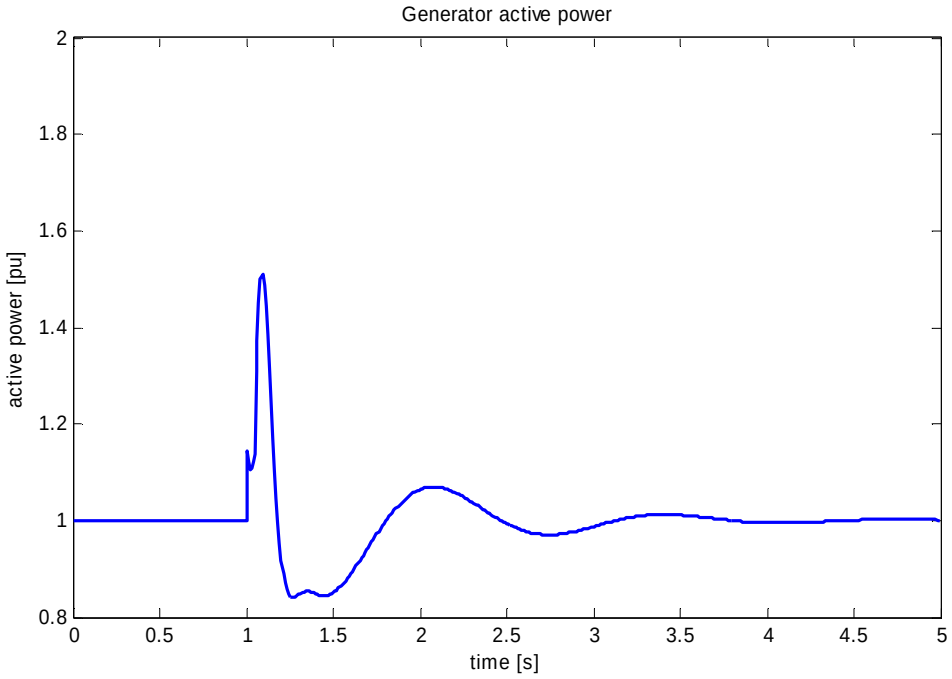

Figure 5.9: Active power response in DigSILENT

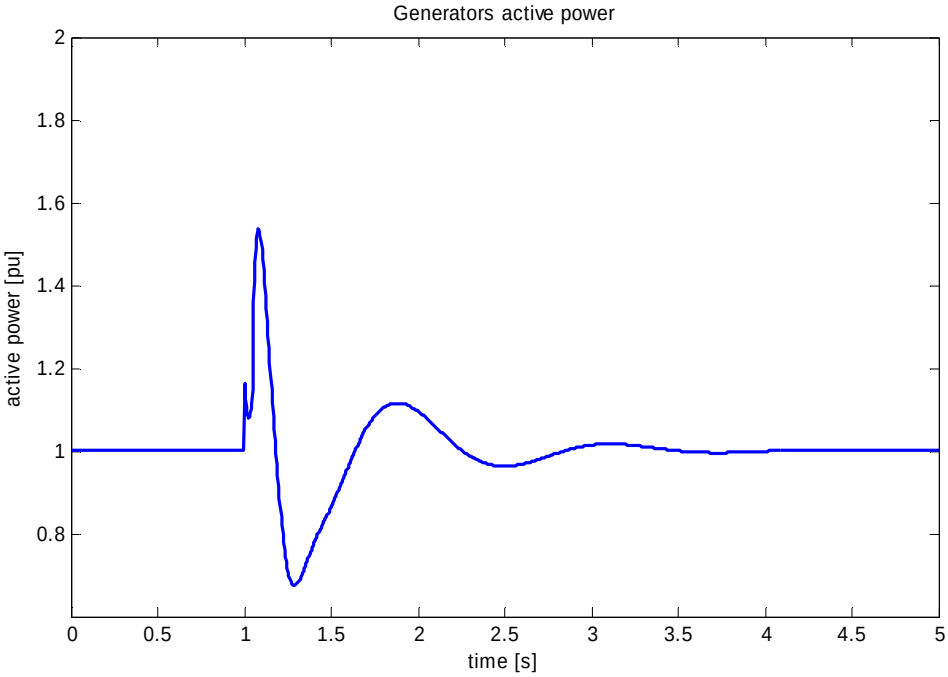

Figure 5.10: Active power response in PST

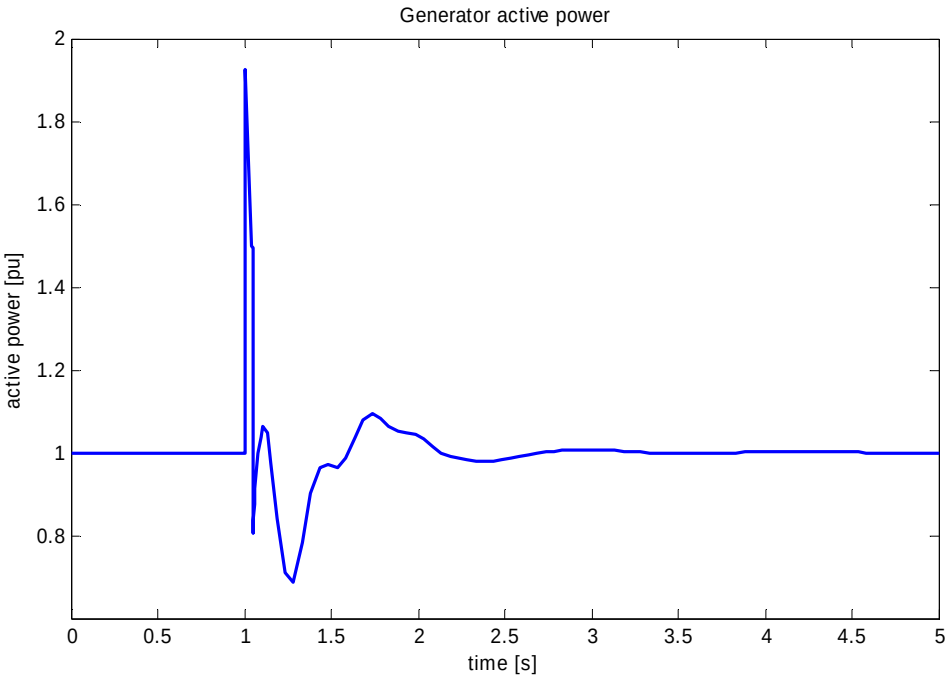

Figure 5.11: Active power response in PSAT

5.4.2 Case 2: HVAC-HVDC system with AVR and PSS

The simulation results obtained for this system are shown in figures 5.12 – 5.20. The generators' terminal voltages on the different packages are shown from figures 5.12 – 5.14; the rotor angle results are shown in figures 5.15 – 5.17 and the active power is shown in figures 5.18-5.20.

- **Generator's terminal voltage**

  The terminal voltage for the generator in DigSILENT (figure 5.12), reaches a minimum of 0.69 pu during the fault and when the fault is cleared it reaches a maximum of 1.07 pu. The voltage stabilizes in less than 3 seconds. As shown in figure 5.13, the terminal voltage of the generator dips in PST from 1 pu to 0.61 pu during the fault and after the fault has been cleared the voltage reaches a maximum of approximately 1.14 pu before stabilizing to 1 pu after only 7 seconds. In figure 5.14, the voltage response of the generator in PSAT is displayed. During the fault the terminal voltage reduces to 0.76 pu and when the fault is cleared reaches a maximum of 1.07 pu before it settles at approximately 3 seconds. When compared to the HVAC system, the HVAC-HVDC system has more oscillations and these observation supports what is discussed in [37, 38], where it is stated that in a system where HVDC transmission lines are operated in parallel with HVAC transmission lines, the system is prone to both transient and voltage instability and the risk increases during disturbances. This is because when the HVDC scheme is fitted with classical constant power controls, it deprives the parallel AC system from much needed synchronizing torque during disturbances. This is visible in PST for the voltage and active power responses.

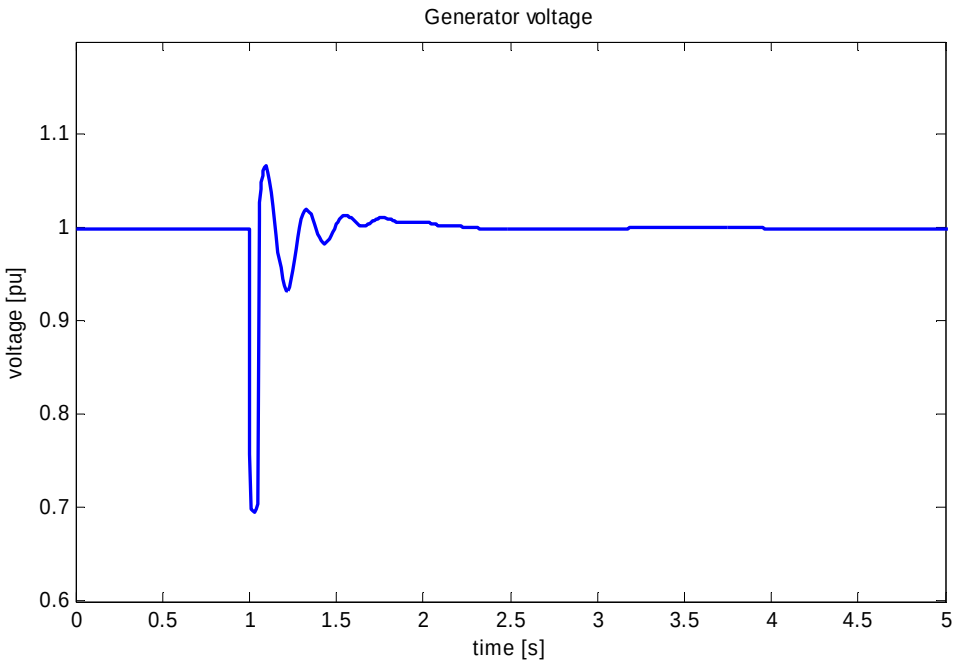

Figure 5.12: Voltage response in DigSILENT

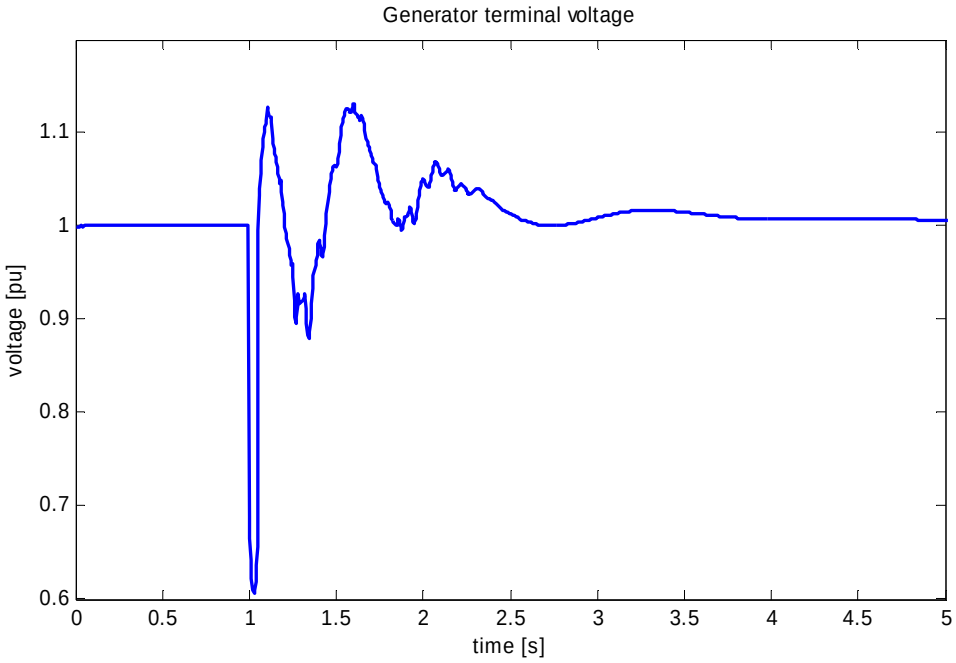

Figure 5.13: Voltage response in PST

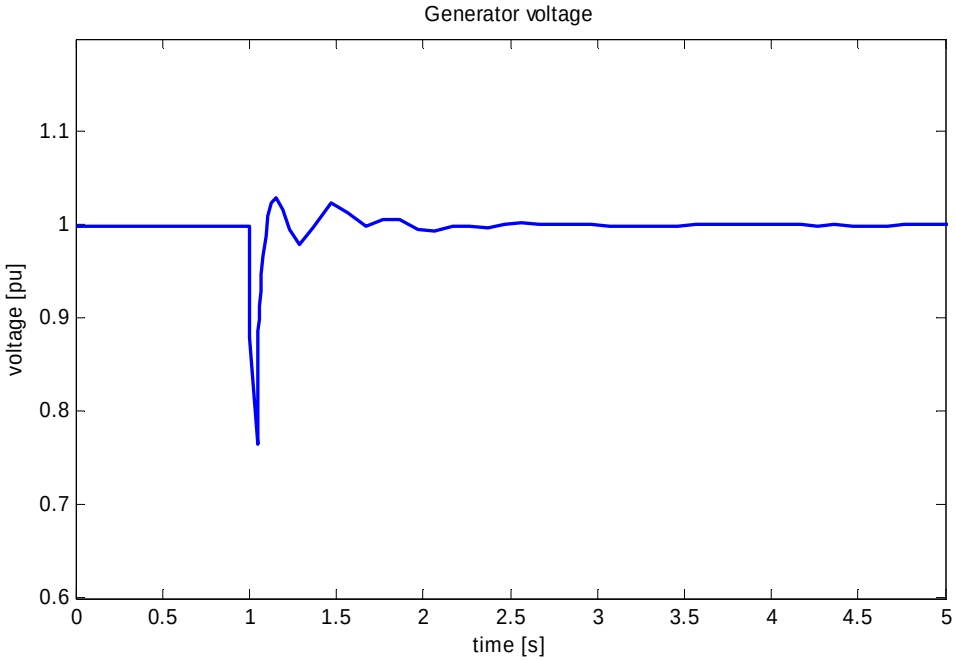

Figure 5.14: Voltage response in PSAT

- **Generator rotor angle**

Figures 5.15, 5.16 and 5.17 show the rotor angle response of the generator in DigSILENT, PST and PSAT respectively. In DigSILENT the rotor angle reduces from -71º to 85º and then increases to -79º before settling to -80º in 4 seconds. In PST, the rotor angle reduces from approximately 16º once the fault is applied to approximately -36º and settles to 19 º in less than 10 seconds. The rotor angle response in PSAT shows that the angle reduces during the fault from the pre-fault value of approximately 19º to 14.3º and stabilizes at the initial value in 6 seconds. Only the responses seen in DigSILENT and PST agree the with expectation that the absolute value of the rotor angle must increase from the pre-fault value and settle at a higher post-fault value when the fault is applied and a line is removed.

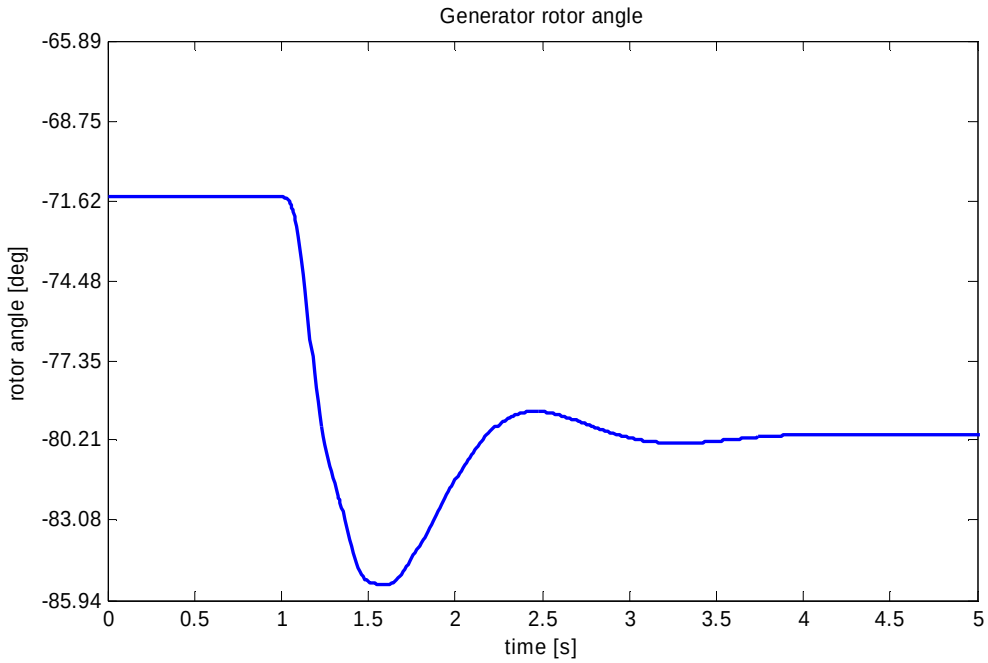

Figure 5.15: DigSILENT rotor angle response

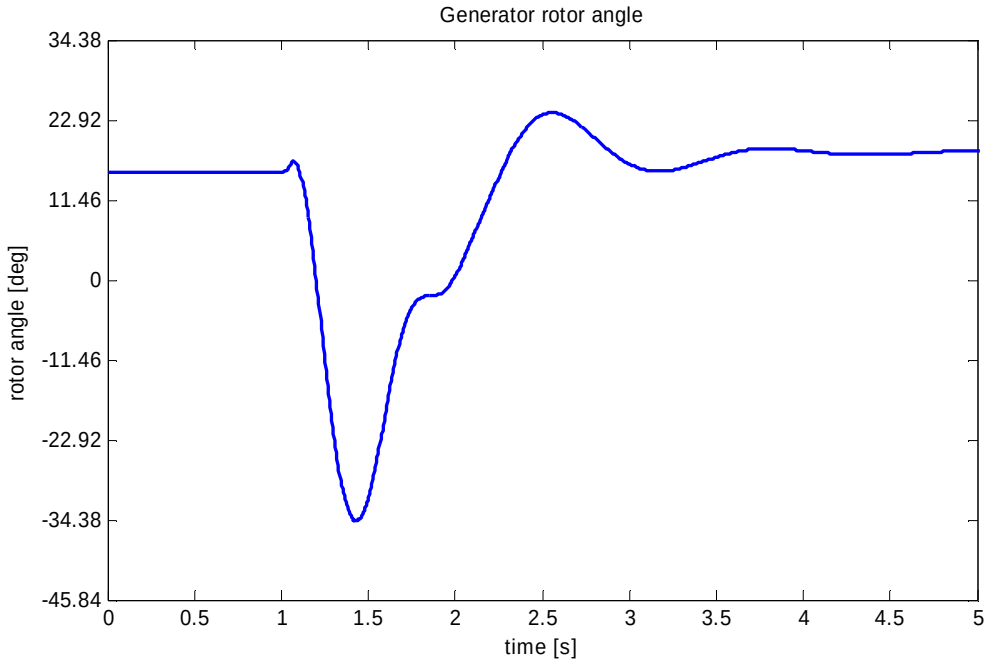

Figure 5.16: PST rotor angle response

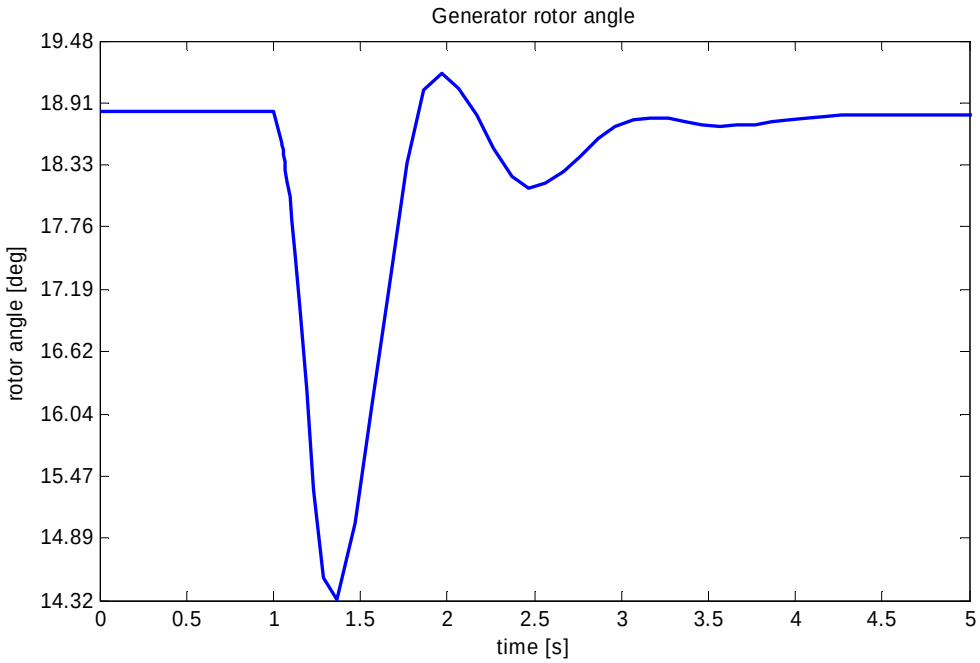

Figure 5.17: PSAT rotor angle response

- **Generator active power**

Figures 5.18, 5.19 and 5.20 show the effect of the fault on the generator's active power output for DigSILENT, PST and PSAT respectively. In DigSILENT the active power increases to a maximum of 1.6 pu after the fault is applied and a minimum of 0.48 pu before stabilizing at 2.5 seconds. In PST, during the fault the generator's active power reaches a minimum of -2 pu and once the fault is cleared the active power reaches a maximum of 4.8 pu before settling in approximately 4 seconds. In addition there are some oscillations up to about 2.5 seconds. The behaviour seen in PST is not expected, as the active power is supposed to increase and not decrease in order to cater for the load requirements. This behaviour may be due to the interaction of the HVAC system with the HVDC system for this specific software package for the single machine infinite bus system. In PSAT, the active power reaches a maximum of 1.4 pu and a minimum of 0.8 pu. The system settles in less than 7 seconds. The HVAC-HVDC system has larger overshoots when compared to the HVAC system.

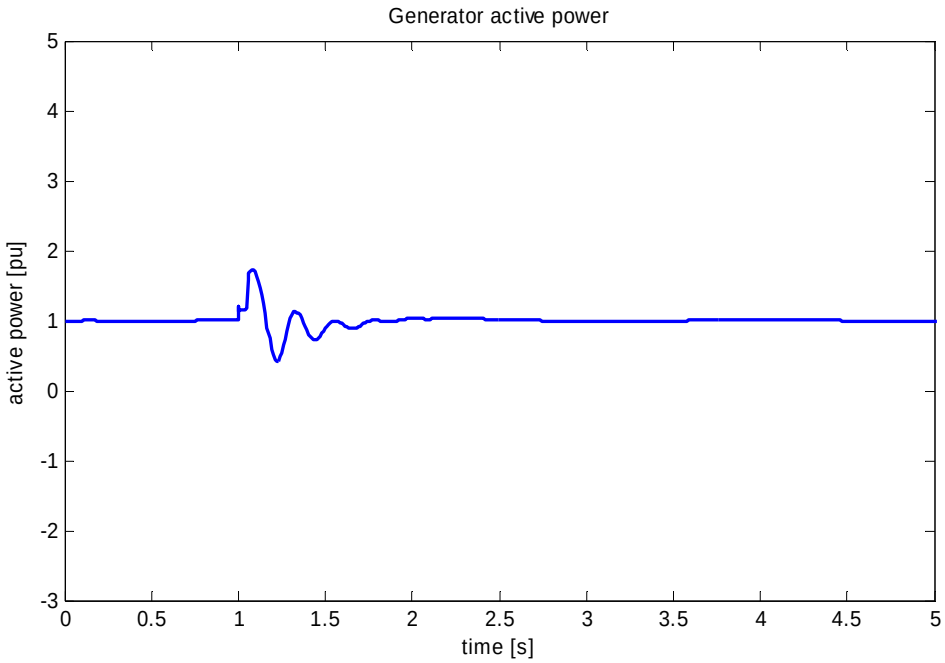

Figure 5.18: DigSILENT active power response

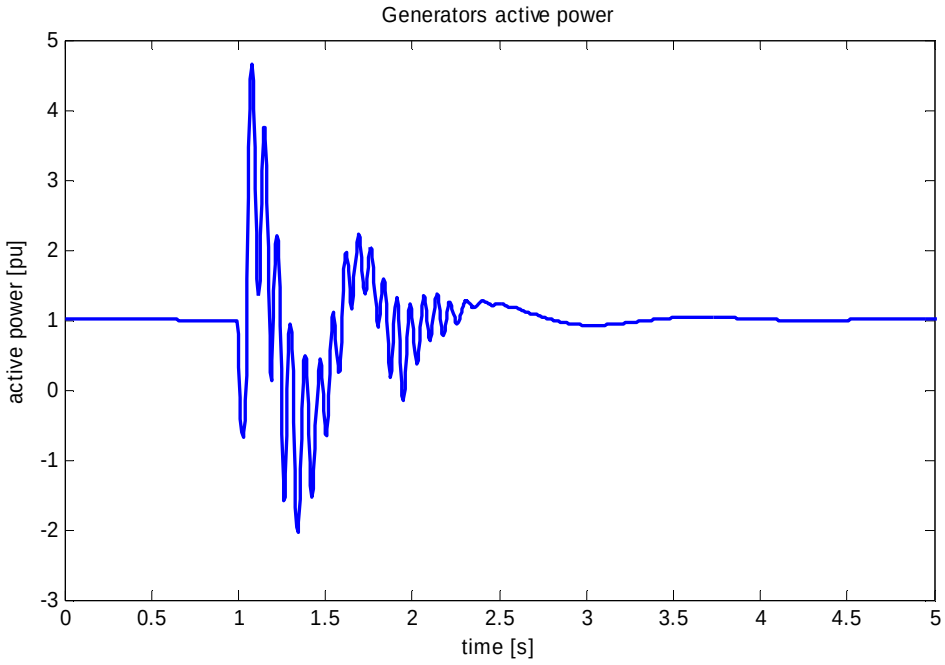

Figure 5.19: PST active power response

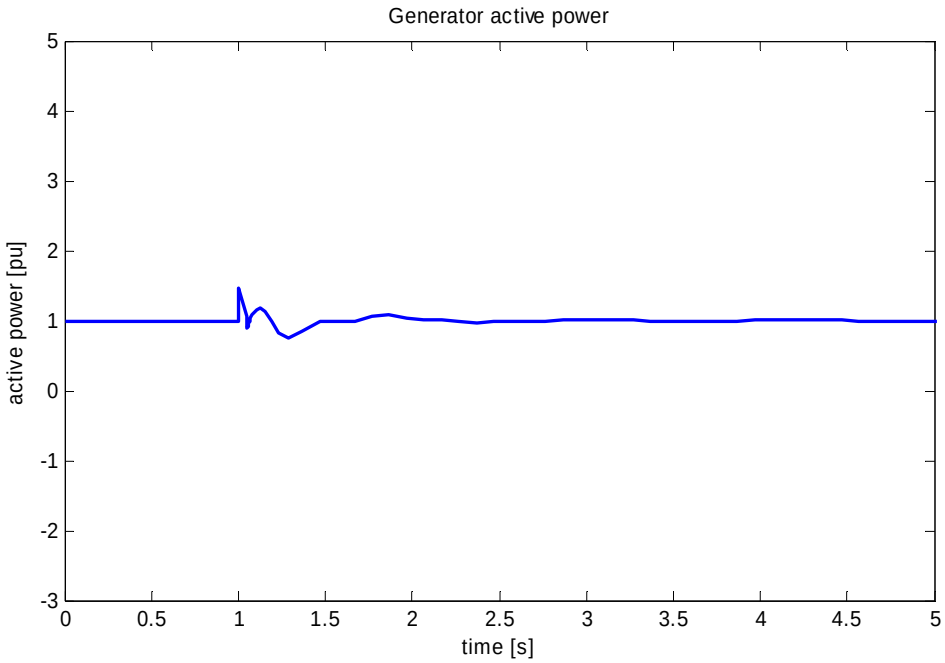

Figure 5.20: PSAT active power response

5.5 Summary

All packages obtained similar results for the load flow, for both the HVAC system and the HVAC-HVDC system. When the load flow was performed on the HVAC system, it was found that the voltages ranged from 1 to 1.09 pu across the buses on the system, with the highest voltage encountered at bus 4 in the middle of the HVAC transmission lines. Close to 500 MW was transmitted through the HVAC lines. Each line had a loss of approximately 4.2 MW, corresponding to 1.65% of the power transmitted through each line. The active and reactive power across the packages differed slightly owing to modelling differences discussed in chapter 4. The HVAC-HVDC system transmitted the same amount of active power with each system, HVAC and HVDC, transmitting 50% of the power. It was observed that the voltages ranged from 1 to 1.1 pu, with the highest voltage at bus 4, in the middle of the HVAC transmission lines. The HVDC buses were operating at 1.04 pu and 1.03 pu for the rectifier and inverter stations respectively. The HVDC system had a power loss of approximately 1% while the HVAC lines had a combined loss of 1.5%. The power being absorbed by the external grid reduced when

compared to the HVAC system. This is due to the fact that the converter stations consumed some of the power on the conversion process of AC to DC.

When small-signal analysis was performed on the HVAC system it was observed that the system was stable for all scenarios (with no AVR and no PSS, with AVR only and with AVR and PSS) across all packages. The damping of the local area model improved when the AVR was incorporated and further improvement was obtained when the AVR and PSS were used on the generator. However, the changes in damping ratios observed in PSAT were smaller when compared to DigSILENT and PST. The HVAC-HVDC system was found to be stable for all scenarios and it behaved in a similar manner when compared to the HVAC system. When the AVR was incorporated, the damping of the system as well as the frequency improved. When the AVR and PSS were used, the damping and frequency improved further. The HVAC-HVDC system improved by a higher percentage if compared to the HVAC system. For both the HVAC and the HVAC-HVDC systems, PSAT gave higher values for the damping ratios and frequency of oscillations than those observed in DigSILENT and PST.

A three-phase fault was applied at bus 3 on the HVAC and HVAC-HVDC systems. The HVAC system remained stable across all three packages, with DigSILENT and PST having similar voltage and active power responses. The effect of the fault was less severe in PSAT; however it displayed more oscillations for the voltage and active power responses. Of the three packages, only the rotor angle response seen in DigSILENT and PST agreed with the expectations. When the HVAC-HVDC system was subjected to the same fault, the system remained stable across all packages. PST however displayed very large oscillations for the active power, which is attributed to the interaction of the HVAC system with the HVDC system for the single machine infinite bus system.

Chapter 6

Simulation Results for the Two-Area Multi-machine system

6.1 Introduction

The results shown in this section are for the Two Area Multi-machine System. It covers the load flow, small signal and transient stability analysis.

Figure 6.1 and figure 6.2 show the single line diagram for case 1 (HVAC system) and case 2 (HVAC-HVDC system) respectively. In both cases, the base MVA and base voltage for the systems are 100 MVA, 230 kV respectively and operate at 60 Hz.

The HVAC system is composed of four generators with a rating of 20 kV and 900 MVA. Generators 1, 2 and 4 are respectively connected to buses 1, 2 and 4 which are PV buses, and set to supply 700 MW. Generator 3 is the reference generator and is connected to bus 3 (slack bus). All other buses in the system are set as PQ buses. Generators 1 and 2 are in area 1 and generators 3 and 4 are in area 2. Power is transferred from area 1 to area 2.

The system has two loads. The first load of (976 + j100) MVA is connected to bus 7 and the second load of (1767 + j 100) MVA is connected to bus 9. To boost the voltage in the system, capacitor banks are connected to buses 7 and 9. A capacitor bank (cap 1) of 300 Mvar is connected to bus 7 and another capacitor bank (cap 2) of 450 Mvar is connected to bus 9. Areas 1 and 2 are connected through a weak tie of double-circuit HVAC transmission lines rated at 230 kV. These transmission lines are 220 km each. The transformers connected between buses 1 and 5 and 2 and 6 in area 1 and between buses 3 and 11 and 4 and 10 in area 2 are rated at 900 MVA each.

The HVAC-HVDC system is similar to the HVAC system; however a HVDC transmission line is added between bus 7 and bus 9 without altering the previous HVAC

system. The HVDC system used is modified from the CIGRE benchmark model [29] (power and current ratings modified). This is a monopolar system rated at 500 kV, 230 MVA, 0.46 kA HVDC link with 12 pulse converters on both the rectifier and inverter sides. To control the power transmitted across the HVDC link, current control is used on the rectifier station, which is set to 0.4 kA. No filters were used, as PST and PSAT do not cater for the modelling of these components; however not much difference in the results is expected owing to the absence of filters. The system parameters are given in Appendix D

In both systems, power flows from area 1 to area 2 to supply load 2 that is much bigger than the total available generation in area 2.

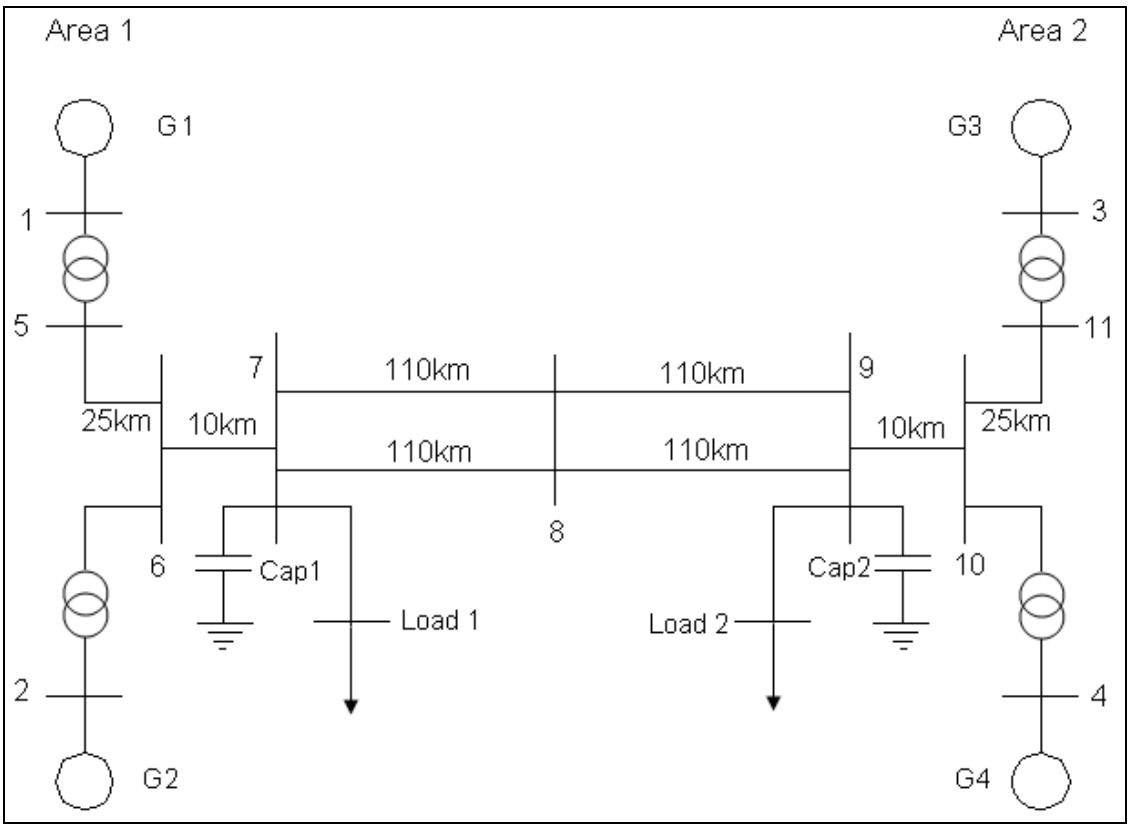

Figure 6.1: HVAC system

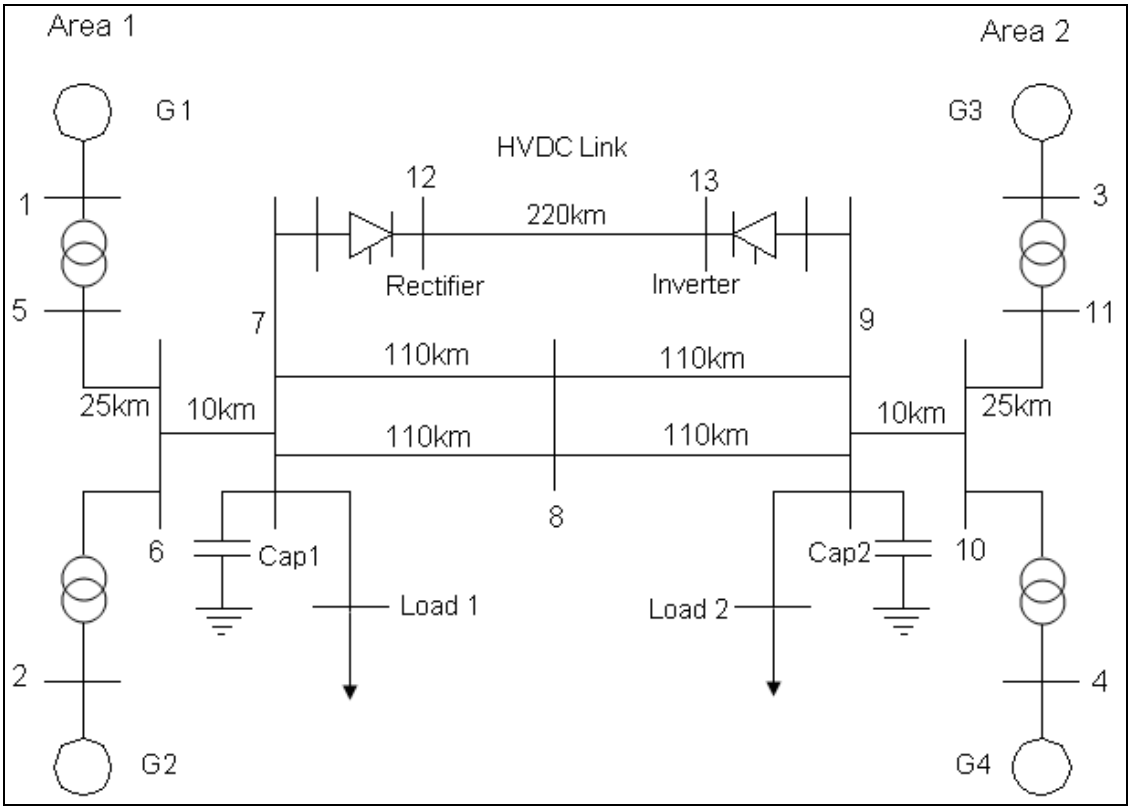

Figure 6.2: HVAC-HVDC system

6.2 Load flow

The load flow results for the two cases are discussed below.

6.2.1 Case 1: HVAC system

The double-circuit HVAC transmission system is used to transmit power from area 1 to area 2, as the generators in area 2 do not generate enough power to supply load 2. Tables 6.1, 6.2 and 6.3 show the voltages and powers at all the busbars in the system.

The negative signs seen in table 6.2 and table 6.3 come from the assumption that the flow of power on the transmission lines is from bus 7 to bus 9. For example, in table 6.2, when looking at HVAC lines 1 and 2, at bus 9 the value for the active power is negative because power is flowing toward bus 9.

.

Table 6.1: Voltage magnitude and angle for HVAC TAMM system

Element	Rated voltage (kV)	Voltage (pu) and angle (deg)		
		DigSILENT	PST	PSAT
Bus 1	20	1.03 ∠18.78º	1.03 ∠18.81º	1.03 ∠18.94º
Bus 2	20	1.01∠9.13º	1.01∠9.15º	1.01∠9.27º
Bus 3	20	1.03∠-6.8º	1.03∠-6.8º	1.03∠-6.8º
Bus 4	20	1.01∠-16.79º	1.01∠-16.79º	1.01∠-16.8º
Bus 5	230	1.01∠12.36º	1.01∠12.37º	1.01∠12.52º
Bus 6	230	0.99∠2.45º	0.99∠2.46º	0.99∠2.59º
Bus 7	230	0.99∠-5.65º	0.99∠-5.65º	0.99∠-5.52º
Bus 8	230	0.98∠-18.72º	0.98∠-18.72º	0.98∠-18.65º
Bus 9	230	1∠-31.49º	1∠-31.52º	1∠-31.55º
Bus 10	230	1∠-23.42º	1∠-23.44º	1∠-23.44º
Bus 11	230	1.02∠-13.35º	1.02∠-13.36º	1.01∠-13.36º

Table 6.2: Active power for HVAC TAMM system

Element	Bus	Active power (MW)		
		DigSILENT	PST	PSAT
Gen 1	1	700	700	700
Gen 2	2	700	700	700
Gen 3	3	715.62	715.67	715.91
Gen 4	4	700	700	700
HVAC Line 1	7	200.73	200.73	200.71
	9	-191.78	-191.76	-191.68
HVAC Line 2	7	200.73	200.73	200.71
	9	-191.78	-191.76	-191.68
Load 1	7	967	967	967
Load 2	9	1767	1767	1767
Cap 1	7	0	0	0
Cap 2	9	0	0	0

Table 6.3: Reactive power for HVAC TAMM system

Element	Bus	Reactive power (Mvar)		
		DigSILENT	PST	PSAT
Gen 1	1	144.1	144.67	146.18
Gen 2	2	136.11	137.2	141.07
Gen 3	3	131.62	132.23	135.67
Gen 4	4	97.34	98.52	106.67
HVAC Line 1	7	0.93	1.36	4.63
	9	-50.45	-50.72	-52.95
HVAC Line 2	7	0.93	1.36	4.63
	9	-50.45	-50.72	-52.95
Load 1	7	100	100	100
Load 2	9	100	100	100
Cap 1	7	300	300	300
Cap 2	9	450	450	450

The lowest voltage is 0.98 pu obtained at bus 8, and the highest voltage of 1.03 is observed at buses 1 and 3. Generator 3 supplies approximately 716 MW and all other generators supply 700 MW. The active power delivered across the HVAC line at bus 9 is close to 382 MW, with each HVAC line having a loss of close to 4.5%. The generators in PSAT supply a relatively larger amount of reactive power when compared to PST and DigSILENT (the difference being in the range of 1.5% in generators 1 and 3 to 8 % in generator 4). The transmission lines absorb more reactive power in PSAT when compared to PST (close to 32 % at bus 7) and DigSILENT (close to 80% at bus 7), and the reasons may be linked to the internal modelling of the software packages, since the transmission line modelling that was chosen (π equivalent circuit with lumped parameters) was the same for all the packages.

6.2.2 Case 2: HVAC-HVDC TAMM system

As in the HVAC case, power is transferred from area 1 to area 2. The lowest voltage on the system is observed at bus 7 (0.98 pu) and the highest voltage of 1.03 pu is observed at buses 1 and 3. The HVDC line operates at a voltage of 1.01 pu in DigSILENT and PST, as seen in table 6.4. PSAT does not display the voltage for the HVDC line. The voltages at buses 12 and 13 differ, but the software packages round them off to 1.01 pu. From table 6.5, it is seen that the HVDC line transmits close to 200 MW with a loss of approximately 0.5% and the HVAC lines each transmit close to 100 MW with a loss of approximately 2% each. When compared to the HVAC system, the HVAC transmission lines experience half the power loss in the HVAC-HVDC system. Generator 3 supplies approximately 703 MW and all other generators supply 700 MW (Table 6.5). In PST, generators 1 and 2 in area 1 supply slightly more reactive power than in DigSILENT and PSAT. The rectifier stations consume approximately 87 Mvar in DigSILENT and PSAT and 82 Mvar in PST, while the inverter stations consume close to 113 Mvar in DigSILENT and 98 Mvar in PST and PSAT (Table 6.6).

Table 6.4: Voltage magnitude and angle for HVAC-HVDC TAMM system

Element	Rated voltage (kV)	Voltage (pu) and angle (deg)		
		DigSILENT	PST	PSAT
Bus 1	20	1.03∠6.56°	1.03∠6.67°	1.03∠6.49°
Bus 2	20	1.01∠-3.14º	1.01∠-3.04º	1.01∠-3.2º
Bus 3	20	1.03∠-6.8º	1.03∠-6.8º	1.03∠-6.8º
Bus 4	20	1.01∠-16.51º	1.01∠-16.51º	1.01∠-16.5º
Bus 5	230	1.01∠0.12º	1.01∠0.21º	1.01∠0.05º
Bus 6	230	0.99∠-9.85º	0.99∠-9.79º	0.99∠-9.91º
Bus 7	230	0.98∠-18.05º	0.98∠-18.07º	0.98∠-18.11º
Bus 8	230	0.99∠-24.76º	0.99∠-25.79º	0.99∠-24.76º
Bus 9	230	1∠-31.24º	1∠-31.24º	1∠-31.2º
Bus 10	230	1∠-23.17º	1∠-23.19º	1∠-23.15º
Bus 11	230	1.01∠-13.24º	1.01∠-13.25º	1.01∠-13.24º
Bus 12	500	1.01	1.01	*
Bus 13	500	1.01	1.01	*

* Results not displayed in PSAT

Table 6.5: Active power for HVAC-HVDC TAMM system

Element	Bus	Active power (MW)		
		DigSILENT	PST	PSAT
Gen 1	1	700	700	700
Gen 2	2	700	700	700
Gen 3	3	703.07	703.36	703.09
Gen 4	4	700	700	700
HVAC Line 1	7	100.69	100.58	100.9
	9	-98.41	-98.25	-98.59
HVAC Line 2	7	100.69	100.58	100.9
	9	-98.41	-98.25	-98.59
HVDC Line	12	199.74	199.7	199.35
	13	-198.78	-198.7	-198.25
Rectifier	7	199.74	199.7	199.35
Inverter	9	198.78	198.7	198.25
Load 1	7	967	967	967
Load 2	9	1767	1767	1767
Cap 1	7	0	0	0
Cap 2	9	0	0	0

Table 6.6: Reactive power for HVAC-HVDC TAMM system

Element	Bus	Reactive power (Mvar)		
		DigSILENT	PST	PSAT
Gen 1	1	158.3	168.2	157.39
Gen 2	2	170.32	193.81	168.08
Gen 3	3	137.79	136.29	135.29
Gen 4	4	119.2	115.17	131.11
HVAC Line 1	7	-24.16	-27	-21.95
	9	9.05	12.89	12.08
HVAC Line 2	7	-24.16	-27	-21.95
	9	9.05	12.89	12.08
HVDC Line	12	0	0	0
	13	0	0	0
Rectifier	7	87.3	82.87	86.77
Inverter	9	113.18	99.71	97.74
Load 1	7	100	100	100
Load 2	9	100	100	100
Cap 1	7	300	300	300
Cap 2	9	450	450	450

6.3 Small Signal Stability

The results shown in this section are for the small signal stability analysis of the Two-Area Multi-machine system. The eigenvalues, damping ratios and frequencies are presented for different excitation system control strategies, namely without AVR and PSS, with AVR and no PSS and with AVR and PSS.

To calculate the percentage changes, the following equations are used:

$$\%\Delta f = \left(\frac{f - f_0}{f_0} \right) \times 100\% \tag{6.1}$$

$$\%\Delta \zeta = \left(\frac{\zeta - \zeta_0}{\zeta_0} \right) \times 100\% \tag{6.2}$$

where:

Δf , $\Delta \zeta$ - change in frequency and damping ratio respectively

f , ζ - current/actual values of frequency and damping ratio respectively

f_0 , ζ_0 - previous values of frequency and damping ratio respectively

6.3.1 Case 1: HVAC TAMM system

Tables 6.7, 6.8 and 6.9 show the eigenvalue results when the system has no AVR, with only AVRs in the system and with AVRs and PSSs in all machines. As in the case of the SMIB systems, the bold values in tables 6.8 and 6.9 show the percentage changes that occurred in the system as AVRs and PSSs were added. Without any AVR and PSS, the system has 24 modes which come from the four 6^{th} order machines. The negative sign for the frequency indicates that it has decreased, while the negative sign for the damping ratio indicates that it has decreased making the mode(s) less damped.

- **No AVR**

Table 6.7: TAMM HVAC system with no AVR and no PSS

Mode	Eigenvalue, frequency, damping ratio		
	DigSILENT	PST	PSAT
Inter-area	-0.1402 ± j3.5166 (f = 0.5596; ζ = 0.0398)	-0.0949 ± j3.5115 (f = 0.5589; ζ = 0.027)	-0.1234 ± j3.5172 (f = 0.5598; ζ = 0.035)
Local area 1	-0.6058 ± j6.9444 (f = 1.1052; ζ = 0.0869)	-0.5463 ± j7.0662 (f = 1.1246; ζ = 0.0771)	-0.826 ± j7.3831 (f = 1.1751; ζ = 0.1112)
Local area 2	-0.6029 ± j6.7156 (f = 1.0688; ζ = 0.0894)	-0.5496 ± j6.8386 (f = 1.0884; ζ = 0.0801)	-0.8054 ± j7.1386 (f = 1.1361; ζ = 0.1121)

With no AVRs on the generators (Table 6.7), the system is stable, with all software packages having similar results for the frequency of oscillation of the inter-area mode. DigSILENT gives the highest damping ratio of 0.0398 for the inter-area mode, while PST shows the lowest damping ratio of 0.027. For the local area modes, PSAT has higher frequency of oscillation (1.1751 Hz and 1.1361 Hz) and damping ratios (0.1112 and 0.1121). DigSILENT has the lowest frequency of oscillation for the local area modes and PST has the lowest damping ratios.

- **AVR only**

Table 6.8: TAMM HVAC TAMM system with AVR only

Mode	Eigen-value (frequency, damping ratio)		
	DigSILENT	PST	PSAT
Inter-area	0.0615 ± j3.9477 (f = 0.6283; **12.28%** ζ = -0.0156; **-139.2%**)	0.04 ± j3.98 (f = 0.63; **12.72** ζ = -0.01; **-137.03%**)	-0.1104 ± j3.5933 (f = 0.5719; **2.16%** ζ = 0.0307; **-12.29%**)
Local area 1	-0.6246 ± j7.2932 (f = 1.1607; **5.02%** ζ = 0.0853; **-1.84%**)	-0.55 ± j7.56 (f = 1.2; **6.7%** ζ = 0.07; **-9.2%**)	-2.0997 ± j6.0771 (f = 0.9672; **-17.69%** ζ = 0.3266; **193.7%**)
Local area 2	-0.6272 ± j7.0773 (f = 1.1264; **5.39%** ζ = 0.0883; **-1.23%**)	-0.57 ± j7.34 (f = 1.17; **7.49%** ζ = 0.08; **-7.08%**)	-2.2697 ± j6.2366 (f = 0.9926; **-12.64%** ζ = 0.3419; **204.99%**)

As the generators are equipped with AVRs only, the system becomes unstable (when looking at the inter-area mode), as seen in Table 6.8 for DigSILENT and PST, agreeing with what is expected from the system when only AVRs are used. The inter-area mode for PSAT, on the other hand, remains stable. This is in disagreement with the expectation that the inter-area mode will become unstable when only the AVRs are used on the generators. The frequency of oscillation increases while the damping ratio decreases for the inter-area mode across all packages. PSAT shows the lowest percentage change for the frequency of 2.16%, while DigSILENT and PST show a change of approximately 12%. The damping ratio shows the lowest percentage change of 12.29% in PSAT and a change of 139% and 137% in DigSILENT and PST respectively. For the local area modes, DigSILENT and PST show that the frequency increases and damping ratios worsen, as is expected when only AVR is being used. However, PSAT shows that the frequency of oscillation and damping ratio improve for the local area modes which does not agree with what is seen in literature. The same behaviour seen in PSAT was observed in the studies performed by Mudau in [13] where it was the only package, out of three, to behave in this manner.

- **AVR and PSS**

Table 6.9: TAMM HVAC system with AVR and PSS

Mode	Eigenvalue, frequency, damping ratio		
	DigSILENT	PST	PSAT
Inter-area	-0.7542 ± j3.9597 (f = 0.6302; **0.3%** ζ = 0.1871; **1299.4%**)	-0.76 ± j3.93 (f = 0.63; **0%** ζ = 0.19; **2000%**)	-0.4832 ± j3.4782 (f = 0.5536; **3.2%** ζ = 0.1376; **348.2%**)
Local area 1	-1.5533 ± j10.0525 (f = 1.5999; **37.8%** ζ = 0.1527; **79%**)	-1.47 ± j10.27 (f = 1.63; **35.8%** ζ = 0.14; **100%**)	-1.8766 ± j8.6159 (f = 1.3713; **41.78%** ζ = 0.2128; **-34.84%**)
Local area 2	-1.7059 ± j9.6841 (f = 1.5413; **36.83%** ζ = 0.1735; **96.49%**)	-1.65 ± j9.91 (f = 1.58; **35.04%** ζ = 0.16; **100%**)	-1.8349 ± j8.3361 (f = 1.3267; **33.66%** ζ = 0.2149; **-37.14%**)

When the generators in the system are equipped with AVRs and PSS (Table 6.9), the system in DigSILENT and PST becomes stable. The damping ratio and frequency of oscillation improve for the inter-area mode. In DigSILENT and PST, the frequency remains quasi-steady and the damping ratio improves to approximately 0.19. PSAT shows the same pattern, but with smaller percentage changes and smaller frequency of oscillation (~ 0.56) and damping ratio (~ 0.14). In PSAT, the frequency increases and damping ratios deteriorate for the local area modes when compared to using only AVRs on the system. This behaviour is not expected, as when the generators are equipped with AVRs and PSSs, the damping ratios are expected to increase. However it still shows the highest damping ratios for the local area modes and the lowest frequency of oscillation when compared to DigSILENT and PST.

6.3.2 Case 2: HVAC-HVDC TAMM system

In tables 6.10, 6.11 and 6.12, the results for the small signal stability analysis on the HVAC-HVDC system are presented. Table 6.10 depicts the results for the system with no AVR. Table 6.11 shows the results with only AVRs installed on the generators and table 6.12 shows the results for the system with AVRs and PSSs installed on all generators.

- **No AVR**

The system is stable across all packages when no AVRs are used. DigSILENT has the highest damping ratio of 0.0871 (1879.8 % more than PST) for the inter-area mode, followed by PSAT with 0.0272 (518.2 % more than PST) while PST has the lowest

damping ratio of 0.0044. The frequency of oscillation for the inter-area mode shows the lowest value of 0.2941 Hz in PST, followed by 0.4035 Hz in DigSILENT (37 % more than PST) and the highest of 0.6584 Hz in PSAT (123.9% more than PST). Damping ratios for the local area modes have the lowest values in PST, followed by DigSILENT, and PSAT shows the highest values. The frequencies of oscillation for the local modes are to a certain extent similar across all packages. The big differences in the damping ratios and frequency of oscillations may be due to the modelling of the HVDC system (looking at section 4.5 it can be seen that in DigSILENT the HVDC system has no modes, in PST has five modes and in PSAT has three modes).

Table 6.10: HVAC-HVDC TAMM with no AVR and no PSS

Mode	Eigenvalue, frequency, damping ratio		
	DigSILENT	PST	PSAT
Inter-area	-0.2216 ± j2.5355 (f = 0.4035; ζ = 0.0871)	-0.0082 ± j1.8481 (f = 0.2941; ζ = 0.0044)	-0.1125 ± j 4.1371 (f = 0.6584; ζ = 0.0272)
Local area 1	-0.6105 ± j6.9798 (f = 1.1109; ζ = 0.0871)	-0.5479 ± j7.2696 (f = 1.157; ζ = 0.0752)	-0.9041 ± j8.2515 (f = 1.3133; ζ = 0.1089)
Local area 2	-0.61 ± j6.7179 (f = 1.0692; ζ = 0.0904)	-0.571 ± j6.8461 (f = 1.0896; ζ = 0.0831)	-0.8846 ± j7.93 (f = 1.2621; ζ = 0.1109)

- **AVR only**

When AVRs are added to the generators, the inter-area mode becomes unstable for DigSILENT and PST, while it remains stable in PSAT, and this behaviour is similar to case 1. Literature supports the behaviour seen in DigSILENT and PST for HVAC; however no example has been encountered where HVDC links were incorporated. PST shows that the damping ratio for the inter-area mode is affected negatively when AVRs are incorporated into system, while PSAT shows an improvement. The damping ratios for the local modes show large improvement in PSAT where they are almost three times better than when no AVR was used. DigSILENT shows a slight reduction in damping ratios and PST shows a slight improvement on the damping ratios for the local area modes. For the inter-area mode, it is observed that the behaviour in DigSILENT and PST is similar to case 1, suggesting that when only the AVR is used, the inter-area mode becomes unstable, but no comments can be made

on what the correct values are for the frequency and damping ratios for this benchmark system since the three packages used disagree on the values obtained.

Table 6.11: HVAC-HVDC TAMM with AVR only

Mode	Eigenvalue, frequency, damping ratio		
	DigSILENT	PST	PSAT
Inter-area	0.1351 ± j3.1059 (f = 0.4943; **-22.5%** ζ = -0.0434; **-149.8%**)	0.45 ± j1.78 (f = 0.28; **5.04%** ζ =-0.24; **-5554.5%**)	-0.1454 ± j3.9585 (f = 0.63; **4.31%** ζ = 0.0367; **34.9%**)
Local area 1	-0.6066 ± j7.0689 (f = 1.1251; **-1.28%** ζ = 0.0855; **-1.84%**)	-0.57 ± j7.49 (f = 1.19; **-2.85%** ζ = 0.08; **6.38%**)	-2.0325± j6.0937 (f = 0.9698; **26.16%** ζ = 0.3164; **190.54%**)
Local area 2	-0.6389 ± j7.3403 (f = 1.1682; **-9.26%** ζ = 0.0867; **-4.1%**)	-0.63 ± 7.35 (f = 1.17; **-1.12%** ζ = 0.09; **8.3%**)	-2.2817 ± j6.2314 (f = 0.9918; **21.42%** ζ = 0.3438; **210.01%**)

- **AVR and PSS**

The system is stable when AVRs and PSSs are used on all generators. DigSILENT and PST show similar results for the inter-area (damping ratio ≈ 0.6) and local area modes (damping ratio ≈ 0.14 and 0.18 for local modes 1 and 2 respectively). PSAT shows a reduction in the damping ratios for the local area modes when compared to the case without PSS; however it has the highest damping ratios when compared to the other two packages. PSAT has the highest frequency of oscillation for the inter-area mode while having the highest frequency for the local area modes and PST has the lowest frequency for the inter-area mode while having the highest frequency for the local area modes. Assuming that the behaviour of the system is the same as in the HVAC case, the system does behave as expected in DigSILENT and PST.

Table 6.12: HVAC-HVDC TAMM with AVR and PSS

Mode	Eigenvalue, frequency, damping ratio		
	DigSILENT	PST	PSAT
Inter-area	-2.0782 ± j2.7819 (f = 0.4428; **10.42%** ζ = 0.5985; **1479.1%**)	-1.15 ± j1.52 (f = 0.24; **14.29%** ζ = 0.6; **350%**)	-0.3991 ± j3.5758 (f = 0.5691; **9.67%** ζ = 0.1109; **224.25%**)
Local area 1	-1.4997 ± j10.3563 (f = 1.6482; **-46.49%** ζ = 0.1433; **67.6%**)	-1.45 ± j10.1 (f = 1.61; **-35.29%** ζ = 0.14; **75%**)	-1.766 ± j8.0331 (f = 1.2785; **-31.83%** ζ = 0.215; **-32.05%**)
Local area 2	-1.6373 ± j9.6649 (f = 1.5382; **-31.67%** ζ = 0.167; **92.27%**)	-1.77 ± 9.92 (f = 1.58; **-35.04%** ζ = 0.18; **100%**)	-1.8225 ± j8.3421 (f = 1.3277; **-33.86%** ζ = 0.2134; **-37.93%**)

6.4 Transient Stability

A large disturbance was applied to the system in the form of a three-phase fault at bus 8 and this fault was cleared by removing the transmission line between bus 8 and bus 9. The fault is applied at 1 s and lasts for 50 ms. The same fault is applied on the HVAC system as well as on the HVAC-HVDC system. The results are discussed below. The results discussed below are for the case where the system includes AVRs and PSSs only.

6.4.1 Case 1: HVAC TAMM system

Figures 6.3 to 6.11 show the effect of the fault on the HVAC system. Figures 6.3-6.5 show the effect of the fault on the terminal voltages of the generators, figures 6.6-6.8 show the effect on the rotor angle and figures 6.9-6.11 show the effect on the active power output of the generators.

- **Generator terminal voltage**

  When the fault is applied, in DigSILENT and PST (figures 6.3 and 6.4 respectively), the lowest voltage of 0.82 pu is reached at the terminals of machine 4 and once the fault is cleared the maximum voltage of 1.09 pu is observed at the terminals of machine 1. The system settles in approximately 6 seconds. When the fault is applied in PST, the lowest voltage of 0.86 is observed at the terminals of machine 4 and when the fault is cleared the maximum voltage of 1.08 is seen at the terminals of machine 1. The system in PSAT shows more oscillations and settles in approximately 9 seconds. As seen in table 6.9, PSAT has the lowest damping ratio of all software packages; hence in responses to the fault, it is the system that has most oscillations. In other words, it is less damped. The effect of this low damping ratio can be seen in figure 6.5.

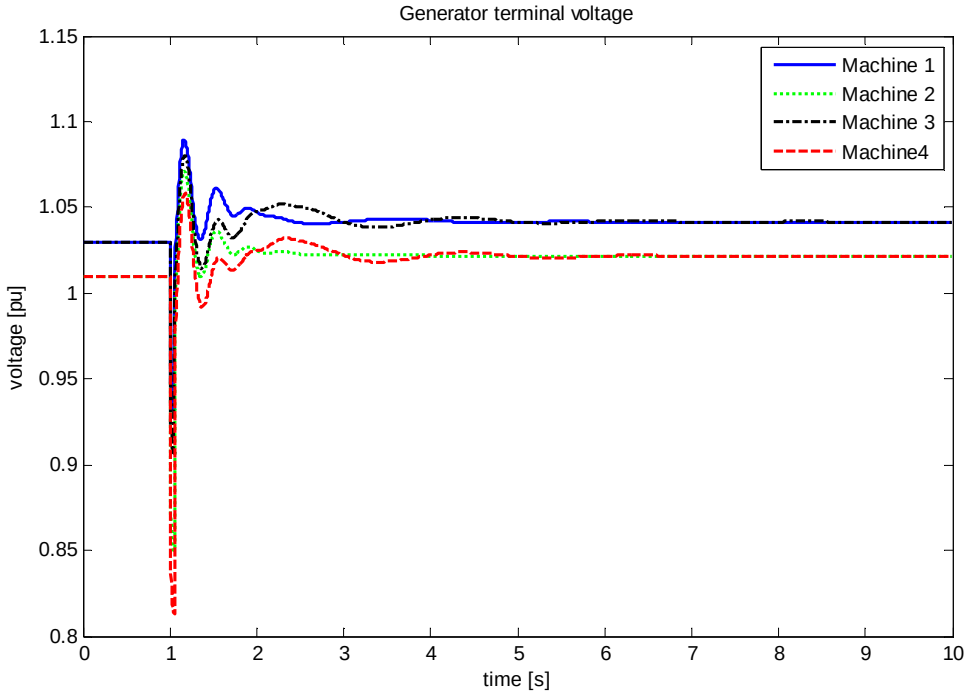

Figure 6.3: Generator terminal voltage responses in DigSILENT

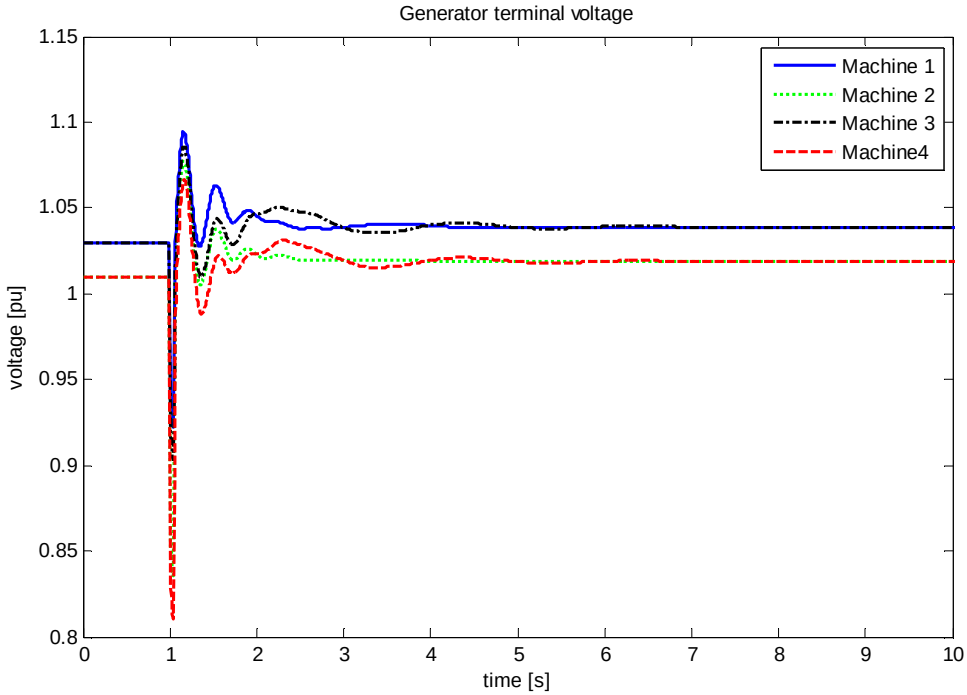

Figure 6.4: Generator terminal voltage responses in PST

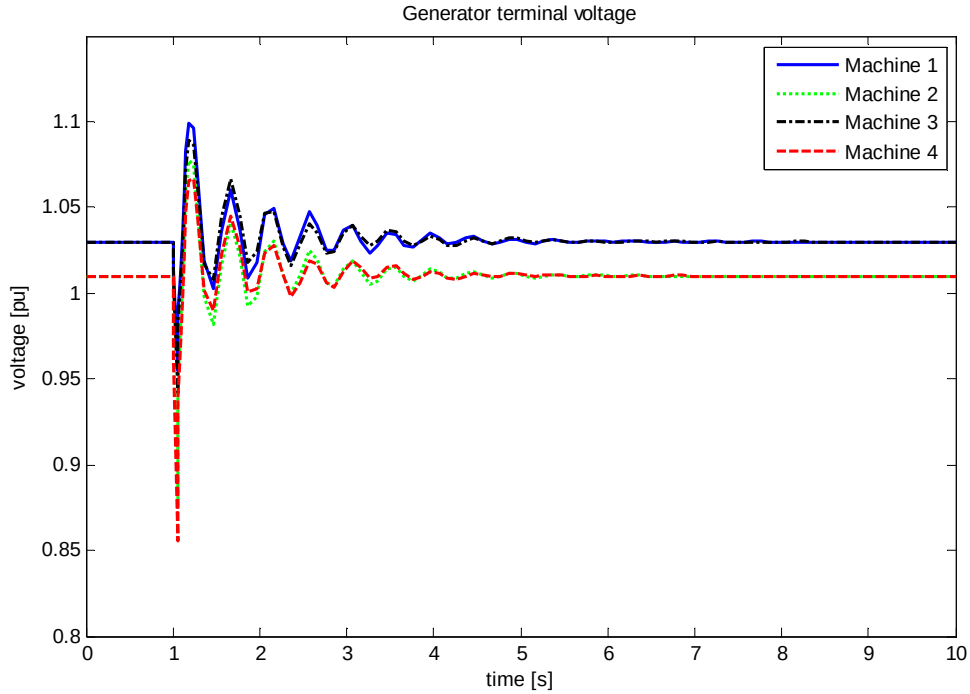

Figure 6.5: Generator terminal voltage responses in PSAT

- **Generator rotor angle**

Figure 6.6 and figure 6.7 show the result for the rotor angles in DigSILENT and PST. During the fault, the rotor angles increase owing to the excess energy that the machines have. This kinetic energy causes an increase in the machines rotor angular velocities. After the fault is cleared, the rotor angles of machines' 1 and 2 settle at a slightly higher value than the initial. This is due to the increase in machine speeds from the machines in one area with respect to the other area. The rotor angle for machine 4 returns to a lower value than its pre-fault value in DigSILENT and PST and it returns to its pre-fault value in PSAT. The rotor angle for machine 3 is at zero in PST and in PSAT, while in DigSILENT it is at approximately -53º. This is due to the fact that DigSILENT automatically calculates the rotor angle, taking machine 3 as the reference. In PST and PSAT, the results are given as individual rotor angles for each machine. To obtain the graphs displayed below for the rotor angle, machine 3 was used as the reference machine, and hence the rotor angle is at zero. The response of the rotor angles in PSAT, where the rotor angles of all machines return to the initial value once the fault is cleared, is not ideal. This is because when a line is removed a

new operating angle is expected and machines 1 and 2 are supposed to settle at higher values. In DigSILENT and PST the system settles in approximately 8.5 seconds, while in PSAT the system settles in approximately 7.5 seconds.

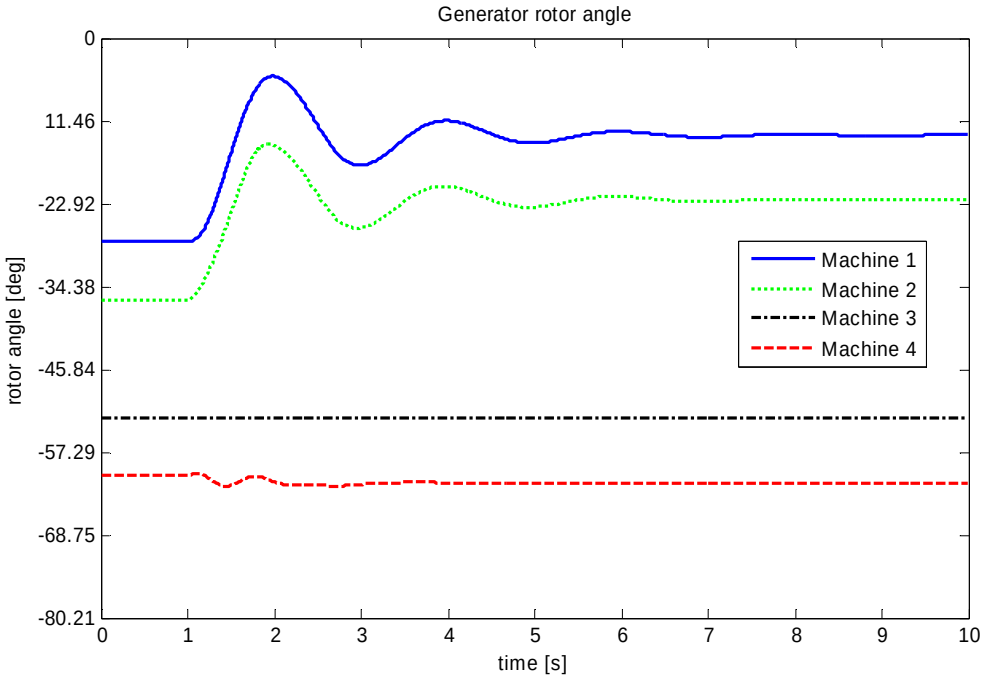

Figure 6.6: Rotor angle responses in DigSILENT

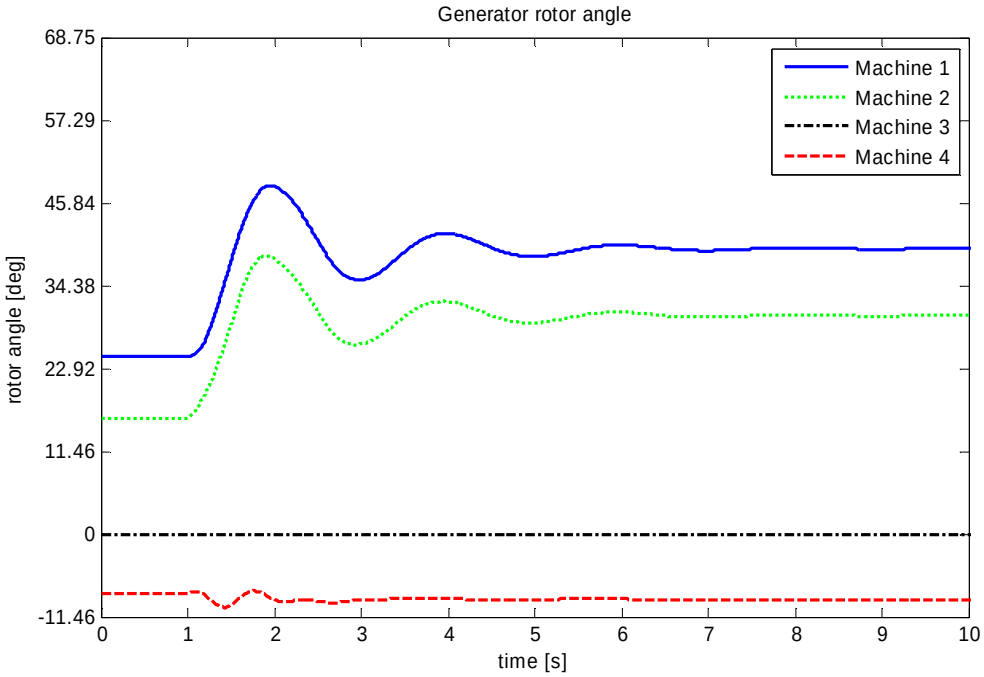

Figure 6.7: Rotor angle responses in PST

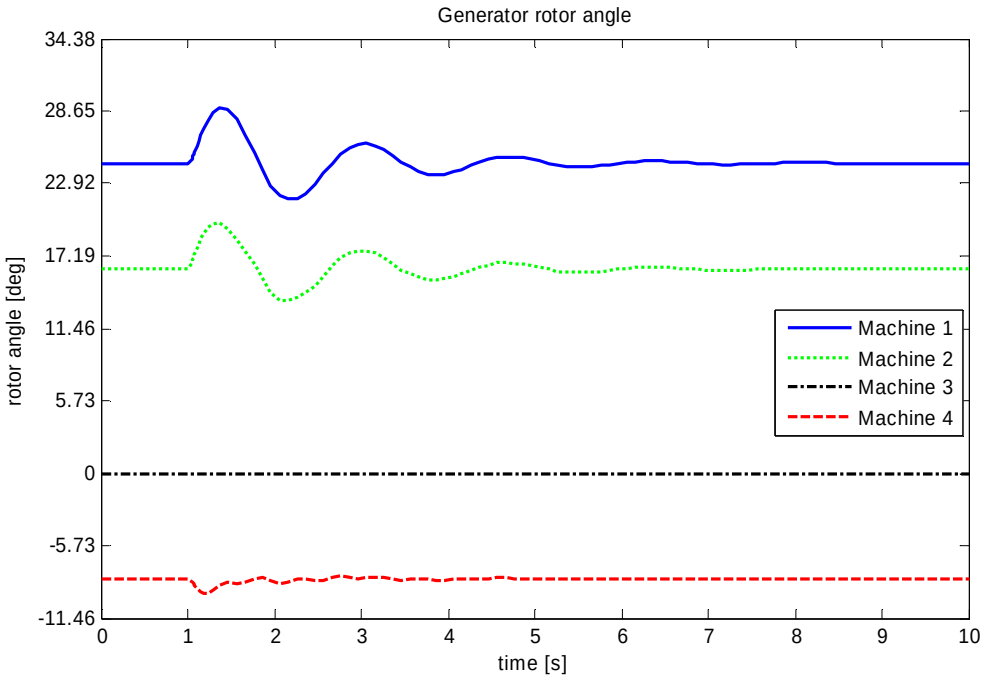

Figure 6.8: Rotor angle responses in PSAT

- **Generators' active power**

Figure 6.9 shows the active power output for all machines in DigSILENT, where machine 2 has the lowest power output of 2.1 pu during the fault and once the fault is cleared machine 4 has the maximum output of 8.3 pu, and the system settles in under 7 seconds. Figure 6.10 displays the output for PST, where machine 2 has the lowest power output of 1.9 pu during the fault and machine 4 has the maximum output of 8.5 pu once the fault is cleared. The system in PST settles in approximately 7 seconds. Figure 6.11 depicts the results for the power output in PSAT. During the fault, machine 2 shows the lowest power output of approximately 3.4 pu and once the fault is cleared machine 1 shows the highest output of 7.7 pu with the system stabilizing at approximately 6 seconds. The impact of the fault in the three packages is less severe in PSAT even though it has smaller oscillations that last longer when compared to DigSILENT and PST, making the system in PSAT more robust.

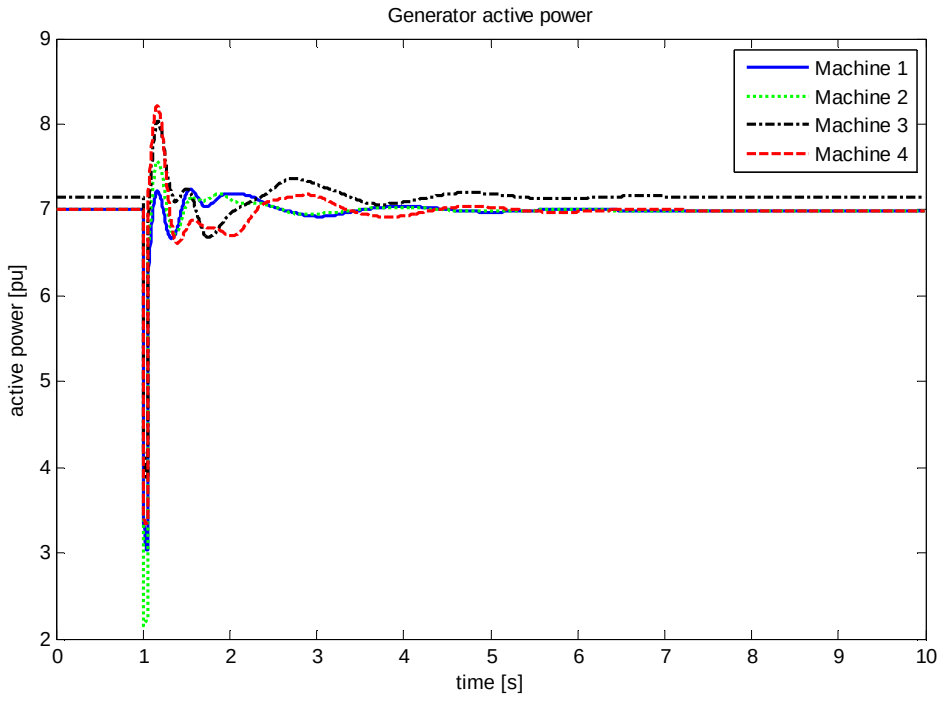

Figure 6.9: Active power responses in DigSILENT

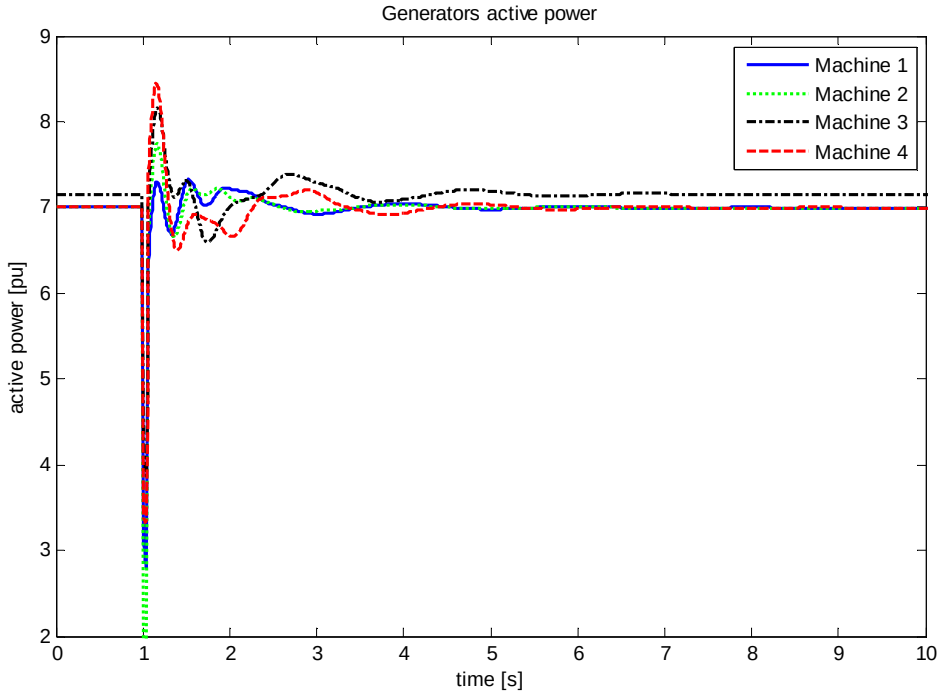

Figure 6.10: Active power responses in PST

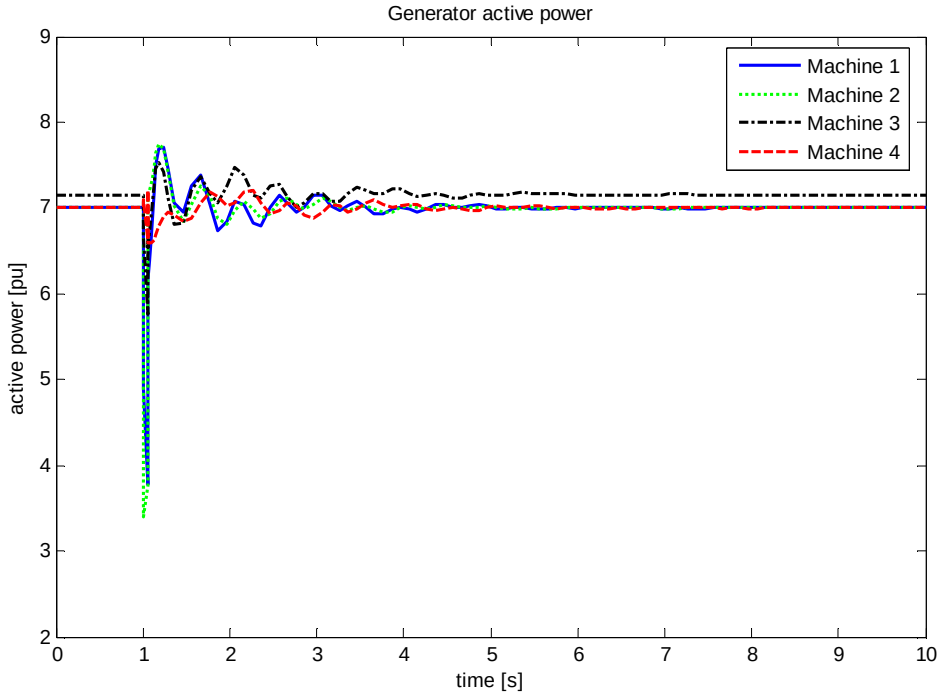

Figure 6.11: Active power responses in PSAT

6.4.2 Case 2: HVDC-HVAC TAMM system

Figures 6.12-6.20 show the effect of a three-phase fault on the HVAC-HVDC system. Figures 6.12-6.14 show the effect on the terminal voltage of the machines, figures 6.15-6.17 show the rotor angle response and figures 6.18-6.20 show the response of the machines' active power across the three packages.

- **Generators' terminal voltage**

Figures 6.12, 6.13 and 6.14 show the responses of the machine voltages for DigSILENT, PST and PSAT, respectively. It can be seen from figure 6.12 and figure 6.13 that the system stabilizes in less than 4 seconds. During the fault, machine 4 reaches the lowest voltage of 0.82 pu and machine 1 reaches the highest voltage of 1.08p.u. The voltage responses in PSAT, shown in figure 6.14, have more oscillations and take longer to stabilize, approximately 6 seconds. During the fault, machine 4 reaches a minimum voltage of 0.86 pu and machine 1 reaches a maximum of 1.08 when the fault is cleared.

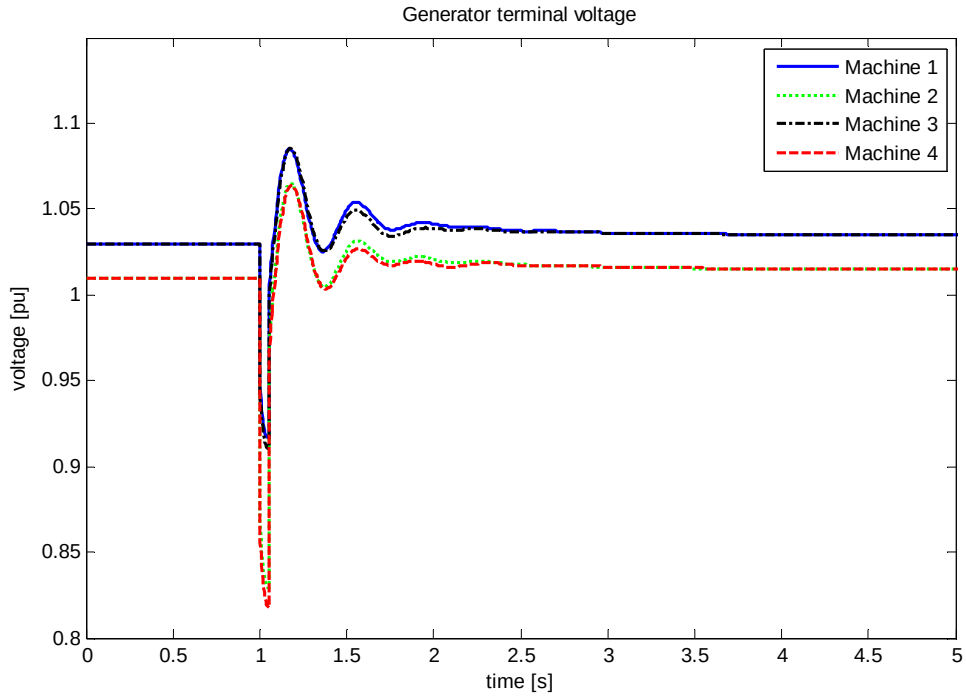

Figure 6.12: Generator terminal voltage responses in DigSILENT

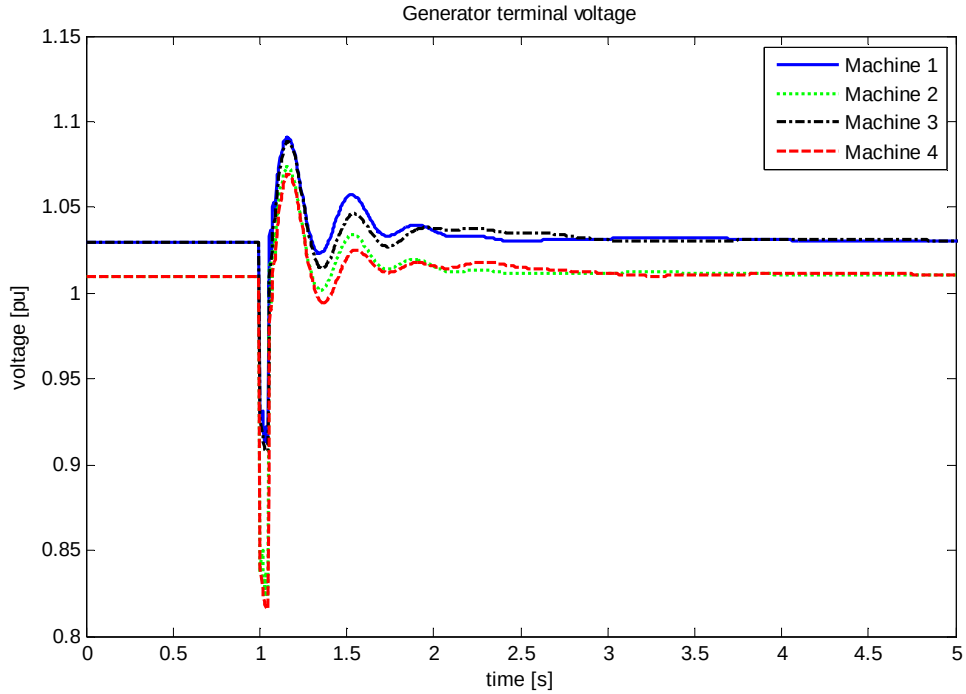

Figure 6.13: Generator terminal voltage responses in PST

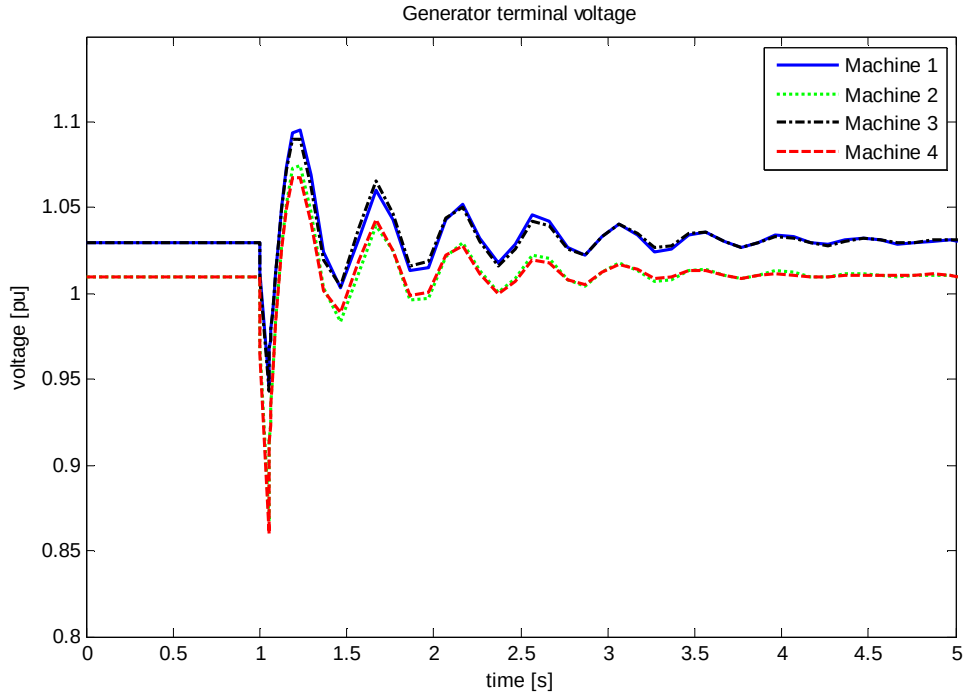

Figure 6.14: Generator terminal voltage responses in PSAT

- **Generators' rotor angle**

Figures 6.15, 6.16 and 6.17 show the results for the machine rotor angle differences, taking machine 3 as the reference rotor angle. The rotor angle response in DigSILENT, shown in figure 6.15, settles in less than 3.5 seconds, while the rotor angle responses for PST and PSAT, shown in figures 6.16 and 6.17, respectively settle at approximately 5 seconds. DigSILENT displays the rotor angle with respect to machine 3, while PST and PSAT display individual rotor angles as discussed in the previous section 6.4.1. The graphs displayed here were calculated manually. The response of the rotor angles of machines 1 and 2 decreases in DigSILENT and then increases settling at a higher value. This behaviour is not normal as the rotor angles are expected to increase when the fault is applied. In PST the rotor angles of machines 1 and 2 increase and settle at a higher value than expected and in PSAT they do increase; however they settle at the same value once the fault is cleared. When comparing the HVAC-HVDC system to the HVAC system, among the three packages, the HVAC system operates and settles at higher rotor angle values. In the HVAC-HVDC system the rotor angle values may be smaller because half of the power is still transmitted through the HVDC system.

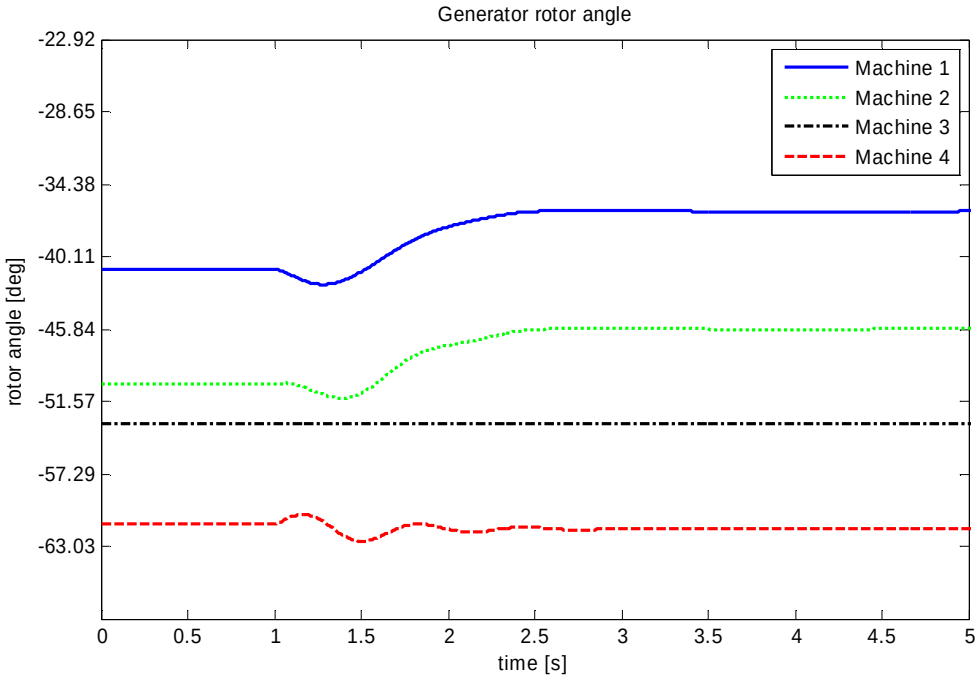

Figure 6.15: Rotor angle responses in DigSILENT

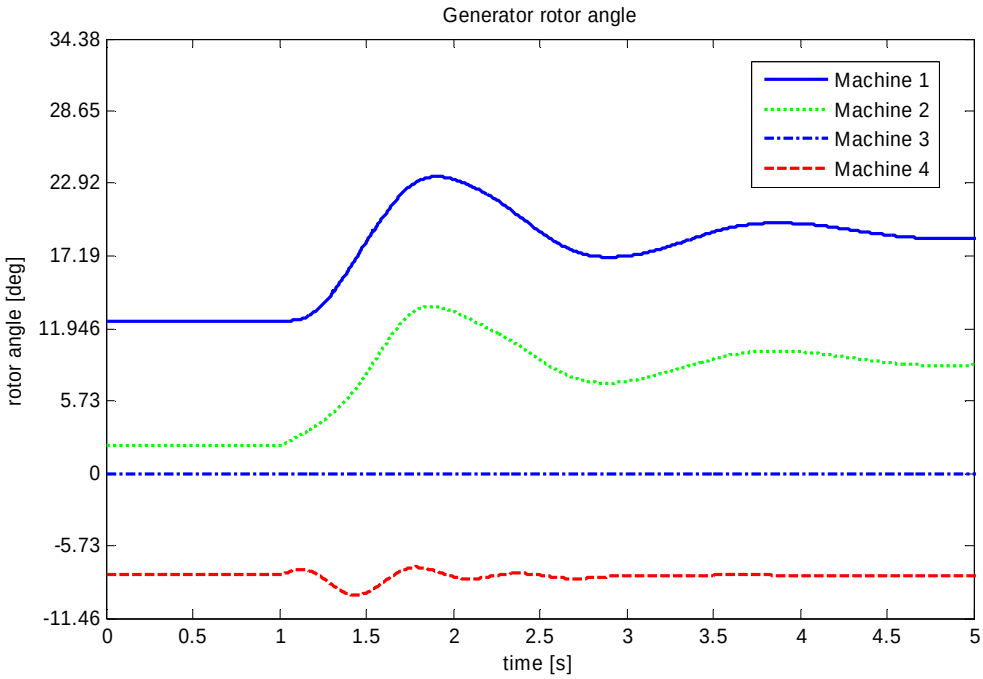

Figure 6.16: Rotor angle responses in PST

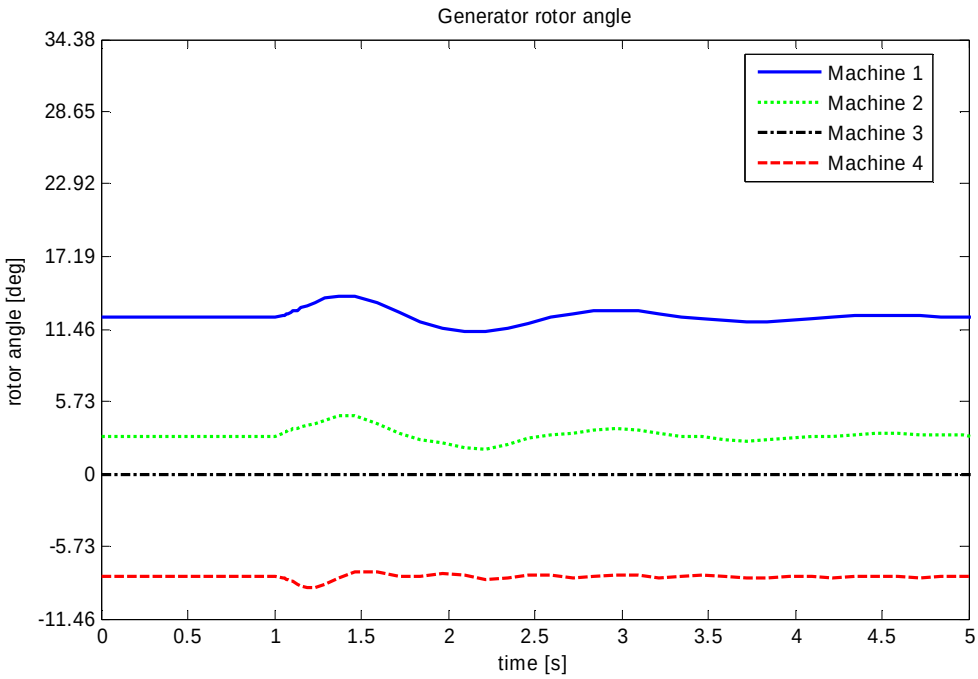

Figure 6.17: Rotor angle responses in PSAT

- **Generators' active power**

The responses of the machines' electric power are shown in Figures 6.18, 6.19 and 6.20. In DigSILENT the electric power of machine 4 reduces to 2.3 pu and that of machine 2 reduces to 2.8 pu during the fault; after it is cleared machine 4 reaches a maximum of 8 pu before stabilizing in 3 seconds. In PST machine 2 shows the lowest active power at 2.3 pu and machine 4 is at 2.5 pu during the fault. When the fault is cleared, machine 4 displays the maximum at 8.4 pu and the system settles in approximately 6 seconds, as shown in figure 6.19. The electric power displays more oscillations in PSAT (figure 6.20) when compared to the other packages. The active power at machine 4 dips to 4.3 pu, that at machine 2 reduces to 4.35 pu during the fault and machine 1 reaches a maximum of 7.7 pu and the system settles after 5 seconds.

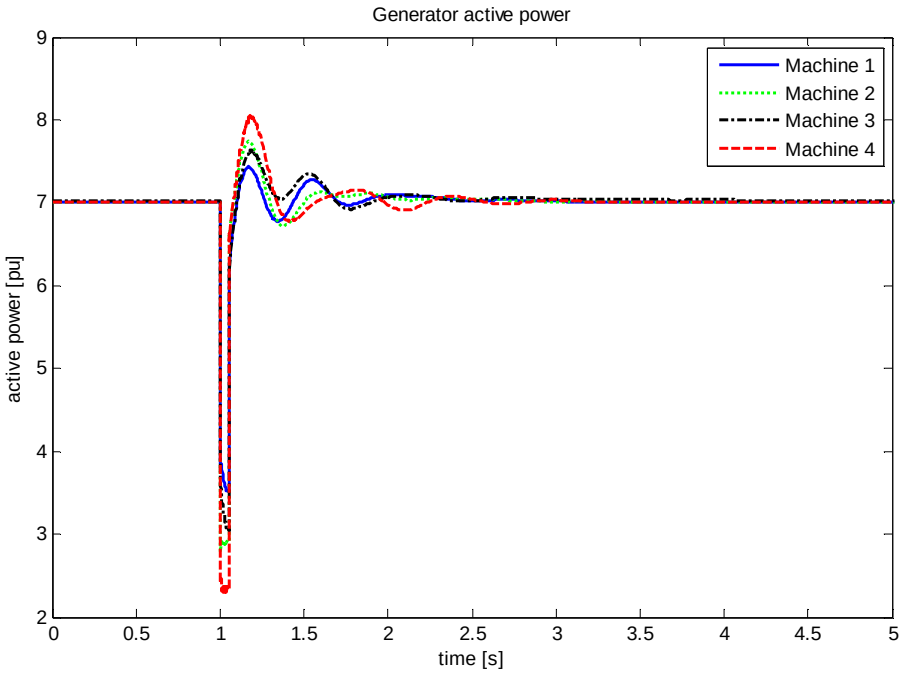

Figure 6.18: DigSILENT active power responses

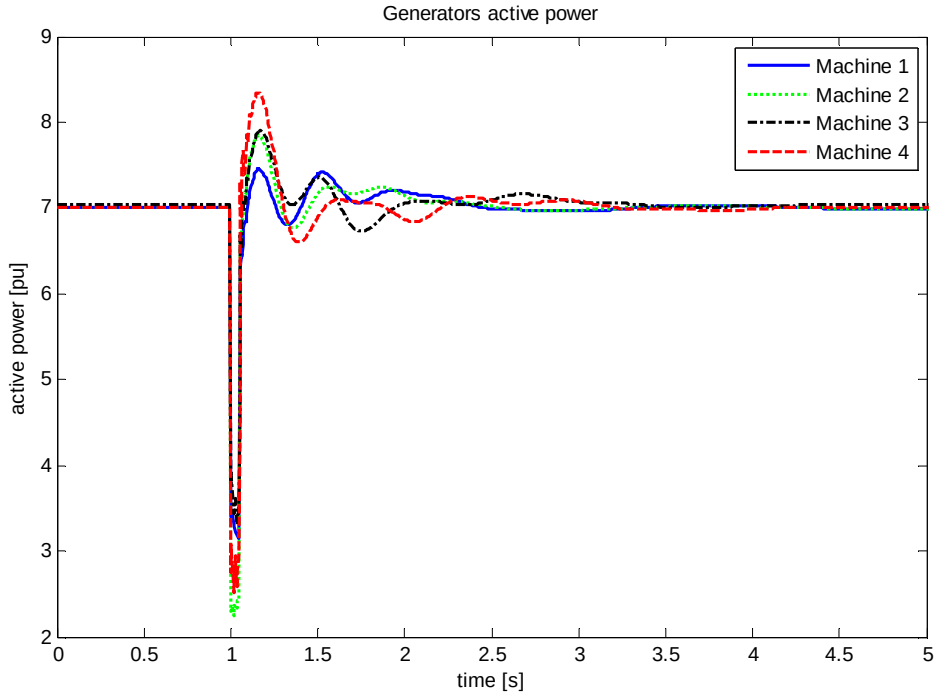

Figure 6.19: PST active power responses

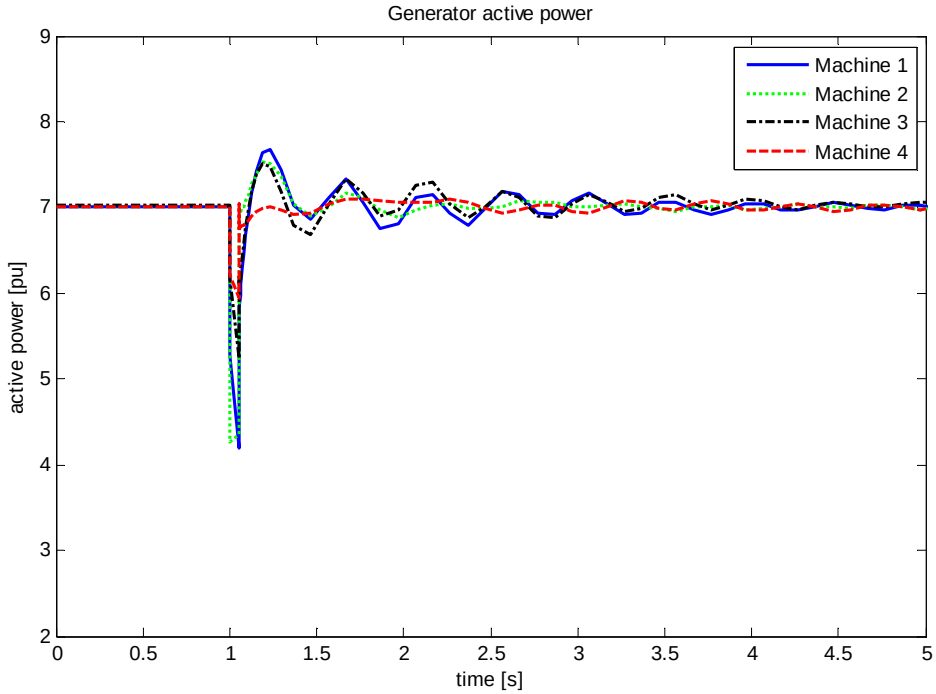

Figure 6.20: PSAT active power responses

6.5 Summary

The performance of the HVAC system is similar across all packages. Each of the HVAC lines has a loss of 4.5% of the power transmitted. When the load flow is performed on the HVAC-HVDC system, the HVDC line has a loss of 0.5% of the power transmitted while each of the HVAC lines has a loss of 2%. The HVAC-HVDC system has fewer losses than the HVAC system. The power supplied by generator 3 reduces, as the losses on the system decrease when compared to the HVAC system.

When small signal stability is performed, it is observed that in PSAT the system is stable for all scenarios (with no AVR and no PSS, with AVR only and with AVR and PSS) disagreeing with literature on the case where only AVRs are used, as according to the literature the system becomes unstable. In DigSILENT and PST the system is stable when no AVR or PSS is used, as well as when AVR and PSS are incorporated on the generators. When only the AVR is used, DigSILENT and PST show that the system is unstable, as stated in literature. When small signal stability is performed on the HVAC-

HVDC system, the system is stable for all scenarios in PSAT. In DigSILENT and PST the system is unstable when only the AVR is used. In PST, the damping ratio when no AVR or PSS is used is much smaller than in the other packages. The damping ratio is similar for DigSILENT and PST when AVR and PSS are used; however PSAT shows the smallest damping ratio, almost five times smaller than in the other packages, which is not desirable, as the highest damping ratio is what is desired. The results obtained in this simulation, which are in accordance with the results obtained by Mudau [13], for the HVAC case without AVR, raise the question of the accuracy of PSAT, since it disagrees completely with literature.

When the transient stability was performed, where only the case that incorporates AVR and PSS was considered, on the HVAC system the system was stable across all packages. PSAT had more oscillations on the voltage and active power curves when compared to DigSILENT and PST. It also had the smallest variation in terms of the voltage and active power, as it had the smallest drop and the smallest increase once the fault was cleared. The voltage settles in almost 8 seconds across all packages, while the active power stabilizes in 7 seconds across all packages. The HVAC-HVDC system remains stable across all packages and after the fault has been cleared the system stabilizes much faster when compared to the HVAC system, settling in less than 5 seconds in most cases. DigSILENT and PST show similar results, with small differences on the minimum and maximum values for the voltage and active power, but the trend is very similar for both packages. PSAT, on the other hand shows more oscillations for the HVAC-HVDC system when compared to the other packages

Chapter 7

Conclusions and Recommendations

7.1 Conclusions

A comparative study of three software packages, namely DigSILENT, Matlab PST and PSAT, has been carried out in this dissertation. The comparisons of the software packages are primarily aimed at their modelling capabilities and performance when studying HVDC systems. DigSILENT was found to model the HVDC system and other HVAC components in more detail than PST and PSAT; however no modifications are allowed without using the DSL (DigSILENT Simulation Language). PST and PSAT allow users to modify the HVDC system and other components, but in-depth knowledge of these software packages is needed to benefit from this option, as these packages are based on Matlab. The modelling differs from package to package even though the order of the generators, HVDC systems and all other components are assumed to be the same. These differences can be observed easily on the input parameters entered in each software package. Unfortunately, in DigSILENT the user does not have access to the codes used to run all the simulations. In PST and PSAT the user has access to the m-files that make up the systems used. From the load flow, small-signal and transient stability studies, the following conclusions were drawn:

7.1.1 SMIB systems

The load flow on the HVAC system showed that the software packages obtained similar results for the bus voltages and active power generated by the external grid and generator. The reactive power obtained across the three packages showed different results for the power supplied by the generator and the power absorbed by the external grid. These differences are not very significant.

When the small signal stability study was performed on the HVAC system, the system was found to be stable across all packages for the three scenarios (no AVR and no PSS,

only AVR used and when AVR and PSS were used on the generator). PSAT showed the lowest percentage change for the three packages when the AVR was added as well as when the AVR and PSS were used on the generator. DigSILENT and PST showed results that were not far from each other when looking at the damping ratio, frequency and the percentage changes. Across all packages the results agreed with the expectation, since the direction of power flow was from the grid to the load (which is in the same location as the generator), hence the AVR adds positive damping to the system and not negative, damping as observed in the literature.

When the three-phase fault was applied on the HVAC system, the system regained stability in approximately 4 seconds. The voltage and active power responses for the generator displayed similar results (larger impact on the system) for DigSILENT and PST. The graphs obtained on PSAT have more oscillations, which can be linked to the simplifications done on the AVR used. Looking at the responses from PSAT in Appendixes C and D, under manual control, it can be seen that PSAT does not have as many oscillations as DigSILENT and PST.

The load flow for the HVAC-HVDC system also displayed similar results for the bus voltages as well as the active power supplied by the generator. However, the HVAC lines have a cumulative loss of 1.5%, while the single HVDC line has a loss of 1% of the power transmitted. The reactive power absorbed by the external grid and supplied by the generator are also different across the packages. Compared to the HVAC system, the reactive power increased to cater for the reactive power consumed by the converter stations. The reactive power consumed by the converter stations differs for the three packages, as the modelling of the converter stations in the different software packages is different.

The small-signal stability studies for all scenarios showed that the system is stable across all packages. When the AVR and PSS were incorporated in the system the damping ratio increased, improving the stability of the system. PSAT showed the smallest percentage changes as the scenarios changed while DigSILENT showed the highest percentage

changes. When controllers such as AVR and PSS were used, PST displayed the highest values for the damping ratios, making the system more stable in PST.

The HVAC-HVDC system has higher damping ratios when compared with the HVAC system. This means that when a fault is applied the HVAC-HVDC system can respond better to it as the system is more stable. Comparing the HVAC system to the HVAC-HVDC system, when no AVR or PSS is used, the frequency of oscillation of the local mode is higher in the HVAC-HVDC system and the damping ratio is lower in the HVAC-HVDC system. However, in PST the damping ratio is lower in the HVAC system. When only the AVR is used the frequency of oscillations has higher values on the HVAC-HVDC system and the damping ratio is higher in the HVAC system with the exception of PST. When the AVR and PSS are incorporated into the systems, the HVAC system has lower values on the HVAC-HVDC system and the damping ratio has higher values on the HVAC-HVDC systems, with the exception of PSAT.

The fault applied on the HVAC-HVDC system shows that the system regains stability in all packages. PST shows that the voltage and active power responses have larger oscillations and take longer to stabilize when compared to the results obtained in DigSILENT and PSAT. The HVDC system may contribute to voltage instability on the SMIB system in PST based on the results obtained in this dissertation agreeing with literature, which states that when the HVDC scheme is fitted with classical constant power controls, it deprives the parallel AC system from much needed synchronizing torque during disturbances.

For the Single Machine Infinite Bus system, it can be said that DigSILENT is the only software package that behaves as expected for all studies. PST has very large oscillation when the transient stability studies are performed owing to the interaction of the HVAC with the HVDC system. PSAT behaves as expected for the single machine infinite bus system for all studies; however the values differ significantly from those in literature.

7.1.2 TAMM systems

The load flow performed on the HVAC system shows similar responses across all packages.

The small-signal results for the HVAC system show that the system is stable under manual control across all packages. PST has the lowest values for the damping ratios for the inter-area mode as well as for the local modes and PSAT has the highest values for the damping ratios for the local area modes. DigSILENT has the highest damping ratio for the inter-area mode. Between PST and PSAT, PST fully agrees with literature on the HVAC system, while PSAT displays inconsistencies when only AVR is used for the two area multi machine system. When only AVR is used, PSAT shows that the system is stable even though the damping ratio has worsened by 12.29 %. This behaviour is unexpected, as according to the literature the system is expected to be unstable. In DigSILENT and PST the system is unstable, as the inter-area mode has a negative damping ratio. DigSILENT and PST show similar results when compared to PSAT. When the PSS is added to all machines the system regains stability, with the damping ratio for the inter-area mode improving and becoming positive.

Transient simulation results for the HVAC system show that DigSILENT and PST yield very similar results for the voltage, rotor and active power generator responses. PSAT shows more oscillations on the graphs displayed and has a smaller voltage and active power drop as well as smaller maximum voltage and active power output. However, when no AVR or PSS is used on the system, when compared to the DigSILENT and PST, the responses for the voltage, rotor angle and active power show fewer oscillations. Hence it can be assumed that the simplifications done on the AVR in PSAT have led to these oscillations. The simplifications were done because PSAT does not have the simple AVR that was used in the other packages. None of the generators exceeded its capacity in response to the fault on the system.

The HVAC-HVDC system results for the load flow study is similar across all packages, and when compared to the HVAC system, an improvement is noticed as the losses on the transmission lines decrease. Consequently, the active power supplied by generator 3

reduces to 703 MW. The reactive power supplied by the generators increases, as the converter stations need reactive power for their conversion process.

The small-signal results for the HVAC-HVDC system show that the system is stable without AVR. The inter-area modes are very different across all packages, resulting in different damping ratios for the inter-area mode across all packages. These differences in the results obtained are due to the different modelling of the HVDC system. In PST the HVDC system has five modes, PSAT has three modes and DigSILENT has no modes. PST shows the lowest damping ratio of 0.0044, while DigSILENT has the highest damping ratio of 0.0871. The damping ratios for the local area modes differ across the packages, with PST having the lowest damping ratios and PSAT having the highest damping ratios.

When only AVR is used on the generators, the system becomes unstable in DigSILENT and PST, as the damping ratio for the inter-area mode becomes negative. In PSAT, the system remains stable, as the damping ratio improves by 34.9% for the inter-area mode, remaining positive. When the PSS is added to all generators, the system becomes stable in DigSILENT and PST and it remains stable in PSAT even though the damping of the local modes has decreased. When compared to the HVAC system, the HVAC-HVDC system is much more stable when considering the scenario where AVR and PSS are used on all generators. The damping ratio for the inter-area mode is approximately three times better in the HVAC-HVDC system. The damping ratio for the local area modes are almost the same in both the HVAC and HVDC systems. Assuming (since there is no base for comparison) that the behaviour of the HVAC-HVDC system is similar to that of the HVAC system, the performance of the HVAC-HVDC system is as expected.

The transient results for the HVAC-HVDC system improved when compared to the HVAC system, as the settling time reduced to approximately 4 seconds. The voltage and active power output for the generators showed similar results in DigSILENT and PST. None of the generators was overloaded in response to the fault on the system.

As in the Single Machine Infinite Bus system, DigSILENT is the only software package recommended for all studies (considered in this dissertation) that can be presented as

standard software to use on HVAC or HVAC-HVDC systems. PST can be fully trusted when performing HVAC studies only as the results agree with the examples used in literature. When considering the HVAC-HVDC, the Two Area Multi-Machine system behaves quite as expected for all studies. PSAT has to be investigated in more detail as it displays large inconsistencies with literature on the HVAC system, introducing serious doubts about its accuracy for the HVAC-HVDC system as well. Further work is necessary to determine the causes of these inconsistencies.

7.2 Recommendations

In this dissertation, it has been observed that different results are obtained for different software packages when using the same power system model in the small-signal and transient stability studies. Among the three software packages, the one that always behaved as expected is DigSILENT. Therefore, the software that the researcher recommends for load flow, small signal and transient stability studies on both HVAC and HVAC-HVDC systems is DigSILENT. PST performed much better than PSAT, hence I recommend that PST be considered as a stepping stone; however the user cannot fully trust the results for the HVAC-HVDC system for the Single Machine Infinite Bus system. Further work is necessary to determine the causes of this behaviour.

When selecting software packages to study HVDC systems, it is advised that these software packages be from the same class - in other words, compare commercial software packages as a group and academic software packages as a group. Commercial packages are well tested and in most cases computationally efficient; however they can be very cumbersome for educational or research purposes. In most cases, these packages do not allow one to change the source code or add new algorithms. For research purposes flexibility and the ability to prototype easily are more important, hence open research tools are advised and in-depth knowledge of these academic tools is needed. Research packages that allow complete and detailed system modelling - in other words, that can model components such as reactors, filters etc. are recommended in order to make a fair comparison of the software packages.

Based on the work done in this dissertation, the HVAC-HVDC system is recommended for power transmission as it offers fewer losses and is more stable in both small-signal and transient studies.

I recommend that in future the effect harmonics and the use of filters to filter out these harmonics be studied as well.

References

[1] P Kundur, "*Power System Stability and Control*", Mc-Graw-Hill, Inc., 1994

[2] K R Padiyar, "*HVDC Power Transmission Systems*". John Wiley & Sons, 1990

[3] J Arrillaga, "*High Voltage Current Transmission*", IEEE Power Engineering Series 6, Peter Peregrinus Ltd, 1988

[4] A V Ubisse, K A Folly, K Awodele, L Azimoh, D T Oyedokun, S P Sheetekela, "*Comparison of Matlab PST, PSAT and DigSILENT for Power Flow Studies on Parallel HVAC-HVDC Transmission lines*", Proceedings of the 19th Souther African Universities Power Engineering Conference, SAUPEC 2010, University of the Witwatersrand, Johannesburg

[5] D T Oyedokun, "*Power flow and rotor angle stability studies of HVAC-HVDC power system interconnections using DigSILENT*", MSc, University of Cape Town, 2010

[6] T Gönen, "*Electric Power Transmission System Engineering Analysis and Design*", 2nd Edition, CRC Press, 2009

[7] D A Woodfrod, "*HVDC Transmission*", Manitoba HVDC Research Centre, Canada, 1998

[8] A Routray, P K Dash, S K Panda, "*A Fussy Self-Tuning PI Controller for HVDC Links*", IEEE Transactions on Power Electronics, Vol. 11, No. 5, September 1996

[9] K BMohanty, "*Development of Neuro-Fuzzy Controller for a Two Terminal HVDC Link*", Paritantra, Vol. 9, No. 1, June 2004

[10] P K Dash, A Routray, A C Liew, "*Design of an Energy Function Based Fuzzy Tuning Controller for HVDC Links*", Elsevier Electrical Power and Energy Systems, Vol. 21, 1999

[11] Cuiging Du, **"***The Control of VSC-HVDC and its Use for Large Industrial Power Systems***"**, Department of Electric Power Engineering, CHALMERS UNIVERSITY OF TECHNOLOGY, GÄoteborg, Sweden 2003

[12] P M Anderson, A A Fouad, "*Power System Control and Stability*", The Iowa University Press, First Edition, 1977

[13] D S Mudau, "*Comparison of Three Power System Software Packages for Small Signal-Stability Analysis*", MSc, University of Cape Town, August 2009

[14] J Khumalo, "*An Investigation into the Effects of Load Modelling on Transient Stability and Analysis of Voltage Collapse* ", MSc, University of Cape Town, 1992

[15] K K Keberere, "*Variations in Modelling and Algorithmic Factors Impacting on Small-signal Stability Results: Assessment of Five Industrial-grade Power System Simulations Tools*", PHD, University of Cape Town, 2006

[16] M Nthombela, "*An Investigation into the Capabilities of Three Simulation Tools for Small-signal Stability Analysis*", MSc, University of Cape Town, 2007

[17] "*IEEE Guide for Synchronous Generator Modelling Practises in Stability Analyses*", IEEE Std 1110-2002, 2003

[18] K R Padiyar, "*Power System Dynamics Stability and Control*", John Wiley & Sons (Asia) Pte Ltd and Interline Publishing Pvt Ltd, 1996

[19] E Kyriakides, G T Heydt, V Vital, "*Online Parameter Estimation of Round Rotor Synchronous Generators Including Magnetic Saturation*" IEEE Transactions on Energy Conversion, Vol. 20, 2005

[20] "*IEEE Recommended Practice for Excitation System Models for Power System Stability Studies*", IEEE Power Engineering Society, IEEE Std 421.5-2005

[21] J D Glover, M S Sarma, "*Power System Analysis and Design*", 3rd edition, Books/Cole, 2002

[22] M E El-Hawary, "*Introduction to Electrical Power Systems*", IEEE Press on Power Engineering, Wiley, 2008

[23] I R Navarro, "*Dynamic Load Models for Power Systems*", Licentiate Thesis, Lund University, 2002

[24] DigSILENT, *Technical Reference V-14.0.513*.DigSILENT GmbH (C), 2009.

[25] Joe Chow, Power System Toolbox Version 2.0 Load Flow Tutorial and Functions Manual, 2003

[26] Federico Milano, Power System Analysis Toolbox Quick Reference Manual for PSAT version 2.1.2, June 26, 2008

[27] M Khatir et al., "*Comparison of HVDC Line Models in PSB/SIMULINK Based on Steady-State and Transient Considerations*", Acta Electrotechnica et Informatica, Vol. 8, No. 2, 2008

[28] M Khatir et al., "*HVDC Transmission Line Models for Steady-State and Transient Analysis in SIMULINK Environment*", IEEE Conference on Industrial Electronics, IECON 2006

[29] Working Group 14.02, "*The Cigre Benchmark Model – A new proposal with revised parameters*", December 2003

[30] K W V To, A K David, A E Hammad, "*A Robust Co-ordinated Control Scheme for HVDC Transmission with Parallel AC Systems*", IEEE Transactions on Power Delivery, Vol. 9, No. 3, July 1994

[31] IEEE Panel Report, "*HVDC Controls for System Dynamic Performance*", IEEE Transactions on Power Systems, Vol. 6, No. 2, May 1991

[32] R J Piwko, E V Larsen, "*HVDC System Control for Damping of Subsynchronous Oscillations*", IEEE Transactions on Power Apparatus and Systems, vol. PAS-101, No. 7, July 1982

[33] M Bahrman, E V Larsen, R J Piwko, H S Patel, "*Experience with HVDC-Turbine-Generator Torsional Interaction at Square Butte*", IEEE Transactions on Power Apparatus and Systems, Vol. PAS-99, No. 3, May/June 1980

[34] Y Jiang-Häfner et al., "*Improvement of Subsynchronous Torsional Damping Using VSC HVDC*", IEEE Proceedings, Vol. 4, 2002

[35] P Zizliauskas, "*Subsynchronous Torque Interaction for HVDC Light B*", Lund University, 2001

[36] G Rogers, "*Power System Oscillations*", Kluwer Academic Publishers, 2000

[37] A E Hammad, "*Stability and Control of HVDC and AC transmission in Parallel*", IEEE Transactions on Power Delivery, Vol. 14, No. 4, October 1999

[38] P Ye, Y Sui, Y Yuan, X Li, J Tao, "*Transient Stability Analysis of Hu-Liao HVDC and AC Parallel Transmission System*", Smart Grid and Renewable Energy, Vol. 1, 2010

Research Publications

---

1. A V Ubisse, K A Folly, Power Flow Studies on HVAC/HVDC Transmission Lines, 18th SAUPEC Proceedings, January 2009, Pages 276-280

2. A V Ubisse, K A Folly, K Awodele, L Azimoh, D T Oyedokun, S P Sheetekela, Comparison of Matlab PST, PSAT and DigSilent for Power Flow Studies on Parallel HVAC-HVDC Transmission Lines, 19th SAUPEC Proceedings, January 2010, Pages 153-157

Appendices

Appendix A: A brief description of small signal and transient stability is given in this appendix.

Appendix B: This appendix gives the data for the SMIB; TAMM and HVDC system used in chapters 5 and 6, as well as the AVR and PSS data

Appendix C: This appendix presents the results obtained when the small signal and transient stability studies were performed on the HVAC and HVAC-HVDC SMIB systems.

Appendix D: This appendix presents the results obtained when the small signal and transient stability studies were performed on the HVAC and HVAC-HVDC TAMM systems.

Appendix A

Small Signal and Transient Stability

Small signal stability

Small signal stability can be described as the ability of a power system to maintain synchronism when subjected to small disturbances, such as small variations in the loads and generation.

Instability can occur either as a result of a steady increase in the rotor angle due to insufficient synchronizing torque or as a result of rotor oscillations which increase in amplitude due to insufficient damping torque.

Small signal stability of power systems focus on the following types of oscillations:

- Local modes are the modes that are associated with the swinging of units at a generating station with respect to the rest of the power system. They are localized at a power station or are a small part of a power system.

- Inter-area modes are the modes that are associated with a group of machines in one part of the system oscillating against a group(s) of machines in another part(s) of the system. This mode results from a weak tie(s) interconnecting the different parts of the system.

- Control modes are the modes that are associated with generating units and other controls. The instability of these modes is a result of poorly tuned exciters, speed governors, HVDC converters and static var compensators.

- Torsional modes are the modes that are associated with the turbine-generator shaft system rotational components. Interaction with excitation controls, speed governors, HVDC controls and series-capacitor-compensated lines may cause instability of torsional modes [2].

Transient stability

Transient stability of a power system refers to the ability of a system to remain stable under transient disturbances, in other words, maintain synchronism when subjected to severe disturbances such as faults and switching of lines. The stability of a system is primarily dependent on the initial state of the system as well as on the severity of the disturbance.

Under transient stability, two forms of instability can be encountered: a case where the rotor angle keeps increasing steadily until synchronism is lost owing to insufficient synchronizing torque, known as first-swing, or a case where the system is stable in the first-swing, but the oscillations keep growing owing to insufficient damping torque [2].

Appendix B

Systems Data

B1 Single machine infinite bus system

The data presented below are valid for both for the HVAC and HVAC-HVDC systems. However, the HVDC data only apply to the HVAC-HVDC SMIB system. The data are given both in pu and in SI units, as DigSILENT uses SI units while PST and PSAT use pu units for most of the components.

Table B.1: HVDC Converter station parameters

Parameter	Rectifier	Inverter
Rated DC voltage (kV)	500	500
Rated power	1000	1000
min α	15	-
max α	26	-
min γ	-	135
max γ	-	170
Commutation reactance	3	3
Control type	CC	CEA
Current setpoint (kA)	0.97	-

Table B.2: HVAC / HVDC Transmission Line parameters

Parameter	HVDC Line		HVAC Line	
	SI/km*	pu/km	SI/km*	pu/km
Resistance (R)	0.0281	0.0001124	0.0281	0.0001124
Reactance (X)	0.027	0.000108	0.27	0.00108
Susceptance (B)	0.433	0.0001075	4.3	0.001075
Rated voltage (kV)	500		500	
Rated Current (kA)	2		0.125	
Length (km)	500		500	

* The SI used for R, X and B are Ohms (R, X) and μS (B).

Table B.3: Transformer parameters

Parameter	HVDC Trs		HVAC Trs	
	Tr1	Tr2	Tr3	Tr4
Voltage (kV)	345/500	500/230	345/500	500/230
Nominal Power (MVA)	1000	1000	1000	1000
Reactance (pu)	0.15	0.15	0.1	0.1

Synchronous generator data

$X_d = 1.81$ $X'_d = 0.3$ $X''_d = 0.23$

$X_q = 1.76$ $X'_q = 0.65$ $X''_q = 0.25$

$X_l = 0.16$ $R_a = 0.003$

$T'_{do} = 8s$ $T''_{do} = 0.03s$

$T'_{qo} = 1s$ $T''_{qo} = 0.07s$

$A_{sat} = 0.031$ $B_{sat} = 6.93$

$H = 3.5$

AVR

$K_A = 200$ $T_A = 0.05s$ $T_R = 0.01s$

PSS

K = 20 T = 10s

$T_1 = 0.05s$ $T_2 = 0.02s$ $T_3 = 3s$ $T_4 = 5.4s$

B2 Two Area Multi-machine System

Table B.4: HVDC Converter Station parameters

Parameter	Rectifier	Inverter
Rated DC voltage (kV)	500	500
Rated power	500	500
min α	15	-
max α	40	-
min γ	-	135
max γ	-	170
Commutation reactance	3	3
Control type	CC	CEA
Current Setpoint (kA)	0.395	-

Table B.5: HVAC / HVDC Transmission Line parameters

Parameter	HVDC Line		HVAC Line	
	SI/km*	pu/km	SI/km*	pu/km
Resistance (R)	0.0281	0.0001124	0.0529	0.0001
Reactance (X)	0.02	0.0001	0.529	0.001
Susceptance (B)	0.439	0.00011	3.371	0.001
Rated voltage (kV)	500		230	
Rated Current (kA)	0.46		1	
Length (km)	220		220	

Table B.6: Transformer parameters

Parameter	HVDC Trs		HVAC Trs	
	Tr	Tr	Tr	Tr
Voltage (kV)	230/500	500/230	20/230	230/20
Nominal Power (MVA)	900	900	900	900
Reactance (pu)	0.15	0.15	0.15	0.15

Synchronous generator data

$X_d = 1.8$ $X'_d = 0.3$ $X''_d = 0.25$

$X_q = 1.7$ $X'_q = 0.55$ $X''_q = 0.25$

$X_l = 0.2$ $R_a = 0.0025$

$T'_{do} = 8s$ $T''_{do} = 0.03s$

$T'_{qo} = 0.4s$ $T''_{qo} = 0.05s$

$A_{sat} = 0.015$ $B_{sat} = 9.6$

$\psi_{TI} = 0.9$

$S_{1.0} = 0.039$ $S_{1.2} = 0.223$

$K_D = 0$

$H = 6.5$(For machines 1 and 2) $H = 6.175$(for machines 3 and 4)

AVR

$K_A = 200$ $T_A = 0.05s$ $T_R = 0.01s$

PSS

K = 20 T = 10s

T_1 = 0.05s T_2 = 0.02s T_3 = 3s T_4 = 5.4s

Appendix C

SMIB Small Signal and Transient Simulations

SMIB eigenvalues, frequency and damping ratios

Presented in the tables below are the complete eigenvalue, frequency and damping ratios for the HVAC and HVAC-HVDC systems discussed in this dissertation.

Table C.1: HVAC SMIB manual control

Mode	Eigen-value (frequency, damping ratio)		
	DigSILENT	PST	PSAT
1 &2	-0.4394 ± j6.0672 (f = 0.965; ζ = 0.0723)	-0.4383 ± j6.2591 (f = 0.996; ζ = 0.0699)	-0.7283 ± 6.3054 (f = 1.0035; ζ = 0.1147)
3	-36.5165 (f = 0; ζ = 1)	-36.2238 (f = 0; ζ = 1)	-34.2857 (f = 0; ζ = 1)
4	-20.5015 (f = 0; ζ = 1)	-21.7903 (f = 0; ζ = 1)	-21.9745 (f = 0; ζ = 1)
5	-10 (f = 0; ζ = 1)	-1.3436 (f = 0; ζ = 1)	-1.4223 (f = 0; ζ = 1)
6	-10 (f = 0; ζ = 1)	-0.2569 (f = 0; ζ = 1)	-0.0672 (f = 0; ζ = 1)
7	-1.4421 (f = 0; ζ = 1)		
8	-1 (f = 0; ζ = 1)		
9	-1 (f = 0; ζ = 1)		
10	-0.2439 (f = 0; ζ = 1)		
11	-0.0106 (f = 0; ζ = 1)		
12	0 (f = 0; ζ = 1)		
13	0 (f = 0; ζ = 1)		

Table C.2: HVAC SMIB with AVR only

Mode	Eigen-value (frequency, damping ratio)		
	DigSILENT	PST	PSAT
1 &2	-0.6734 ± j5.6603 (f = 0.9; ζ = 0.1181)	-0.78 ± j5.87 (f = 0.93; ζ = 0.13)	-0.9385 ± 6.1026 (f = 0.9713; ζ = 0.152)
3	-101.1472 (f = 0; ζ = 1)	-95.5613 (f = 0; ζ = 1)	-1000000 (f = 0; ζ = 1)
4	-43.6611 (f = 0; ζ = 1)	-23.3436 (f = 0; ζ = 1)	-1000000 (f = 0; ζ = 1)
5	-20.7289 (f = 0; ζ = 1)	-19.491 + j14.3765 (f = 2.288; ζ = 0.8048)	-108.46 + j27.34 (f = 4.35; ζ = 0.973)
6	-5.7474 + j15.638 (f = 2.488; ζ = 0.3449)	-19.491 - j14.3765 (f = 2.288; ζ = 0.8048)	-108.46 - j27.34 (f = 4.35; ζ = 0.973)
7	-5.7474 - j5.638 (f = 2.488; ζ = 0.3449)	-1.0519 (f = 0; ζ = 1)	-21.739 (f = 0; ζ = 1)
8	-10 (f = 0; ζ = 1)		-8.729 + j22.438 (f = 3.571; ζ = 0.375)
9	-10 (f = 0; ζ = 1)		-8.729 - j22.438 (f = 3.571; ζ = 0.375)
10	-1.1695 (f = 0; ζ = 1)		-1.19500 (f = 0; ζ = 1)
11	-1 (f = 0; ζ = 1)		
12	-1 (f = 0; ζ = 1)		
13	-0.00004 (f = 0; ζ = 1)		
14	0 (f = 0; ζ = 1)		
15	0 (f = 0; ζ = 1)		
16	0 (f = 0; ζ = 1)		

Table C.3: HVAC SMIB with AVR and PSS

Mode	Eigen-value (frequency, damping ratio)		
	DigSILENT	PST	PSAT
1 &2	-1.5632 ± j5.1205 (f = 0.8149 ζ = 0.2919)	-1.7813 ± j5.2425 (f = 0.8344; ζ = 0.3217)	-1.3942 ± 5.8975 (f = 0.9386; ζ = 0.2301
3	-101.1488 (f = 0; ζ = 1)	-95.5888 (f = 0; ζ = 1)	-1000000 (f = 0; ζ = 1)
4	-41.6568 (f = 0; ζ = 1)	-36.1421 (f = 0; ζ = 1)	-1000000 (f = 0; ζ = 1)
5	-34.8025 (f = 0; ζ = 1)	-21.7165 (f = 0; ζ = 1)	-108.15 + j27.05 (f = 4.3; ζ = 0.969)
6	-20.4873 (f = 0; ζ = 1)	-16.382 + j18.7405 (f = 2.983; ζ = 0.6581)	-108.15 - j27.05 (f = 4.3; ζ = 0.969)
7	-3.6784 + j17.0186 (f = 2.708; ζ = 0.2113)	-16.382 - j18.7405 (f = 2.983; ζ = 0.6581)	-100 (f = 0; ζ = 1)
8	-3.6784 - j17.0186 (f = 2.708; ζ = 0.2113)	-1.0197 (f = 0; ζ = 1)	-32.537 (f = 0; ζ = 1)
9	-10 (f = 0; ζ = 1)	-0.1009 (f = 0; ζ = 1)	-22.099 (f = 0; ζ = 1)
10	-10 (f = 0; ζ = 1)		-7.3 + j22.579 (f = 3.594; ζ = 0.325)
11	-1.1309 (f = 0; ζ = 1)		-7.3 - j22.579 (f = 3.594; ζ = 0.325)
12	-1 (f = 0; ζ = 1)		-1.174 (f = 0; ζ = 1)
13	-10 (f = 0; ζ = 1)		-0.1 (f = 0; ζ = 1)
14	-0.2269 (f = 0; ζ = 1)		
15	-0.00002 (f = 0; ζ = 1)		
16	0 (f = 0; ζ = 1)		
17	0 (f = 0; ζ = 1)		
18	0 (f = 0; ζ = 1)		
19	0 (f = 0; ζ = 1)		

Table C.4: HVAC-HVDC SMIB manual control

Mode	Eigen-value (frequency, damping ratio)		
	DigSILENT	PST	PSAT
1 &2	-0.3009 ± j6.4045 (f = 1.0193; ζ = 0.0469)	-0.4849 ± j6.7043 (f = 1.067; ζ = 0.0721)	-0.7263 ± j6.4062 (f = 1.0196; ζ = 0.1126)
3	-35.6644 (f = 0; ζ = 1)	-36.4086 (f = 0; ζ = 1)	-34.4018 (f = 0; ζ = 1)
4	-17.0484 (f = 0; ζ = 1)	-21.53 (f = 0; ζ = 1)	-21.852 (f = 0; ζ = 1)
5	-10 (f = 0; ζ = 1)	-1.5902 (f = 0; ζ = 1)	-1.4276 (f = 0; ζ = 1)
6	-10 (f = 0; ζ = 1)	-0.5087 (f = 0; ζ = 1)	-0.0693 (f = 0; ζ = 1)
7	-1.2832 (f = 0; ζ = 1)	0 (f = 0; ζ = 1)	-42.9474 (f = 0; ζ = 1)
8	-1 (f = 0; ζ = 1)	0 (f = 0; ζ = 1)	-0.816 (f = 0; ζ = 1)
9	-1 (f = 0; ζ = 1)	0.0417 (f = 0; ζ = -1)	0 (f = 0; ζ = 1)
10	-0.1625 (f = 0; ζ = 1)	0.4433 + j1.4184 (f = 0.2257; ζ = -0.02983)	
11	-0.0062 (f = 0; ζ = 1)	0.4433 - j1.4184 (f = 0.2257; ζ = -0.02983)	
12	0 (f = 0; ζ = 1)		
13	0 (f = 0; ζ = 1)		

Table C.5: HVAC-HVDC SMIB with AVR only

Mode	Eigen-value (frequency, damping ratio)		
	DigSILENT	PST	PSAT
1 &2	-0.6414 ± j5.6508 (f = 0.899; ζ = 0.1128)	-0.99 ± j6.05 (f = 0.96; ζ = 0.16)	-0.9058 ± 6.2434 (f = 0.9937; ζ = 0.1436)
3	-101.4737 (f = 0; ζ = 1)	-95.51 (f = 0; ζ = 1)	-1000000 (f = 0; ζ = 1)
4	-43.9541 (f = 0; ζ = 1)	-23.479 (f = 0; ζ = 1)	-1000000 (f = 0; ζ = 1)
5	-20.3219 (f = 0; ζ = 1)	-19.626 + j14.6993 (f = 2.3395 ζ = 0.8004)	-108.53 + j27.43 (f = 4.37; ζ = 0.955)
6	-3.2506 + j18.974 (f = 3.019; ζ = 0.1688)	-19.626 - j14.6993 (f = 2.3395 ζ = 0.8004)	-108.53 - j27.43 (f = 4.37; ζ = 0.955)
7	-3.2506 - j18.974 (f = 3.019; ζ = 0.1688)	-1.0662 + j0.0868 (f = 0.0138; ζ = 0.0.9967)	-42.85 (f = 0; ζ = 1)
8	-10 (f = 0; ζ = 1)	-1.0662 – j0.0868 (f = 0.0138; ζ = 0.0.9967)	-21.687 (f = 0; ζ = 1)
9	-10 (f = 0; ζ = 1)	-0.0705 (f = 0; ζ = 1)	-8.756 + j22.488 (f = 4.365; ζ = 0.411)
10	-1.2139 (f = 0; ζ = 1)	0 (f = 0; ζ = 1)	-8.756 - j22.488 (f = 4.365; ζ = 0.411)
11	-1 (f = 0; ζ = 1)	0 (f = 0; ζ = 1)	-1.2285 (f = 0; ζ = 1)
12	-1 (f = 0; ζ = 1)	1.7968 (f = 0; ζ = -1)	-0.813 (f = 0; ζ = 1)
13	-0.00035 (f = 0; ζ = 1)		0 (f = 0; ζ = 1)
14	0 (f = 0; ζ = 1)		
15	0 (f = 0; ζ = 1)		
16	0 (f = 0; ζ = 1)		

Table C.6: HVAC-HVDC SMIB with AVR and PSS

Mode	Eigen-value (frequency, damping ratio)		
	DigSILENT	PST	PSAT
1 &2	-1.7403 ± j4.3126 (f = 0.686; ζ = 0.3742)	-1.8351 ± j5.169 (f = 0.823; ζ = 0.3346)	-1.3664 ± 6.0381 (f = 0.9609; ζ = 0.2207)
3	-101.4792 (f = 0; ζ = 1)	-95.5373 (f = 0; ζ = 1)	-1000000 (f = 0; ζ = 1)
4	-39.9048 + j5.0329 (f = 0.801; ζ = 0.9921)	-36.2402 (f = 0; ζ = 1)	-1000000 (f = 0; ζ = 1)
5	-39.9048 - j5.0329 (f = 0.801; ζ = 0.9921)	-21.5054 (f = 0; ζ = 1)	-108.24 + j27.16 (f = 4.33; ζ = 0.945)
6	-18.9241 (f = 0; ζ = 1)	-16.788 + j19.1014 (f = 3.0401; ζ = 0.6602)	-108.24 - j27.16 (f = 4.33; ζ = 0.945)
7	-10 (f = 0; ζ = 1)	-16.788 -+ j19.1014 (f = 3.0401; ζ = 0.6602)	-100 (f = 0; ζ = 1)
8	-10 (f = 0; ζ = 1)	-0.9455 + j0.2204 (f = 0.0351; ζ = 0.9739)	-42.135 (f = 0; ζ = 1)
9	-1.2053 (f = 0; ζ = 1)	-0.9455 - j0.2204 (f = 0.0351; ζ = 0.9739)	-33.307 (f = 0; ζ = 1)
10	-1 (f = 0; ζ = 1)	-0.1086 (f = 0; ζ = 1)	-21.933 (f = 0; ζ = 1)
11	-1 (f = 0; ζ = 1)	-0.0682 (f = 0; ζ = 1)	-7.319 + j22.588 (f = 3.595; ζ = 0.439)
12	-0.02375 + j21.9075 (f = 3.486; ζ = 0.0011)	0 (f = 0; ζ = 1)	-7.319 - j22.588 (f = 3.595; ζ = 0.439)
13	-0.02375 – j21.9075 (f = 3.486; ζ = 0.0011)	0 (f = 0; ζ = 1)	-1.209 (f = 0; ζ = 1)
14	-0.2237 (f = 0; ζ = 1)	2.2033 (f = 0; ζ = -1)	-0.813 (f = 0; ζ = 1)
15	-0.00015 (f = 0; ζ = 1)		-0.1 (f = 0; ζ = 1)
16	0 (f = 0; ζ = 1)		0 (f = 0; ζ = 1)
17	0 (f = 0; ζ = 1)		
18	0 (f = 0; ζ = 1)		
19	0 (f = 0; ζ = 1)		

The figures below display the voltage, angle and active power response of the machine in the SMIB system for the HVAC and HVAC-HVDC systems under manual control only.

HVAC system

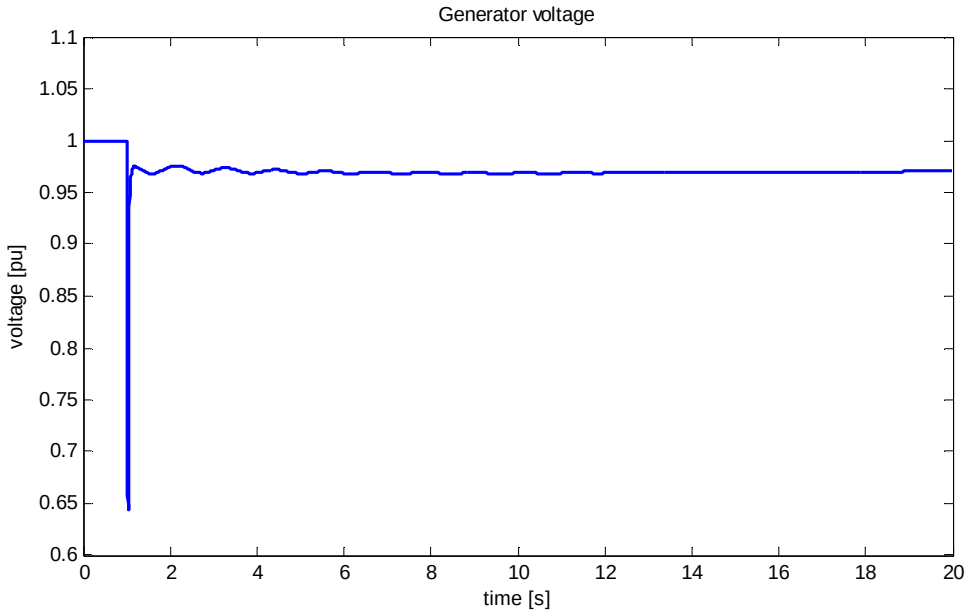

Figure C.1: DigSILENT voltage response

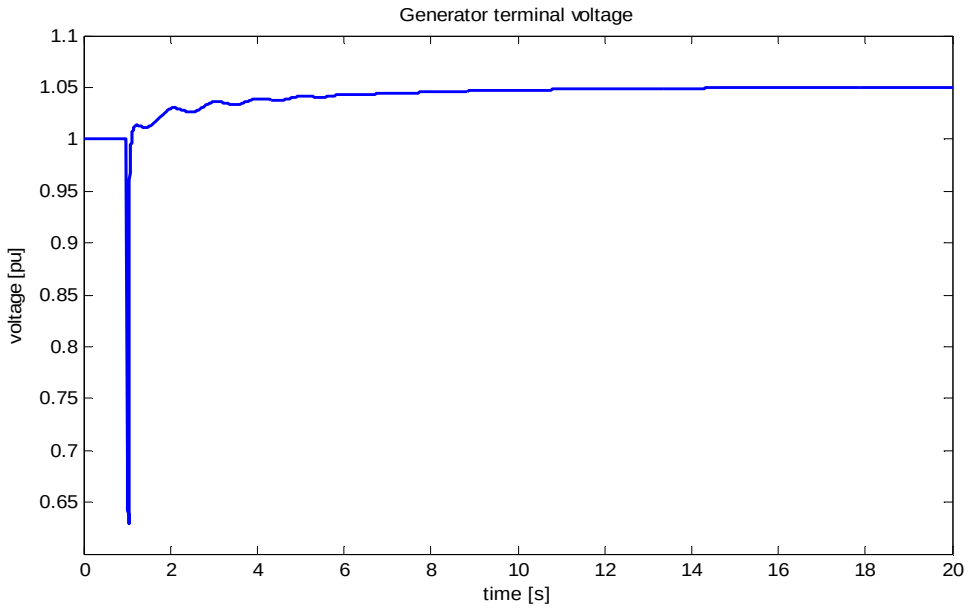

Figure C.2: PST voltage response

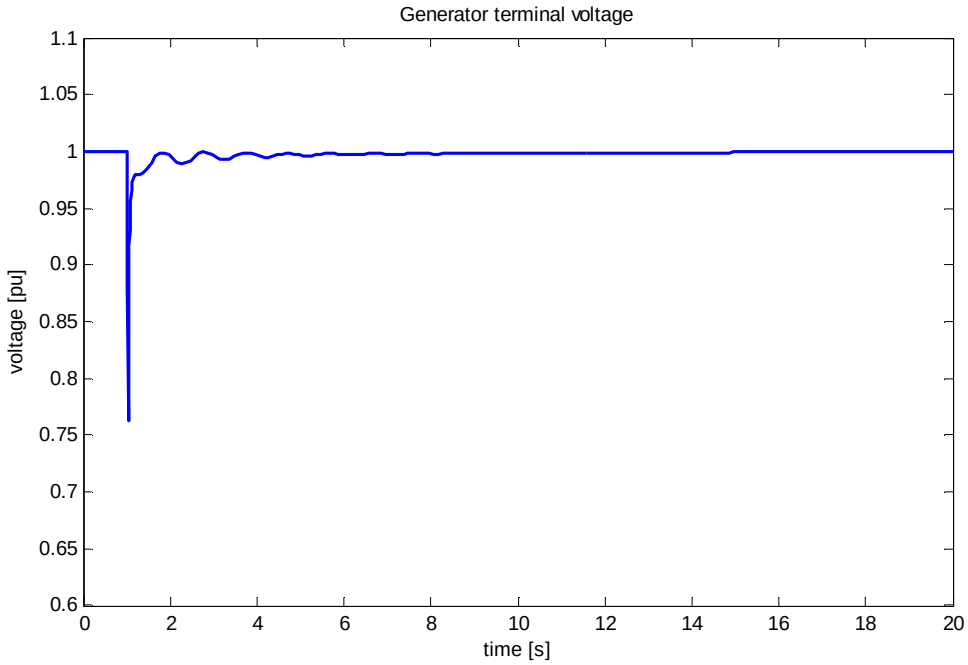

Figure C.3: PSAT voltage response

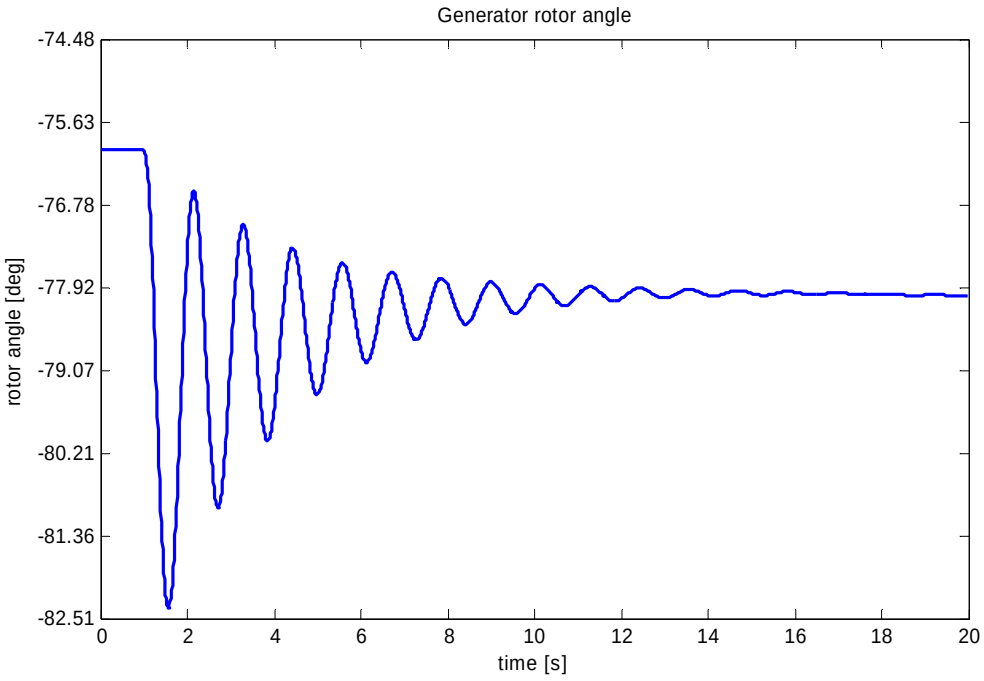

Figure C.4: DigSILENT rotor angle response

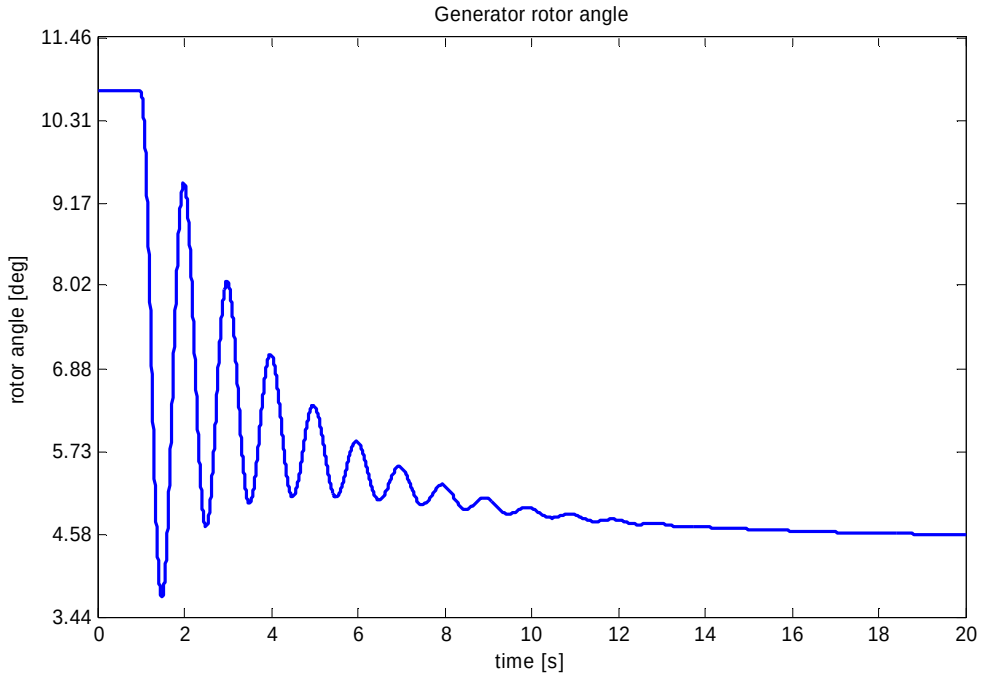

Figure C.5: PST rotor angle response

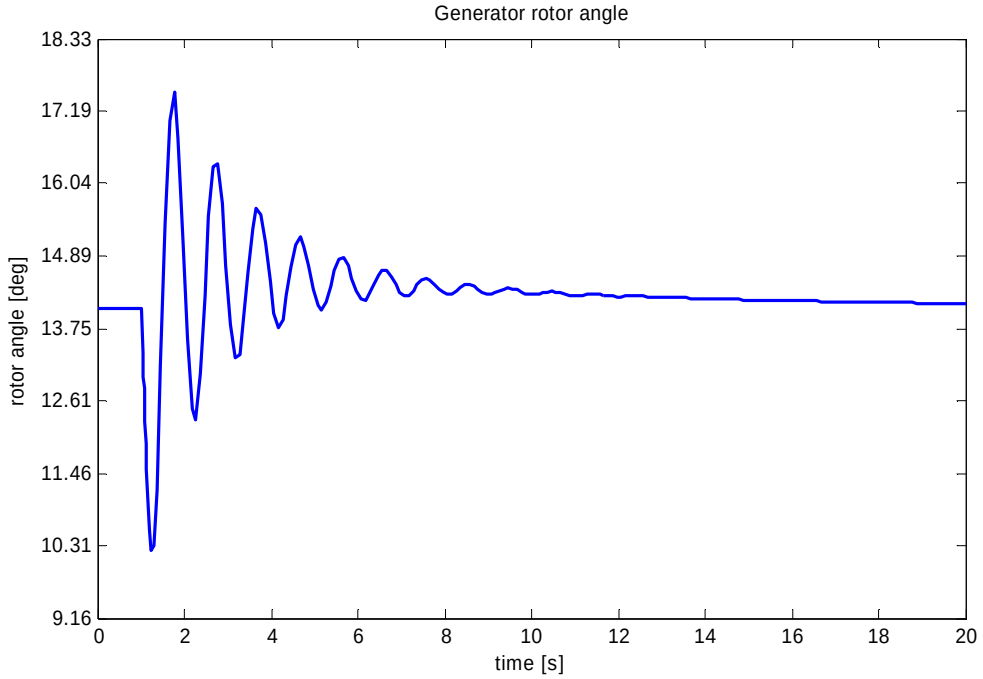

Figure C.6: PSAT rotor angle response

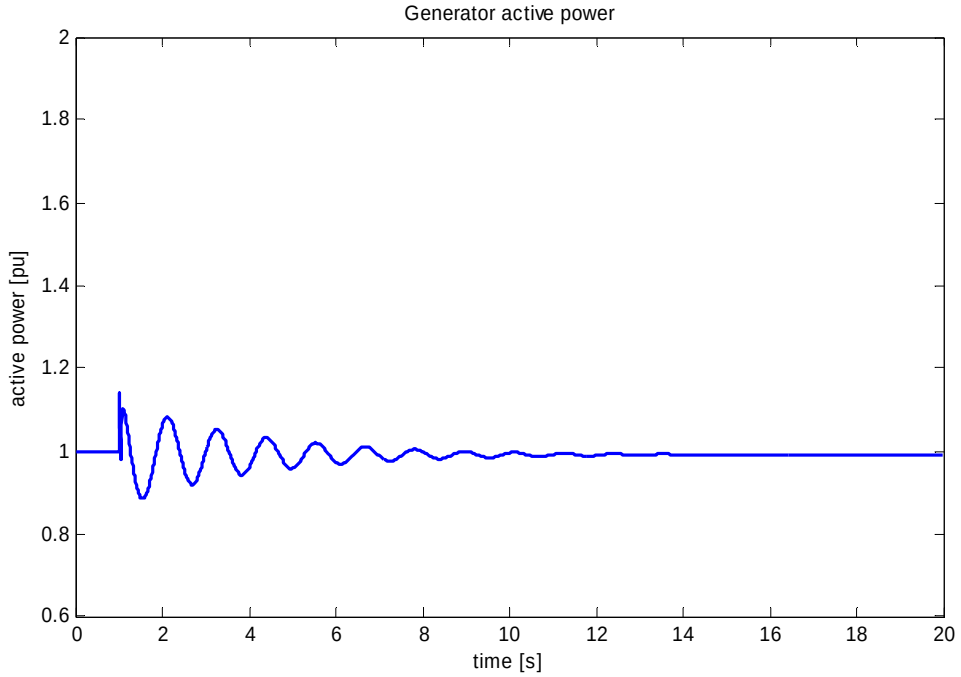

Figure C.7: DigSILENT active power response

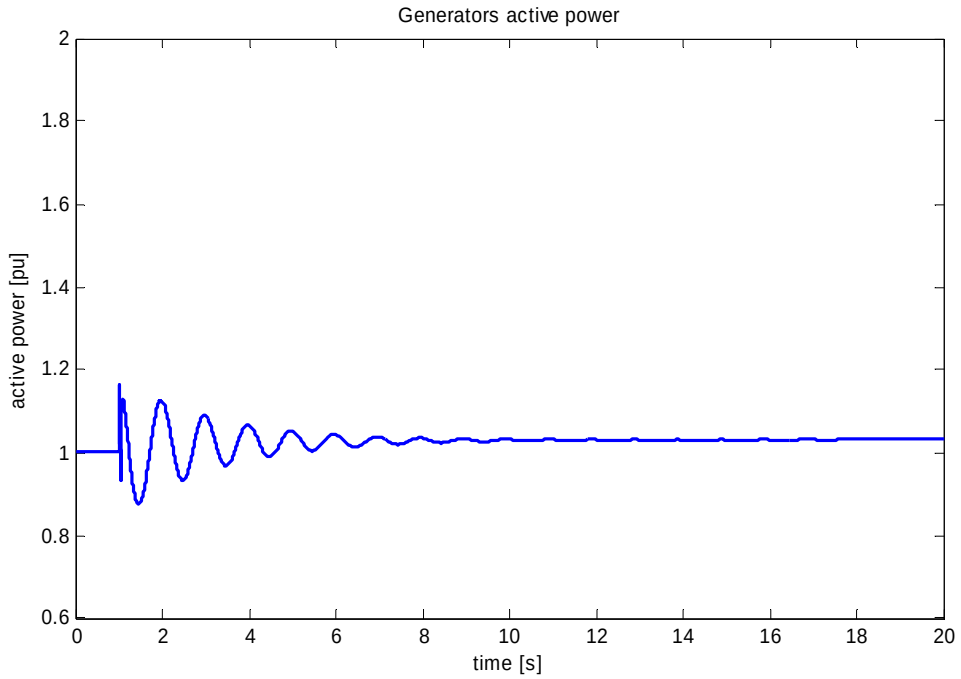

Figure C.8: PST active power response

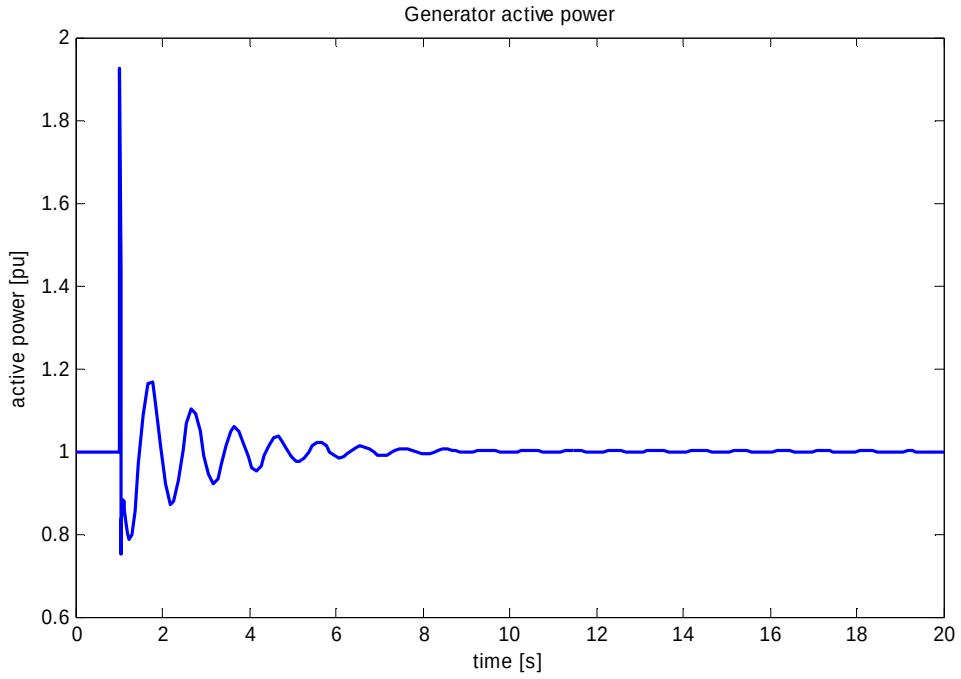

Figure C.9: PSAT active power response

HVAC-HVDC SMIB system

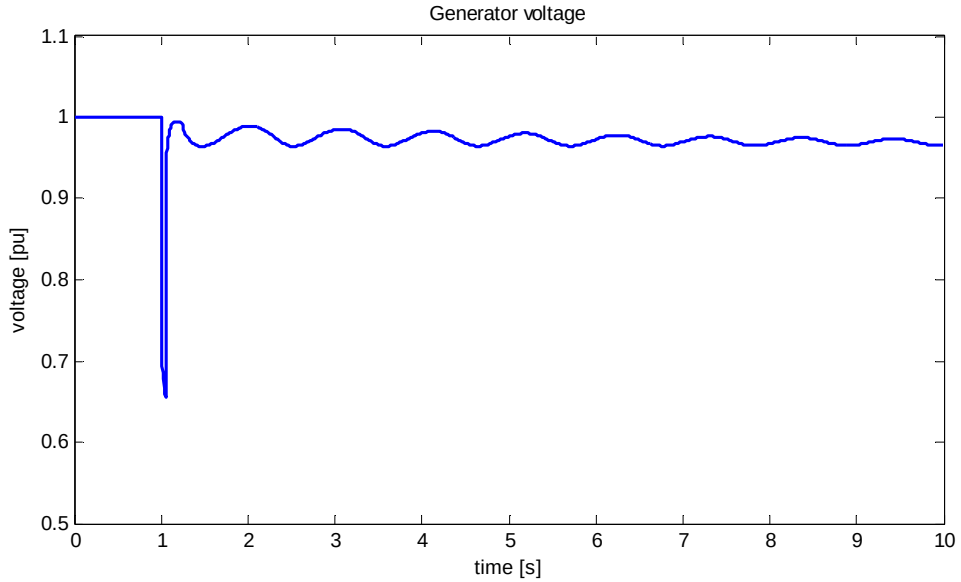

Figure C.10: DigSILENT voltage response

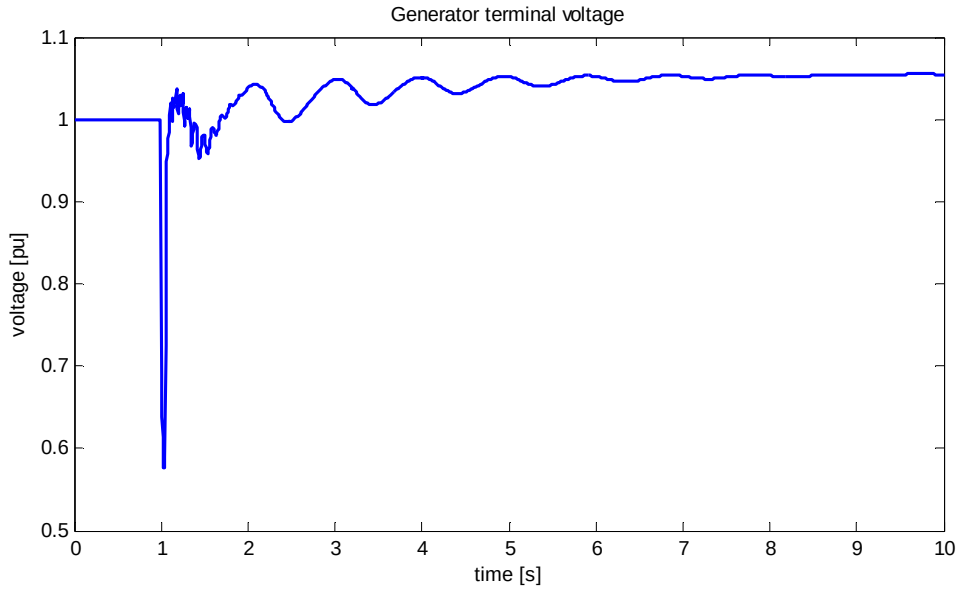

Figure C.11: PST voltage response

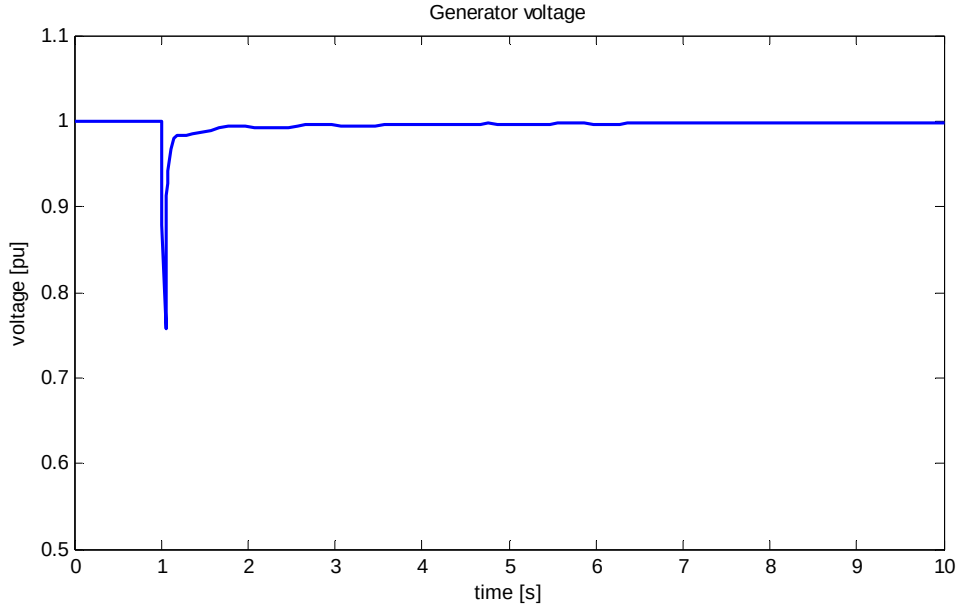

Figure C.13: PSAT voltage response

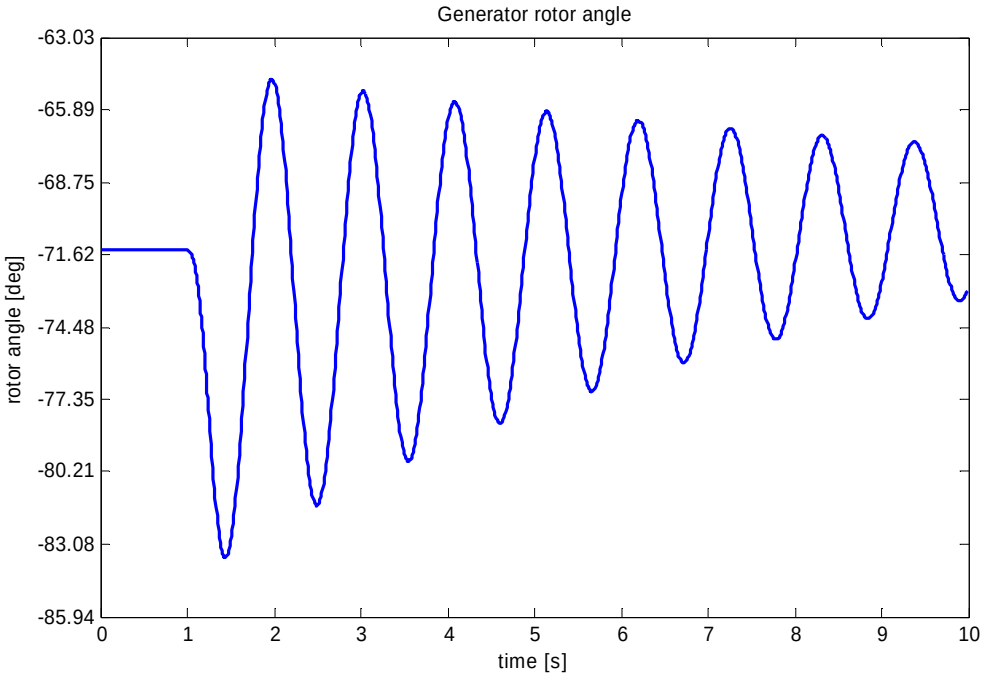

Figure C.13: DigSILENT rotor angle response

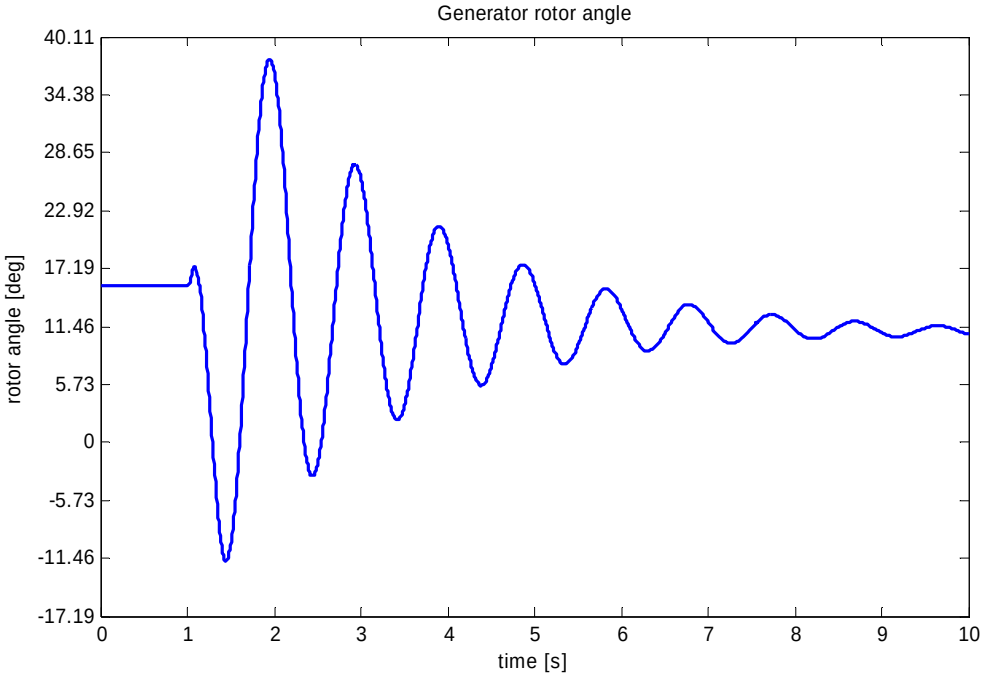

Figure C.12: PST rotor angle response

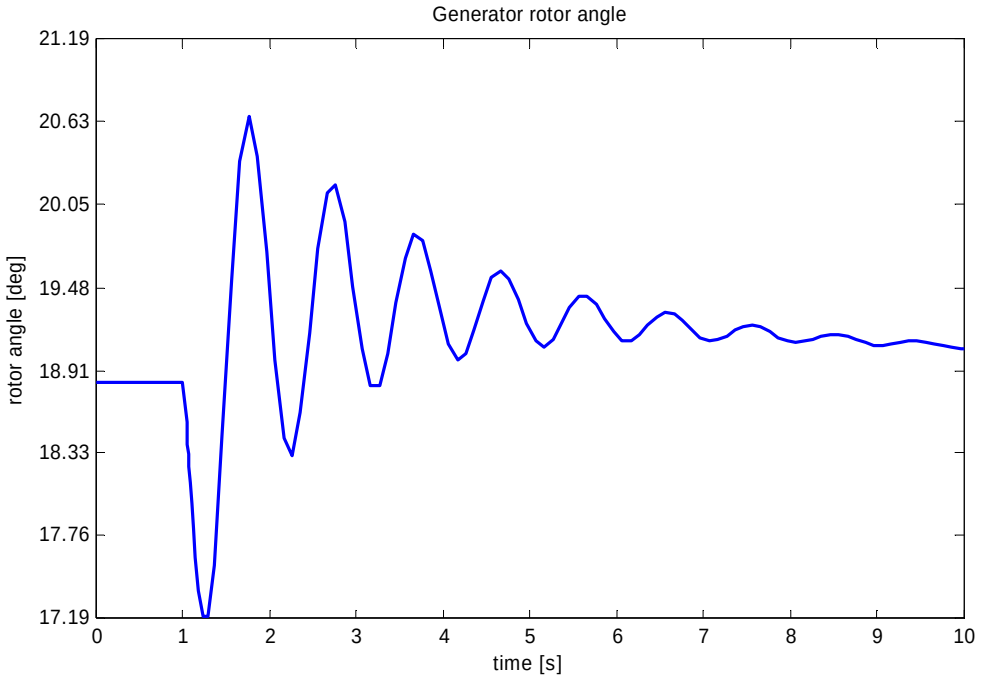

Figure C.15: PSAT rotor angle response

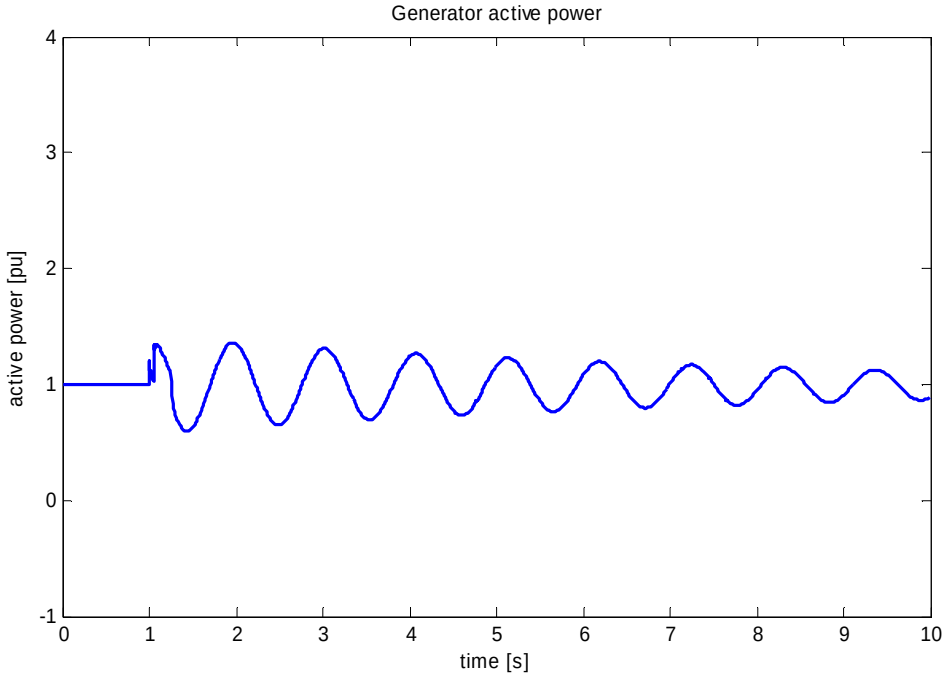

Figure C.16: DigSILENT active power response

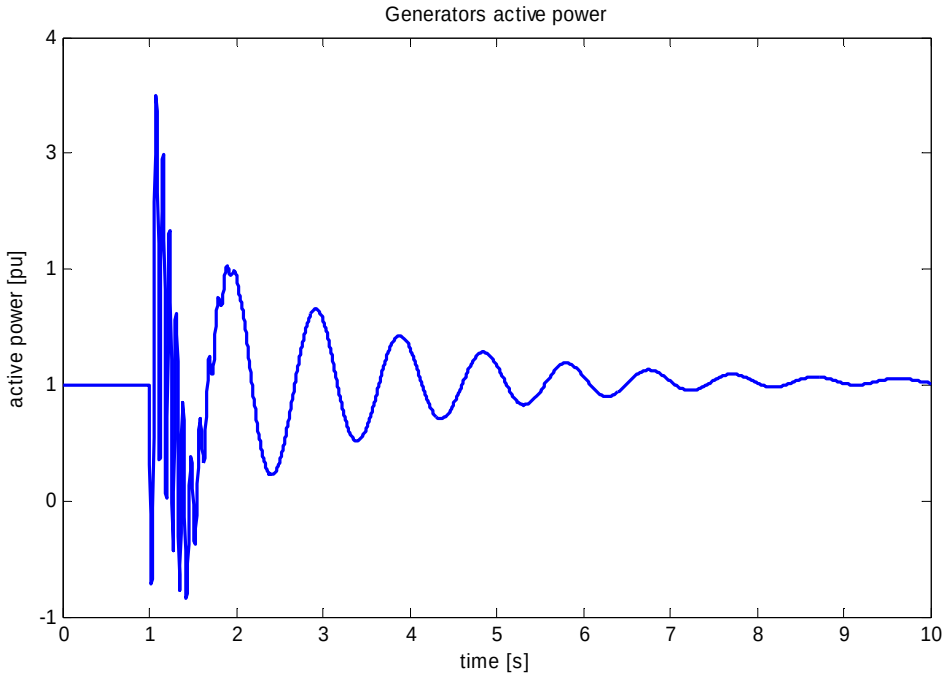

Figure C.17: PST active power response

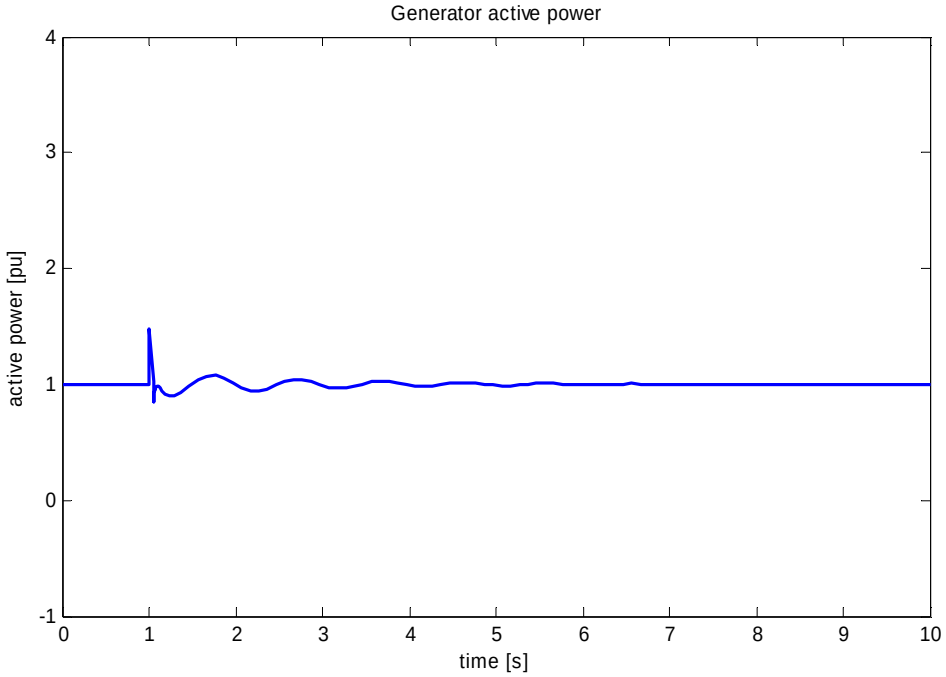

Figure C- 18: PSAT active power response

Appendix D

TAMM Small Signal and Transient Simulations

TAMM eigenvalues, frequency and damping ratios

In the tables below, the complete eigenvalues, frequencies and damping ratios for the HVAC and HVAC-HVDC Two-Area Multi-Machine systems discussed in this dissertation are presented.

Table D.1: TAMM HVAC with manual control

Mode	Eigen-value (frequency, damping ratio)		
	DigSILENT	PST	PSAT
1&2	-0.1402 ± j3.5166 (f = 0.5596; ζ = 0.0398)	-0.0949 ± j3.5115 (f = 0.5589; ζ = 0.027)	-0.1234 ± j3.5172 (f = 0.5598; ζ = 0.035)
3&4	-0.6058 ± j6.9444 (f = 1.1052; ζ = 0.0869)	-0.5463 ± j7.0662 (f = 1.1246; ζ = 0.0771)	-0.826 ± j7.3831 (f = 1.1751; ζ = 0.1112)
5&6	-0.6029 ± j6.7156 (f = 1.0688; ζ = 0.0894)	-0.5496 ± j6.8386 (f = 1.0884; ζ = 0.0801)	-0.8054 ± j7.1386 (f = 1.1361; ζ = 0.1121)
7	-37.2402 (f = 0; ζ = 1)	-37.2323 (f = 0; ζ = 1)	-38.8628 + j0.4617 (f = 0.0735; ζ = 0.9999)
8	-37.1782 (f = 0; ζ = 1)	-37.1659 (f = 0; ζ = 1)	-38.8628 - j0.4617 (f = 0.0735; ζ = 0.9999)
9	-34.9853 (f = 0; ζ = 1)	-36.1519 (f = 0; ζ = 1)	-38.4332 + j0.573 (f = 0.0912; ζ = 0.9999)
10	-33.9951 (f = 0; ζ = 1)	-35.9607 (f = 0; ζ = 1)	-38.4332 - j0.573 (f = 0.0912; ζ = 0.9999)
11	-33.2392 (f = 0; ζ = 1)	-35.0513 (f = 0; ζ = 1)	-33.9525 (f = 0; ζ = 1)
12	-33.1067 (f = 0; ζ = 1)	-34.1425 (f = 0; ζ = 1)	-32.5531 (f = 0; ζ = 1)
13	-26.7786 (f = 0; ζ = 1)	-30.2705 (f = 0; ζ = 1)	-24.0365 (f = 0; ζ = 1)
14	-25.4189 (f = 0; ζ = 1)	-29.1942 (f = 0; ζ = 1)	-21.8372 (f = 0; ζ = 1)
15	-5.6582 (f = 0; ζ = 1)	-4.7782 (f = 0; ζ = 1)	-6.8135 (f = 0; ζ = 1)

16	-5.6106 (f = 0; ζ = 1)	-4.7738 (f = 0; ζ = 1)	-6.7595 (f = 0; ζ = 1)
17	-4.2087 (f = 0; ζ = 1)	-3.2222 (f = 0; ζ = 1)	-4.6339 (f = 0; ζ = 1)
18	-3.3841 (f = 0; ζ = 1)	-2.3807 (f = 0; ζ = 1)	-3.5529 (f = 0; ζ = 1)
19	-0.3851 (f = 0; ζ = 1)	-0.2873 (f = 0; ζ = 1)	-0.2028 (f = 0; ζ = 1)
20	-0.1995 (f = 0; ζ = 1)	-0.1872 (f = 0; ζ = 1)	-0.19861 (f = 0; ζ = 1)
21	-0.1882 (f = 0; ζ = 1)	-0.1675 (f = 0; ζ = 1)	-0.0812 (f = 0; ζ = 1)
22	-0.0521 (f = 0; ζ = 1)	-0.0199 (f = 0; ζ = 1)	-0.0109 (f = 0; ζ = 1)
23	-0.0296 (f = 0; ζ = 1)	0.0033 (f = 0; ζ = -1)	0 (f = 0; ζ = 1)
24	0 (f = 0; ζ = 1)	0.0182 (f = 0; ζ = -1)	0 (f = 0; ζ = 1)

Table D.2: TAMM HVAC with AVR only

Mode	Eigen-value (frequency, damping ratio)		
	DigSILENT	PST	PSAT
1&2	0.0615 ± j3.9477 (f = 0.6283; ζ = -0.0156)	0.04 ± j3.98 (f = 0.63; ζ = -0.01)	-0.1104 ± j3.5933 (f = 0.5719; ζ = 0.0307)
3&4	-0.6246 ± j7.2932 (f = 1.1607; ζ = 0.0853)	-0.55 ± j7.56 (f = 1.2; ζ = 0.07)	-2.0997 ± j6.0771 (f = 0.9672; ζ = 0.3266)
5&6	-0.6272 ± j7.0773 (f = 1.1264; ζ = 0.0883)	-0.57 ± j7.34 (f = 1.17; ζ = 0.08)	-2.2697 ± j6.2366 (f = 0.9926; ζ = 0.3419)
7	-101.015 (f = 0; ζ = 1)	-101.19 (f = 0; ζ = 1)	-1000000 (f = 0; ζ = 1)
8	-100.9567 (f = 0; ζ = 1)	-101.08 (f = 0; ζ = 1)	-1000000 (f = 0; ζ = 1)
9	-100.5957 (f = 0; ζ = 1)	-100.63 (f = 0; ζ = 1)	-1000000 (f = 0; ζ = 1)
10	-100.5771 (f = 0; ζ = 1)	-100.62 (f = 0; ζ = 1)	-1000000 (f = 0; ζ = 1)
11	-42.4138 (f = 0; ζ = 1)	-42.13 (f = 0; ζ = 1)	-1000000 (f = 0; ζ = 1)
12	-42.2865 (f = 0; ζ = 1)	-41.94 (f = 0; ζ = 1)	-1000000 (f = 0; ζ = 1)
13	-41.9621 (f = 0; ζ = 1)	-41.67 (f = 0; ζ = 1)	-1000000 (f = 0; ζ = 1)
14	-41.8372 (f = 0; ζ = 1)	-41.59 (f = 0; ζ = 1)	-1000000 (f = 0; ζ = 1)
15	-32.6163 (f = 0; ζ = 1)	-36.16 + j0.03 (f = 0.01; ζ = 1)	-97.7895 (f = 0; ζ = 1)
16	-32.5376 (f = 0; ζ = 1)	-36.16 - j0.03 (f = 0.01; ζ = 1)	-97.7336 (f = 0; ζ = 1)
17	-27.0379 (f = 0; ζ = 1)	-31.02 (f = 0; ζ = 1)	-97.5537 (f = 0; ζ = 1)
18	-26.2525 (f = 0; ζ = 1)	-30.43 (f = 0; ζ = 1)	-97.4929 (f = 0; ζ = 1)
19	-8.5521 + j9.2746 (f = 1.4761; ζ = 0.6779)	-8.15 + j9.71 (f = 1.55; ζ = 0.64)	-50.7555 (f = 0; ζ = 1)
20	-8.5521 - j9.2746 (f = 1.4761; ζ = 0.6779)	-8.15 - j9.71 (f = 1.55; ζ = 0.64)	-50.6054 (f = 0; ζ = 1)
21	-8.4383 + j9.5285 (f = 1.5165; ζ = 0.6629)	-8.06 + j9.87 (f = 1.57; ζ = 0.63)	-49.7038 (f = 0; ζ = 1)
22	-8.4383 - j9.5285 (f = 1.5165; ζ = 0.6629)	-8.06 - j9.87 (f = 1.57; ζ = 0.63)	-48.783 (f = 0; ζ = 1)
23	-6.0587 + j14.7519 (f = 2.3478; ζ = 0.3799)	-5.23 + j15.58 (f = 2.48; ζ = 0.32)	-39.5047 (f = 0; ζ = 1)

24	-6.0587 - j14.7519 (f = 2.3478; ζ = 0.3799)	-5.23 - j15.58 (f = 2.48; ζ = 0.32)	-39.2782 (f = 0; ζ = 1)
25	-4.8022 + j16.5549 (f = 2.6348; ζ = 0.2786)	-4.51 + j16.67 (f = 2.65; ζ = 0.26)	-25.1813 (f = 0; ζ = 1)
26	-4.8022 - j16.5549 (f = 2.6348; ζ = 0.2786)	-4.51 - j16.67 (f = 2.65; ζ = 0.26)	-23.6787 (f = 0; ζ = 1)
27 & 28	-4.1148 ± j0.0189 (f = 0.0031; ζ = 0.9999)	-3.58 ± j0.03 (f = 0.001; ζ = 0.999)	-5.3531 ± j0.057 (f = 0.001; ζ = 0.999)
29	-3.9989 (f = 0; ζ = 1)	-3.42 + j0.02 (f = 0.001; ζ = 1)	-3.9575 + j13.9698 (f = 2.223; ζ = 0.282)
30	-3.9531 (f = 0; ζ = 1)	-3.42 + j0.02 (f = 0.001; ζ = 1)	-3.9575 - j13.9698 (f = 2.223; ζ = 0.282)
31	-0.0006 (f = 0; ζ = 1)	0 (f = 0; ζ = 1)	-3.9563 + j14.081 (f = 2.241; ζ = 0.289)
32	0 (f = 0; ζ = 1)	0 (f = 0; ζ = 1)	-3.9563 - j14.081 (f = 2.241; ζ = 0.289)
33	0 (f = 0; ζ = 1)		-2.8336 + j15.5391 (f = 2.473; ζ = 0.178)
34	0 (f = 0; ζ = 1)		-2.8336 - j15.5391 (f = 2.473; ζ = 0.178)
35	0 (f = 0; ζ = 1)		-1.8979 + j15.9954 (f = 2.546; ζ = 0.116)
36	0 (f = 0; ζ = 1)		-1.8979 - j15.9954 (f = 2.546; ζ = 0.116)
37			-4.9497 (f = 0; ζ = 1)
38			-4.6634 (f = 0; ζ = 1)
39			-0.0003 (f = 0; ζ = 1)
40			0 (f = 0; ζ = 1)

Table D.3: TAMM HVAC with AVR and PSS

Mode	Eigen-value (frequency, damping ratio)		
	DigSILENT	PST	PSAT
1&2	-0.7542 ± j3.9597 (f = 0.6302; ζ = 0.1871)	-0.76 ± j3.93 (f = 0.63; ζ = 0.19**)**	-0.4832 ± j3.4782 (f = 0.5536; ζ = 0.1376)
3&4	-1.5533 ± j10.0525 (f = 1.5999; ζ = 0.1527)	-1.47 ± j10.27 (f = 1.63; ζ = 0.14**)**	-1.8766 ± j8.6159 (f = 1.3713; ζ = 0.2128)
5&6	-1.7059 ± j9.6841 (f = 1.5413; ζ = 0.1735)	-1.65 ± j9.91 (f = 1.58; ζ = 0.16**)**	-1.8349 ± j8.3361 (f = 1.3267; ζ = 0.2149)
7	-101.0153 (f = 0; ζ = 1)	-101.19 (f = 0; ζ = 1)	-99.9191 (f = 0; ζ = 1)
8	-100.9575 (f = 0; ζ = 1)	-101.09 (f = 0; ζ = 1)	-99.9172 (f = 0; ζ = 1)
9	-100.5962 (f = 0; ζ = 1)	-100.63 (f = 0; ζ = 1)	-99.9101 (f = 0; ζ = 1)
10	-100.5777 (f = 0; ζ = 1)	-100.62 (f = 0; ζ = 1)	-99.9079 (f = 0; ζ = 1)
11	-49.6375 (f = 0; ζ = 1)	-49.66 (f = 0; ζ = 1)	-49.9852 (f = 0; ζ = 1)
12	-49.5594 (f = 0; ζ = 1)	-49.59 (f = 0; ζ = 1)	-49.9728 (f = 0; ζ = 1)
13	-49.3694 (f = 0; ζ = 1)	-49.37 (f = 0; ζ = 1)	-49.9072 (f = 0; ζ = 1)
14	-49.2942 (f = 0; ζ = 1)	-49.3 (f = 0; ζ = 1)	-49.9004 (f = 0; ζ = 1)
15	-43.042 + j0.0459 (f = 0.0073; ζ = 0.9999)	-42.89 (f = 0; ζ = 1)	-37.846 + j0.2004 (f = 0.0319; ζ = 0.9998)
16	-43.042 - j0.0459 (f = 0.0073; ζ = 0.9999)	-42.83 (f = 0; ζ = 1)	-37.846 - j0.2004 (f = 0.1333; ζ = 0.9998)
17	-42.995 + j0.0078 (f = 0.0012; ζ = 0.9999)	-42.7 + j0.02 (f = 0.00005 = 0.9999)	-37.3616 + j0.8378 (f = 0.0319; ζ = 0.9997)
18	-42.995 - j0.0078 (f = 0.0012; ζ = 0.9999)	-42.7 - j0.02 (f = 0.00005 = 0.9999)	-37.3616 - j0.8378 (f = 0.0319; ζ = 0.9997)
19	-32.7498 (f = 0; ζ = 1)	-36.11 + j0.02 (f = 0.00006 = 0.9999)	-33.6512 (f = 0; ζ = 1)
20	-32.6402 (f = 0; ζ = 1)	-36.11 - j0.02 (f = 0.00006 = 0.9999)	-32.7602 (f = 0; ζ = 1)
21	-27.0322 (f = 0; ζ = 1)	-31 (f = 0; ζ = 1)	-24.1707 (f = 0; ζ = 1)
22	-26.2555 (f = 0; ζ = 1)	-30.43 (f = 0; ζ = 1)	-21.9012 (f = 0; ζ = 1)
23	-7.7581 + j6.5745	-7.05 + j7.08	-6.2616

	(f = 1.0464; ζ = 0.7629)	(f = 1.13; ζ = 0.71)	(f = 0; ζ = 1)
24	-7.7581 - j6.5745 (f = 1.0464; ζ = 0.7629)	-7.05 - j7.08 (f = 1.13; ζ = 0.71)	-6.2088 (f = 0; ζ = 1)
25	-7.4619 + j6.9437 (f = 1.1052; ζ = 0.7321)	-6.81 + j7.38 (f = 1.17; ζ = 0.68)	-4.7651 (f = 0; ζ = 1)
26	-7.4619 - j6.9437 (f = 1.1052; ζ = 0.7321)	-6.81 - j7.38 (f = 1.17; ζ = 0.68)	-4.1357 (f = 0; ζ = 1)
27	-5.1282 + j14.7275 (f = 2.3439; ζ = 0.3288)	-4.37 + j15.65 (f = 2.49; ζ = 0.27)	-0.9885 + j2.8136 (f = 0.4478; ζ = 0.2911)
28	-5.1282 - j14.7275 (f = 2.3439; ζ = 0.3288)	-4.37 - j15.65 (f = 2.49; ζ = 0.27)	-0.9885 - j2.8136 (f = 0.4478; ζ = 0.2911)
29	-4.1886 (f = 0; ζ = 1)	-3.71 (f = 0; ζ = 1)	-0.9857 + j2.7391 (f = 0.4359; ζ = 0.2936)
30	-4.0509 (f = 0; ζ = 1)	-3.55 (f = 0; ζ = 1)	-0.9857 - j2.7391 (f = 0.4359; ζ = 0.2936)
31	-3.978 + j16.6268 (f = 2.6462; ζ = 0.2327)	-3.67 + j16.75 (f = 2.67; ζ = 0.21)	-0.4717 + j0.1235 (f = 0.0197; ζ = 0.9326)
32	-3.978 - j16.6268 (f = 2.6462; ζ = 0.2327)	-3.67 - j16.75 (f = 2.67; ζ = 0.21)	-0.4717 - j0.1235 (f = 0.0197; ζ = 0.9326)
33	-3.2338 (f = 0; ζ = 1)	-2.97 + j0.02 (f = 0.000002; ζ = 1)	-0.3144 + j4.9257 (f = 0.7839; ζ = 0.0623)
34	-3.1354 (f = 0; ζ = 1)	-2.97 - j0.02 (f = 0.000002; ζ = 1)	-0.3144 - j4.9257 (f = 0.7839; ζ = 0.0623)
35	-1.2321 (f = 0; ζ = 1)	-1.22 (f = 0; ζ = -1)	-1 (f = 0; ζ = 1)
36	-0.3716 (f = 0; ζ = 1)	-0.37 (f = 0; ζ = -1)	-1 (f = 0; ζ = 1)
37	-0.1782 (f = 0; ζ = 1)	-0.18 (f = 0; ζ = 1)	-1 (f = 0; ζ = 1)
38	-0.1089 (f = 0; ζ = 1)	-0.18 (f = 0; ζ = 1)	-1 (f = 0; ζ = 1)
39	-0.1775 (f = 0; ζ = 1)	-0.18 (f = 0; ζ = -1)	-0.1808 (f = 0; ζ = 1)
40	-0.1036 (f = 0; ζ = 1)	-0.1 (f = 0; ζ = -1)	-0.1791 (f = 0; ζ = 1)
41	-0.1033 (f = 0; ζ = 1)	-0.1 (f = 0; ζ = 1)	-0.1786 (f = 0; ζ = 1)
42	-0.1029 (f = 0; ζ = 1)	-0.1 (f = 0; ζ = 1)	-0.103 (f = 0; ζ = 1)

43	-0.00001 (f = 0; ζ = 1)	0 (f = 0; ζ = -1)	-0.1029 (f = 0; ζ = 1)
44	0 (f = 0; ζ = 1)	0 (f = 0; ζ = -1)	-0.1021 (f = 0; ζ = 1)
45	0 (f = 0; ζ = 1)		-0.00002 (f = 0; ζ = 1)
46	0 (f = 0; ζ = 1)		0 (f = 0; ζ = 1)
47	0 (f = 0; ζ = 1)		0.3376 + j4.8408 (f = 0.7704; ζ = 0.0663)
48	0 (f = 0; ζ = 1)		0.3376 - j4.8408 (f = 0.7704; ζ = 0.0663)

Table D.4: TAMM HVAC-HVDC with manual control

Mode	Eigen-value (frequency, damping ratio)		
	DigSILENT	PST	PSAT
1&2	-0.2216 ± j2.5355 (f = 0.4035; ζ = 0.0871)	-0.0082 ± j1.8481 (f = 0.2941; ζ = 0.0044)	-0.1125 ± j 4.1371 (f = 0.6584; ζ = 0.0272)
3&4	-0.6105 ± j6.9798 (f = 1.1109; ζ = 0.0871)	-0.5479 ± j7.2696 (f = 1.157; ζ = 0.0752)	-0.9041 ± j8.2515 (f = 1.3133; ζ = 0.1089)
5&6	-0.61 ± j6.7179 (f = 1.0692; ζ = 0.0904)	-0.571 ± j6.8461 (f = 1.0896; ζ = 0.0831)	-0.8846 ± j7.93 (f = 1.2621; ζ = 0.1109)
7	-37.639 (f = 0; ζ = 1)	-37.2108 + j0.0219 (f = 0.0035; ζ ≈ 1)	-38.7881 + j 0.4205 (f = 0.0669; ζ = 0.9999)
8	-37.1986 (f = 0; ζ = 1)	-37.2108 - j0.0219 (f = 0.0035; ζ ≈ 1)	-38.7881 - j 0.4205 (f = 0.0669; ζ = 0.9999)
9	-36.2741 (f = 0; ζ = 1)	-36.2701 (f = 0; ζ = 1)	-38.2382 + j0.5923 (f = 0.0943; ζ = 0.9999)
10	-34.0842 (f = 0; ζ = 1)	-35.563 (f = 0; ζ = 1)	-38.2382 - j0.5923 (f = 0.0943; ζ = 0.9999)
11	-33.1789 (f = 0; ζ = 1)	-35.1976 + j0.62 (f = 0.0987; ζ ≈ 1)	-33.966 (f = 0; ζ = 1)
12	-33.0755 (f = 0; ζ = 1)	-35.1976 + j0.62 (f = 0.0987; ζ ≈ 1)	-32.3862 (f = 0; ζ = 1)
13	-26.2621 (f = 0; ζ = 1)	-30.9087 (f = 0; ζ = 1)	-23.9157 (f = 0; ζ = 1)
14	-25.32112 (f = 0; ζ = 1)	-29.4792 (f = 0; ζ = 1)	-20.5934 (f = 0; ζ = 1)
15	-5.6033 + j0.0155 (f = 0.0025; ζ = 0.9999)	-4.7784 (f = 0; ζ = 1)	-6.7938 (f = 0; ζ = 1)
16	-5.6033 - j0.0155 (f = 0.0025; ζ = 0.9999)	-4.6961 (f = 0; ζ = 1)	-6.7265 (f = 0; ζ = 1)
17	-4.0015 (f = 0; ζ = 1)	-3.6848 (f = 0; ζ = 1)	-4.5856 (f = 0; ζ = 1)
18	-3.3087 (f = 0; ζ = 1)	-2.824 (f = 0; ζ = 1)	-2.8377 (f = 0; ζ = 1)
19	-0.378 (f = 0; ζ = 1)	-0.2191 (f = 0; ζ = 1)	-0.1978 (f = 0; ζ = 1)
20	-0.2132 (f = 0; ζ = 1)	-0.1762 (f = 0; ζ = 1)	-0.1753 (f = 0; ζ = 1)
21	-0.1944 (f = 0; ζ = 1)	-0.1172 (f = 0; ζ = 1)	-0.0427 (f = 0; ζ = 1)
22	-0.0919 (f = 0; ζ = 1)	-0.0256 +j0.0112 (f = 0.0018; ζ = 0.9159)	-0.0238 (f = 0; ζ = 1)

23	-0.0372 (f = 0; ζ = 1)	-0.0256 +j0.0112 (f = 0.0018; ζ = 0.9159)	0 (f = 0; ζ = 1)
24	0 (f = 0; ζ = 1)	-0.0881 +j5.3325 (f = 0.8487; ζ = 0.0165)	0 (f = 0; ζ = 1)
25		-0.0881 -5.3325 (f = 0.8487; ζ = 0.0165)	-4668.5834 (f = 0; ζ = 1)
26		0 (f = 0; ζ = 1)	-1.8398 (f = 0; ζ = 1)
27		0 (f = 0; ζ = 1)	-1 (f = 0; ζ = 1)
28		1.2623 (f = 0; ζ = -1)	
29		19.2651 (f = 0; ζ = -1)	

Table D.5: TAMM HVAC-HVDC with AVR only

Mode	Eigen-value (frequency, damping ratio)		
	DigSILENT	PST	PSAT
1&2	0.1351 ± j3.1059 (f = 0.4943; ζ = -0.0434)	0.45 ± j1.78 (f = 0.28; ζ =-0.24)	-0.1454 ± j3.9585 (f = 0.63; ζ = 0.0367)
3&4	-0.6066 ± j7.0689 (f = 1.1251; ζ = 0.0855)	-0.57 ± j7.49 (f = 1.19; ζ = 0.08)	-2.0325 ± j6.0937 (f = 0.9698; ζ = 0.3164)
5&6	-0.6389 ± j7.3403 (f = 1.1682; ζ = 0.0867)	-0.63 ± 7.35 (f = 1.17; ζ = 0.09)	-2.2817 ± j6.2314 (f = 0.9918; ζ = 0.3438)
7	-101.1399 (f = 0; ζ = 1)	-100.19 (f = 0; ζ = 1)	-1000000 (f = 0; ζ = 1)
8	-100.7694 (f = 0; ζ = 1)	-100.66 (f = 0; ζ = 1)	-1000000 (f = 0; ζ = 1)
9	-100.596 (f = 0; ζ = 1)	-100.62 (f = 0; ζ = 1)	-1000000 (f = 0; ζ = 1)
10	-100.5364 (f = 0; ζ = 1)	-100.51 (f = 0; ζ = 1)	-1000000 (f = 0; ζ = 1)
11	-42.4368 (f = 0; ζ = 1)	-42.16 (f = 0; ζ = 1)	-1000000 (f = 0; ζ = 1)
12	-42.1881 (f = 0; ζ = 1)	-41.75 (f = 0; ζ = 1)	-1000000 (f = 0; ζ = 1)
13	-42.0081 (f = 0; ζ = 1)	-41.65 (f = 0; ζ = 1)	-1000000 (f = 0; ζ = 1)
14	-41.5889 (f = 0; ζ = 1)	-40.64 (f = 0; ζ = 1)	-1000000 (f = 0; ζ = 1)
15	-32.6133 (f = 0; ζ = 1)	-36.52 (f = 0; ζ = 1)	-4647.3226 (f = 0; ζ = 1)
16	-32.5206 (f = 0; ζ = 1)	-36.15 (f = 0; ζ = 1)	-97.8023 (f = 0; ζ = 1)
17	-26.6932 (f = 0; ζ = 1)	-31.5 (f = 0; ζ = 1)	-97.7264 (f = 0; ζ = 1)
18	-26.2604 (f = 0; ζ = 1)	-30.77 (f = 0; ζ = 1)	-97.5395 (f = 0; ζ = 1)
19	-8.486 + j8.8003 (f = 1.4006; ζ = 0.6941)	-8.2 + j9.56 (f = 1.52; ζ = 0.65)	-97.4633 (f = 0; ζ = 1)
20	-8.486 - j8.8003 (f = 1.4006; ζ = 0.6941)	-8.2 - j9.56 (f = 1.52; ζ = 0.65)	-49.681 + j0.7262 (f = 0.1156; ζ = 0.9921)
21	-8.4739 + j9.5391 (f = 1.5182; ζ = 0.6642)	-8.07 + j9.68 (f = 1.54; ζ = 0.64)	-49.681 - j0.7262 (f = 0.1156; ζ = 0.9921)
22	-8.4739 - j9.5391 (f = 1.5182; ζ = 0.6642)	-8.07 - j9.68 (f = 1.54; ζ = 0.64)	-49.995 + j0.2479 (f = 0.0395; ζ = 0.9979)
23	-7.0175 + j12.2862 (f = 1.9554; ζ = 0.4959)	-5.93 + j14.68 (f = 2.34; ζ = 0.37)	-49.995 - j0.2479 (f = 0.0395; ζ = 0.9979)
24	-7.0175 - j12.2862 (f = 1.9554; ζ =	-5.93 - j14.68 (f = 2.34; ζ = 0.37)	-39.4542 (f = 0; ζ = 1)

	0.4959)		
25	-4.7867 + j16.5639 (f = 2.6362; ζ = 0.2786)	-2.66 + j16.63 (f = 2.65; ζ = 0.16)	-39.0873 (f = 0; ζ = 1)
26	-4.7867 - j16.5639 (f = 2.6362; ζ = 0.2786)	-2.66 - j16.63 (f = 2.65; ζ = 0.16)	-25.3154 (f = 0; ζ = 1)
27	-4.1358 + j0.08879 (f = 0.0141; ζ = 0.9998)	-0.34 + j5.03 (f = 0.8; ζ = 0.07)	-23.7012 (f = 0; ζ = 1)
28	-4.1358 - j0.08879 (f = 0.0141; ζ = 0.9998)	-0.34 - j5.03 (f = 0.8; ζ = 0.07)	-4.7946 + j15.7036 (f = 2.4993; ζ = 0.2826)
29	-4.0235 (f = 0; ζ = 1)	-3.96 (f = 0; ζ = 1)	-4.7946 - j15.7036 (f = 2.4993; ζ = 0.2826)
30	-3.9448 (f = 0; ζ = 1)	-3.45 (f = 0; ζ = 1)	-4.7563 + j15.7189 (f = 2.5017; ζ = 0.2752)
31	-0.0015 (f = 0; ζ = 1)	-3.42 (f = 0; ζ = 1)	-4.7563 - j15.7189 (f = 2.5017; ζ = 0.2752)
32	0 (f = 0; ζ = 1)	-3.39 (f = 0; ζ = 1)	-3.168 + j15.9559 (f = 2.5394; ζ = 0.2293)
33	0 (f = 0; ζ = 1)	-0.04 (f = 0; ζ = 1)	-3.168 - j15.9559 (f = 2.5394; ζ = 0.2293)
34	0 (f = 0; ζ = 1)	0 (f = 0; ζ = 1)	-1.9202 + j16.3007 (f = 2.5943; ζ = 0.1276)
35	0 (f = 0; ζ = 1)	0 (f = 0; ζ = 1)	-1.9202 - j16.3007 (f = 2.5943; ζ = 0.1276)
36	0 (f = 0; ζ = 1)	1.34 (f = 0; ζ = -1)	-5.3206 (f = 0; ζ = 1)
37		21.08 (f = 0; ζ = -1)	-5.2845 (f = 0; ζ = 1)
38			-4.8775 (f = 0; ζ = 1)
39			-4.657 (f = 0; ζ = 1)
40			-1.3497 (f = 0; ζ = 1)
41			-1 (f = 0; ζ = 1)
42			-0.0003 (f = 0; ζ = 1)
43			0 (f = 0; ζ = 1)

Table D.6: TAMM HVAC-HVDC with AVR and PSS

Mode	Eigen-value (frequency, damping ratio)		
	DigSILENT	PST	PSAT
1&2	-2.0782 ± j2.7819 (f = 0.4428; ζ = 0.5985)	-1.15 ± j1.52 (f = 0.24; ζ = 0.6)	-0.3991 ± j3.5758 (f = 0.5691; ζ = 0.1109)
3&4	-1.4997 ± j10.3563 (f = 1.6482; ζ = 0.1433)	-1.45 ± j10.1 (f = 1.61; ζ = 0.14)	-1.766 ± j8.0331 (f = 1.2785; ζ = 0.215)
5&6	-1.6373 ± j9.6649 (f = 1.5382; ζ = 0.167)	-1.77 ± 9.92 (f = 1.58; ζ = 0.18)	-1.8225 ± j8.3421 (f = 1.3277; ζ = 0.2134)
7	-101.1406 (f = 0; ζ = 1)	-101.19 (f = 0; ζ = 1)	-4647.3226 (f = 0; ζ = 1)
8	-100.7701 (f = 0; ζ = 1)	-100.66 (f = 0; ζ = 1)	-100.0233 (f = 0; ζ = 1)
9	-100.5965 (f = 0; ζ = 1)	-100.63 (f = 0; ζ = 1)	-100.0226 (f = 0; ζ = 1)
10	-100.5371 (f = 0; ζ = 1)	-100.61 (f = 0; ζ = 1)	-100.021 (f = 0; ζ = 1)
11	-49.6074 (f = 0; ζ = 1)	-49.72 (f = 0; ζ = 1)	-100.0204 (f = 0; ζ = 1)
12	-49.4361 (f = 0; ζ = 1)	-49.4 (f = 0; ζ = 1)	-50.0674 (f = 0; ζ = 1)
13	-49.3568 (f = 0; ζ = 1)	-49.34 (f = 0; ζ = 1)	-50.0569 (f = 0; ζ = 1)
14	-48.9741 (f = 0; ζ = 1)	-47.13 (f = 0; ζ = 1)	-50.0171 (f = 0; ζ = 1)
15	-43.3134 (f = 0; ζ = 1)	-43.62 (f = 0; ζ = 1)	-50.0094 (f = 0; ζ = 1)
16	-43.118 + j0.0511 (f = 0.0081; ζ = 0.9999)	-42.87 (f = 0; ζ = 1)	-38.9599 (f = 0; ζ = 1)
17	-43.118 - j0.0511 (f = 0.0081; ζ = 0.9999)	-42.81 (f = 0; ζ = 1)	-38.0887 (f = 0; ζ = 1)
18	-43.0973 (f = 0; ζ = 1)	-42.65 (f = 0; ζ = 1)	-34.7112 + j0.0259 (f = 0.0041; ζ = 0.9999)
19	-32.7082 (f = 0; ζ = 1)	-36.36 (f = 0; ζ = 1)	-34.7112 - j0.0259 (f = 0.0041; ζ = 0.9999)
20	-32.6281 (f = 0; ζ = 1)	-36.13 (f = 0; ζ = 1)	-31.5173 (f = 0; ζ = 1)
21	-26.6874 (f = 0; ζ = 1)	-31.46 (f = 0; ζ = 1)	-30.5926 (f = 0; ζ = 1)
22	-26.2637 (f = 0; ζ = 1)	-30.77 (f = 0; ζ = 1)	-23.7364 + j1.6829 (f = 0.2678; ζ = 0.9589)
23	-7.5335 + j6.6423 (f = 1.1049; ζ =	-7.24 + j6.97 (f = 1.11; ζ = 0.72)	-23.7364 - j1.6829 (f = 0.2678; ζ =

	0.7354)		0.9589)
24	-7.5335 - j6.6423 (f = 1.1049; ζ = 0.7354)	-7.24 - j6.97 (f = 1.11; ζ = 0.72)	-22.4214 + j2.5826 (f = 0.4118; ζ = 0.8817)
25	-7.3667 + j5.7679 (f = 0.9179; ζ = 0.7874)	-6.89 + j7.13 (f = 1.13; ζ = 0.69)	-22.4214 - j2.5826 (f = 0.4118; ζ = 0.8817)
26	-7.3667 - j5.7679 (f = 0.9179; ζ = 0.7874)	-6.89 - j7.13 (f = 1.13; ζ = 0.69)	-22.5898 (f = 0; ζ = 1)
27	-4.9049 + j12.0259 (f = 1.9139; ζ = 0.3776)	-5.27 + j14.42 (f = 2.29; ζ = 0.37)	-22.4709 (f = 0; ζ = 1)
28	-4.9049 - j12.0259 (f = 1.9139; ζ = 0.3776)	-5.27 - j14.42 (f = 2.29; ζ = 0.37)	-10 (f = 0; ζ = 1)
29	-4.2743 (f = 0; ζ = 1)	-4.22 (f = 0; ζ = 1)	-10 (f = 0; ζ = 1)
30	-4.1208 (f = 0; ζ = 1)	-3.44 (f = 0; ζ = 1)	-10 (f = 0; ζ = 1)
31	-3.9544 + j16.6217 (f = 2.6454; ζ = 0.2314)	-2.44 + j18.37 (f = 2.92; ζ = 0.13)	-10 (f = 0; ζ = 1)
32	-3.9544 - j16.6217 (f = 2.6454; ζ = 0.2314)	-2.44 - j18.37 (f = 2.92; ζ = 0.13)	-6.1012 (f = 0; ζ = 1)
33	-3.1661 + j0.0659 (f = 0.0105; ζ = 0.9998)	-2.92 (f = 0; ζ = 1)	-6.0658 (f = 0; ζ = 1)
34	-3.1661 - j0.0659 (f = 0.0105; ζ = 0.9998)	-2.88 (f = 0; ζ = 1)	-4.8262 (f = 0; ζ = 1)
35	-1.2449 (f = 0; ζ = 1)	-0.99 + j1.81 (f = 0.29; ζ = 0.48)	-4.2166 (f = 0; ζ = 1)
36	-0.3712 (f = 0; ζ = 1)	-0.99 - j1.81 (f = 0.29; ζ = 0.48)	-1.35 (f = 0; ζ = 1)
37	-0.1781 (f = 0; ζ = 1)	-0.18 (f = 0; ζ = 1)	-1 (f = 0; ζ = 1)
38	-0.1777 (f = 0; ζ = 1)	-0.18 (f = 0; ζ = 1)	-0.7897 + j2.8601 (f = 0.4552; ζ = 0.2666)
39	-0.1561 (f = 0; ζ = 1)	-0.18 (f = 0; ζ = 1)	-0.7897 - j2.8601 (f = 0.4552; ζ = 0.2666)
40	-0.1159 (f = 0; ζ = 1)	-0.13 (f = 0; ζ = 1)	-0.7675 + j2.9378 (f = 0.4676; ζ = 0.2421)
41	-0.1035 (f = 0; ζ = 1)	-0.13 (f = 0; ζ = 1)	-0.7675 - j2.9378 (f = 0.4676; ζ = 0.2421)
42	-0.1033	-0.1	-0.4683 + j0.1273

	(f = 0; ζ = 1)	(f = 0; ζ = 1)	(f = 0.0203; ζ = 0.8012)
43	-0.00006 (f = 0; ζ = 1)	-0.1 (f = 0; ζ = 1)	-0.4683 - j0.1273 (f = 0.0203; ζ = 0.8012)
44	0 (f = 0; ζ = 1)	-0.1 (f = 0; ζ = 1)	-0.1811 (f = 0; ζ = 1)
45	0 (f = 0; ζ = 1)	-0.04 (f = 0; ζ = 1)	-0.1791 (f = 0; ζ = 1)
46	0 (f = 0; ζ = 1)	0 (f = 0; ζ = 1)	-0.1787 (f = 0; ζ = 1)
47	0 (f = 0; ζ = 1)	0 (f = 0; ζ = 1)	-0.1031 (f = 0; ζ = 1)
48	0 (f = 0; ζ = 1)	1.21 (f = 0; ζ = -1)	-0.1028 (f = 0; ζ = 1)
49		23.25 (f = 0; ζ = -1)	-0.1019 (f = 0; ζ = 1)
50			-0.00002 (f = 0; ζ = 1)
51			0 (f = 0; ζ = 1)
52			0.0487 + j4.6935 (f = 0.747; ζ = -0.0107)
53			0.0487 - j4.6935 (f = 0.747; ζ = -0.0107)
54			0.6615 + j4.6106 (f = 0.7338; ζ = -0.1379)
55			0.6615 - j4.6106 (f = 0.7338; ζ = -0.1379)

The figures below, display the voltage response, angle response and active power response for the four generators in the Two Area Multi Machine system for the HVAC and HVAC-HVDC systems under manual control only.

HVAC system

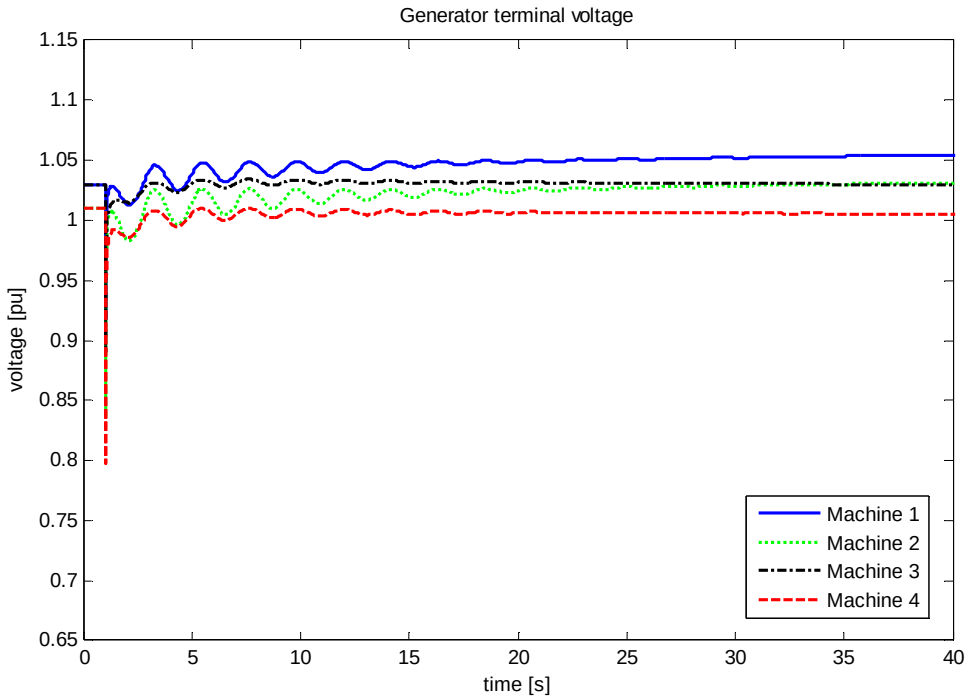

Figure D.1: DigSILENT voltage

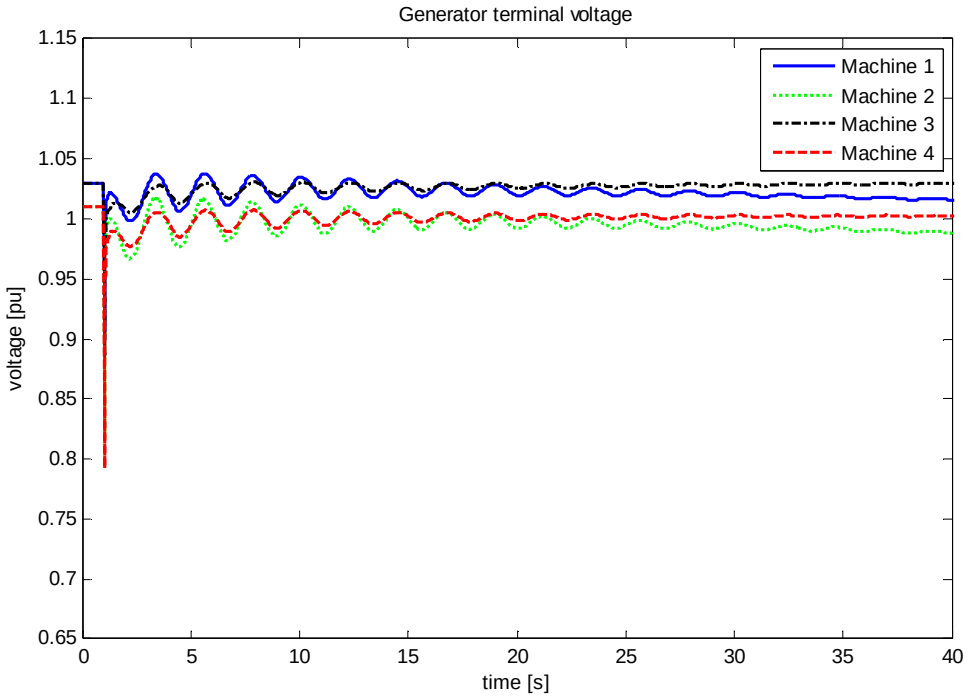

Figure D.2: PST voltage

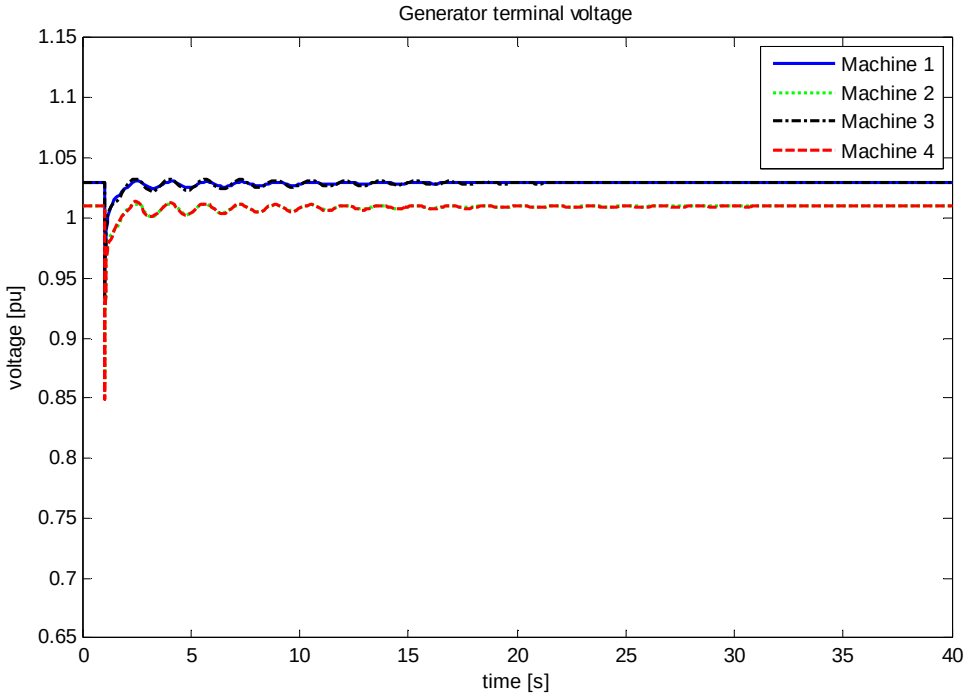

Figure D.3: PSAT voltage

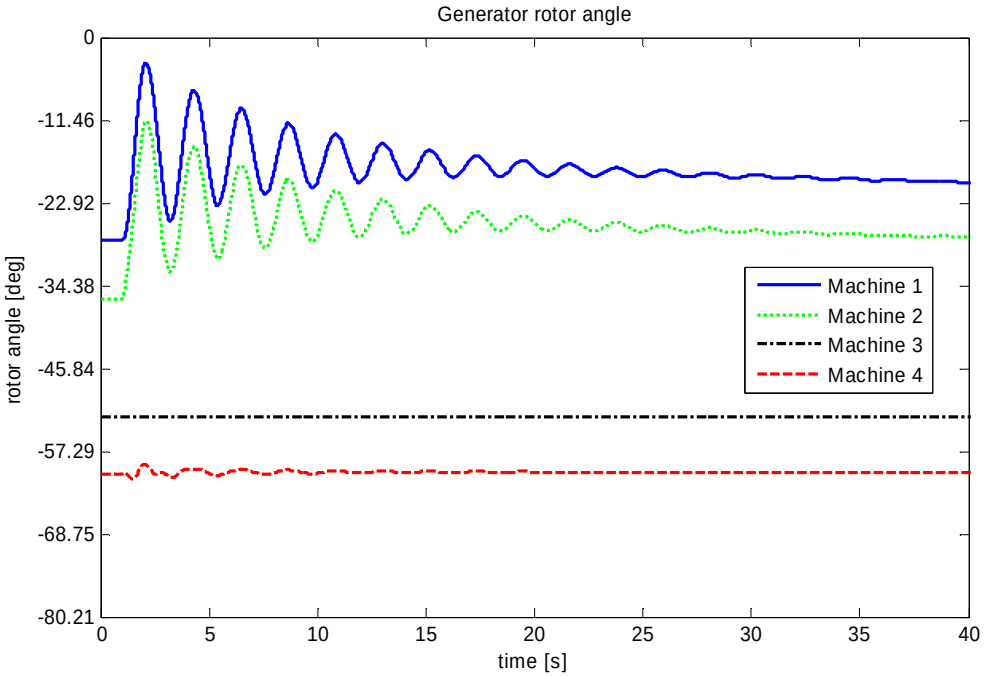

Figure D.4: DigSILENT rotor angle

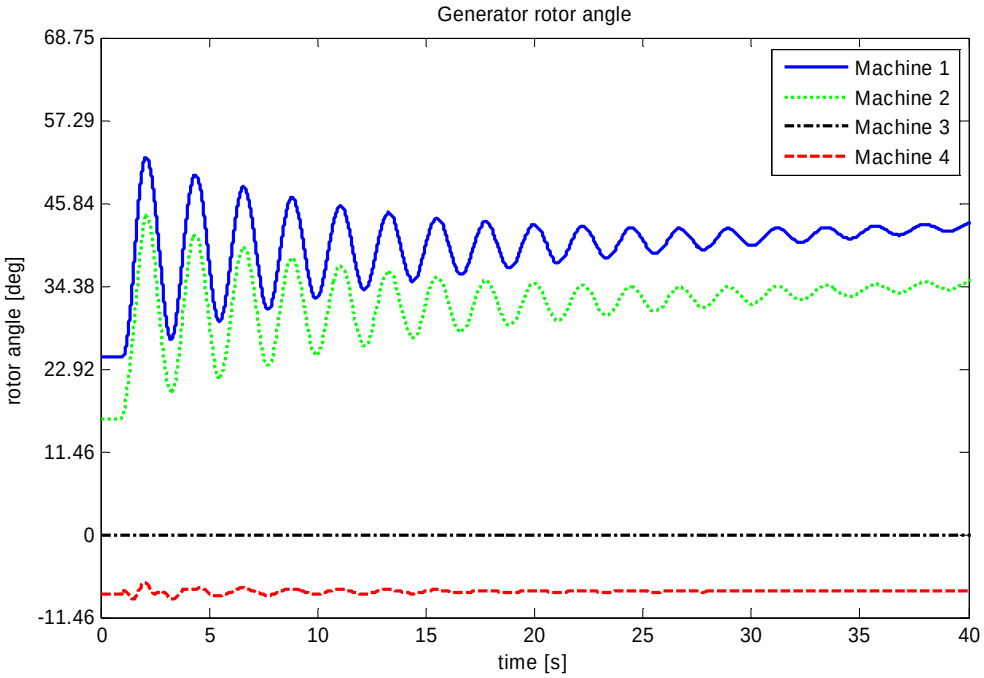

Figure D.5: PST rotor angle

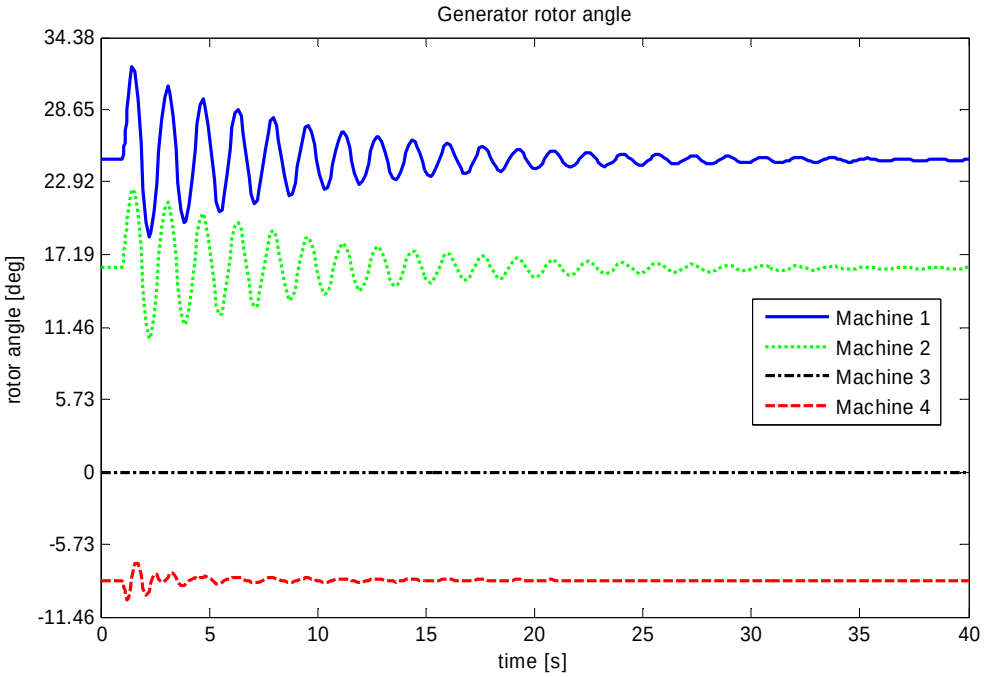

Figure D.6: PSAT rotor angle

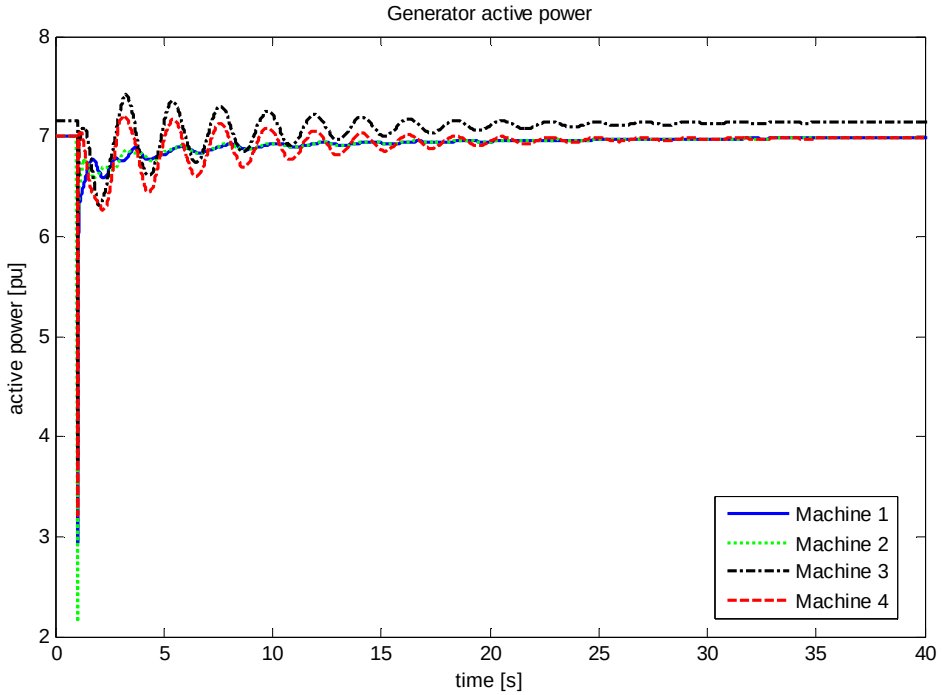

Figure D.7: DigSILENT active power

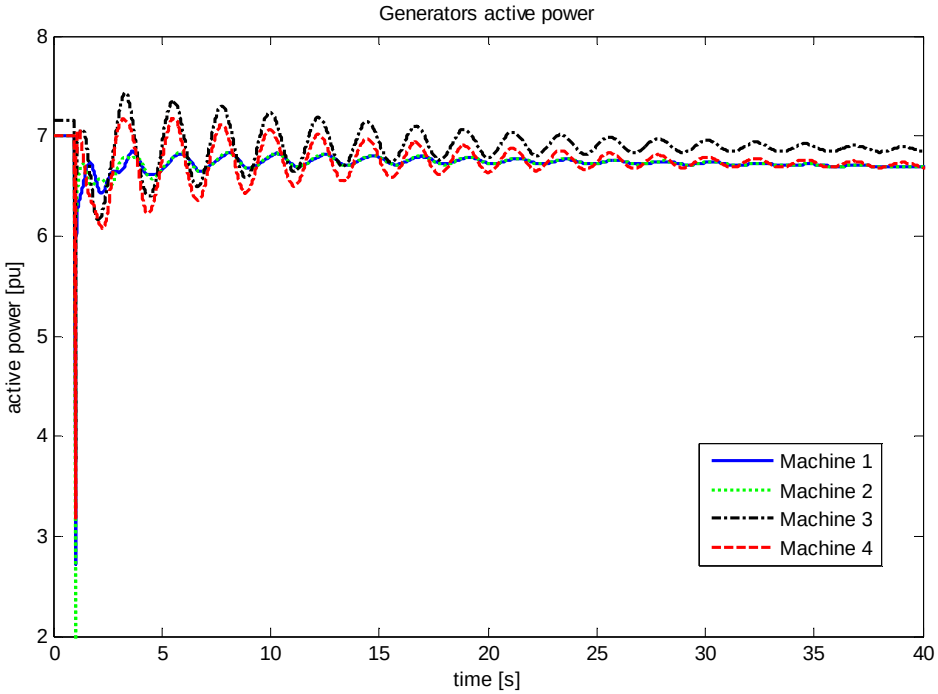

Figure D.8: PST active power

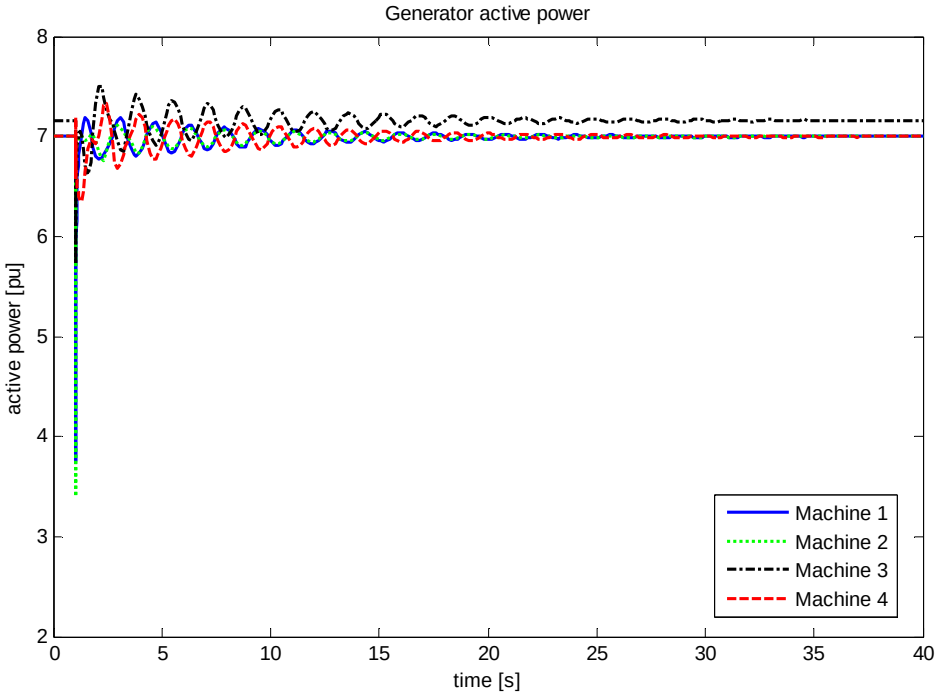

Figure D.9: PSAT active power

HVAC-HVDC TAMM system

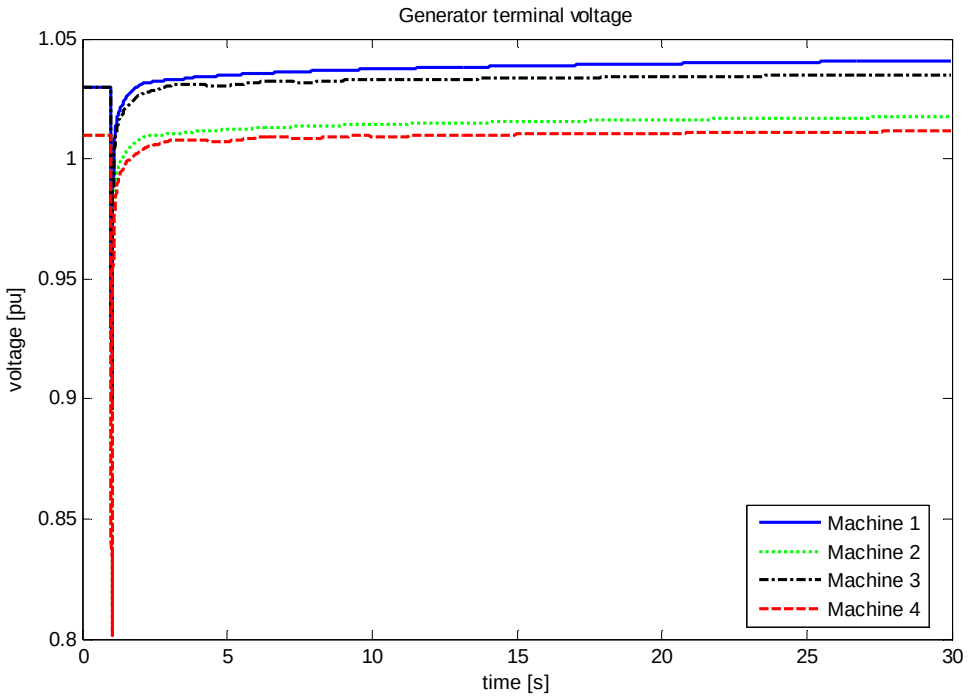

Figure D.10: DigSILENT voltage

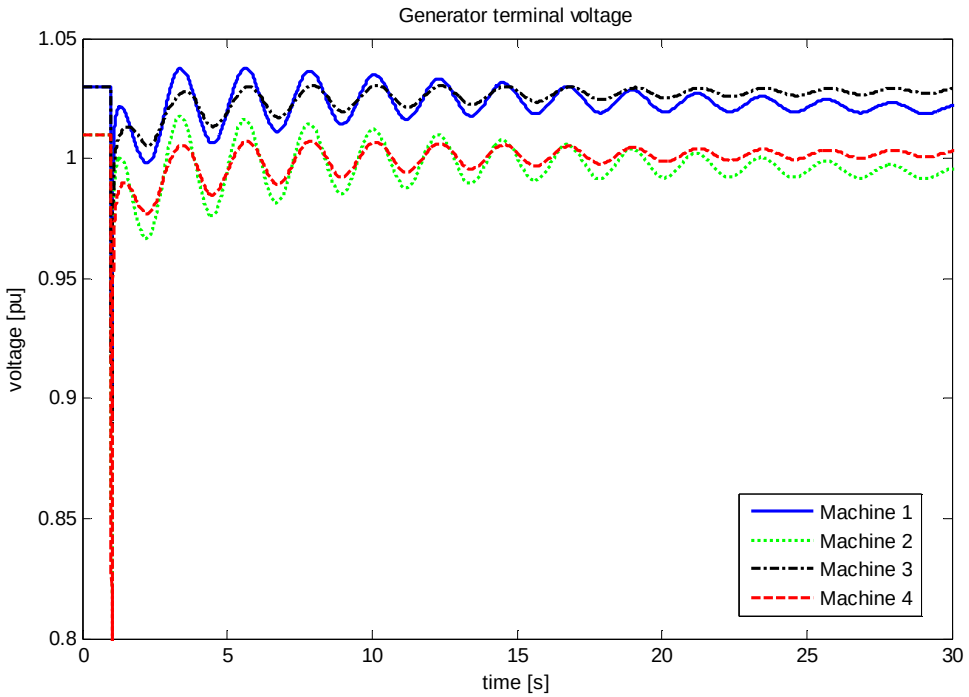

Figure D.11: PST voltage

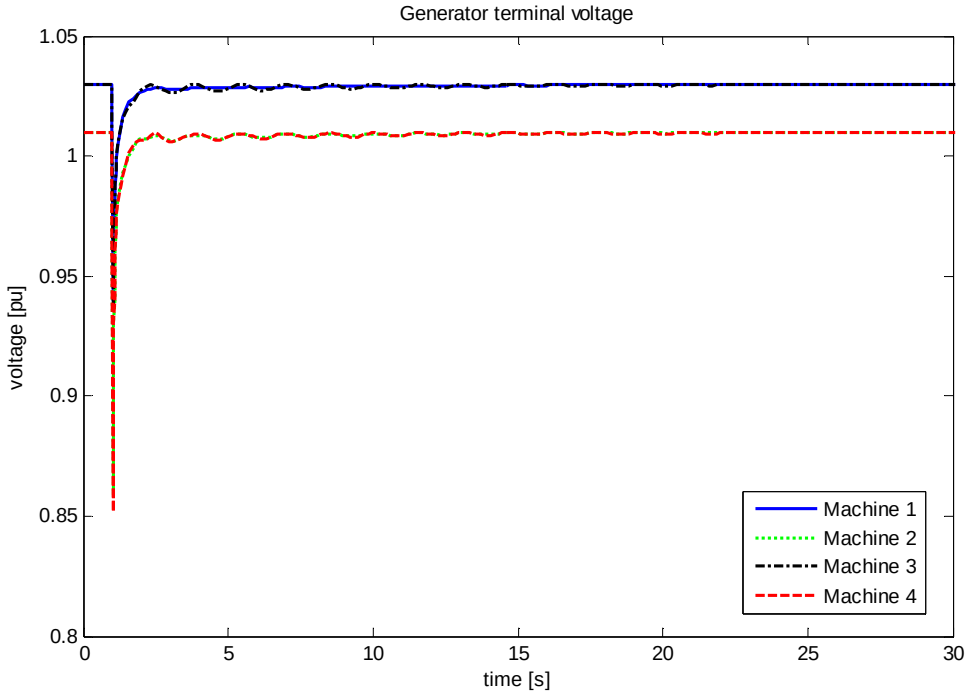

Figure D.12: PSAT voltage

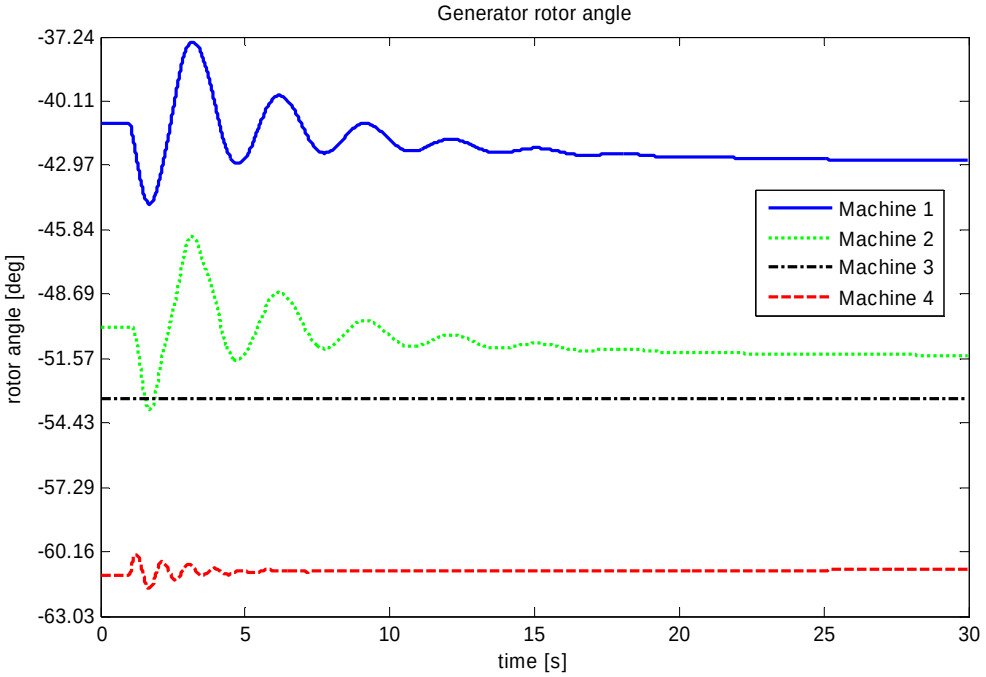

Figure D.13: DigSILENT rotor angle

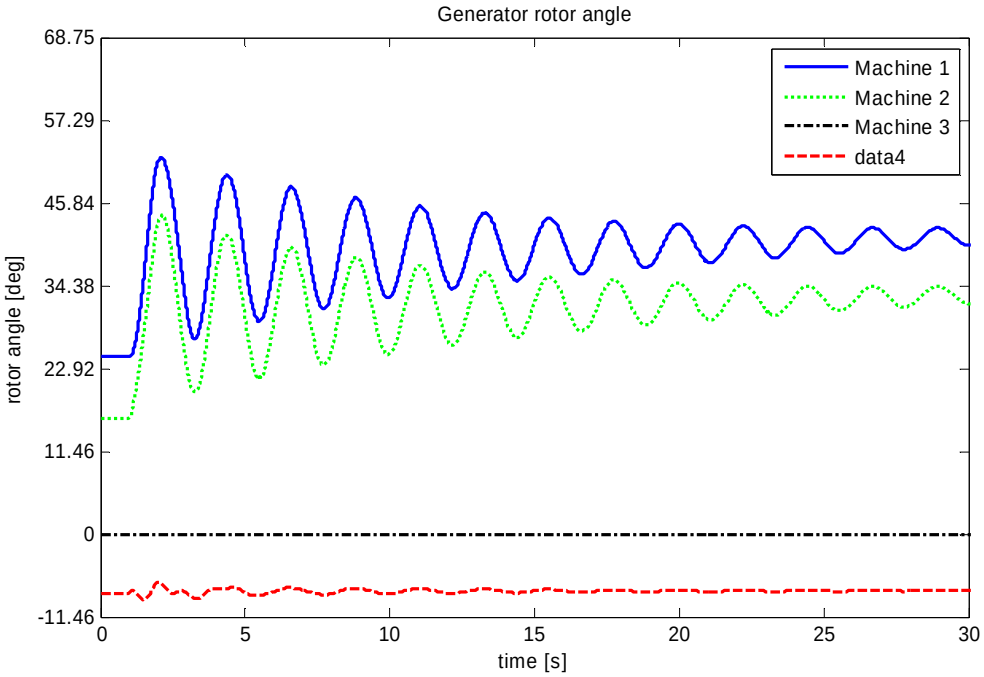

Figure D.14: PST rotor angle

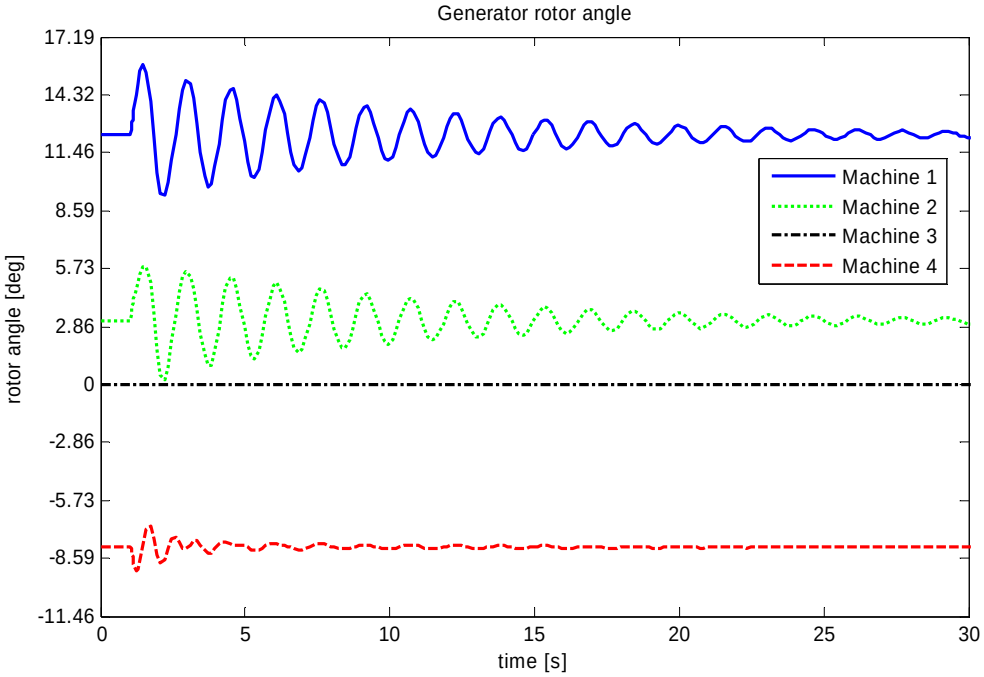

Figure D.15: PSAT rotor angle

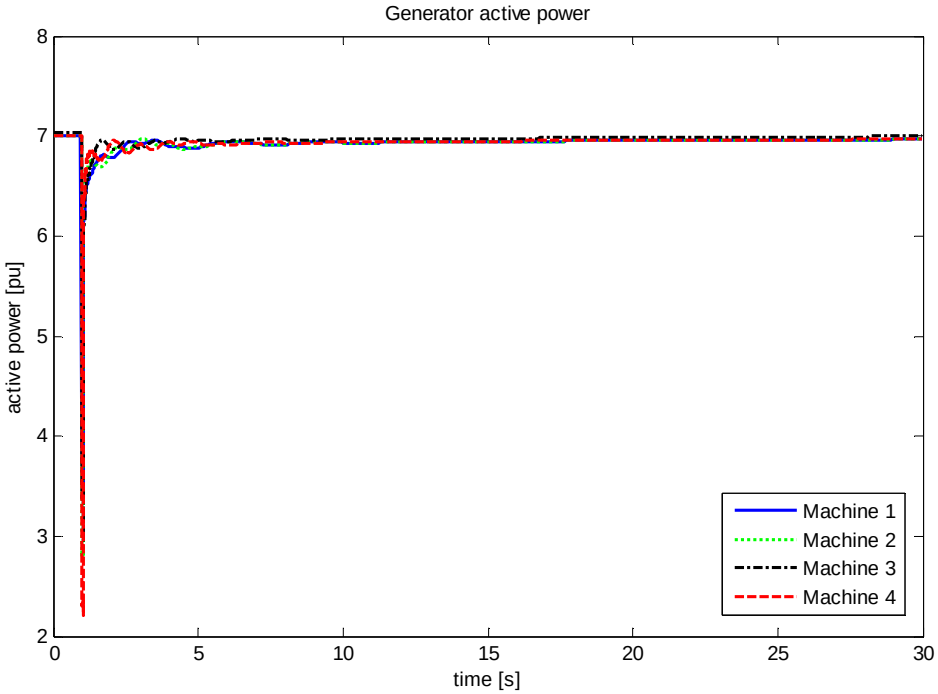

Figure D.16: DigSILENT active power

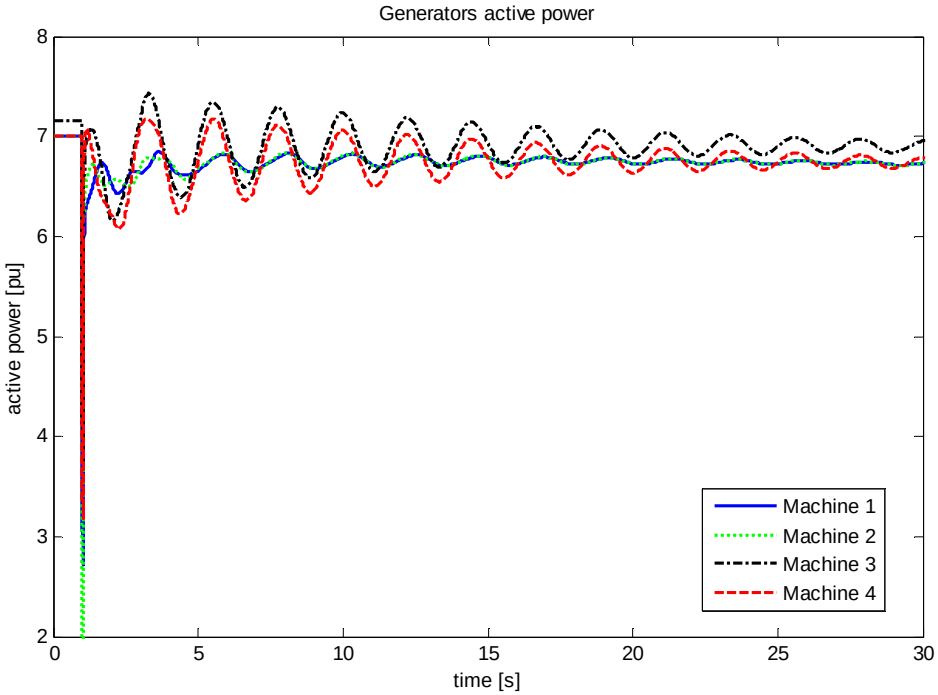

Figure D.17: PST active power

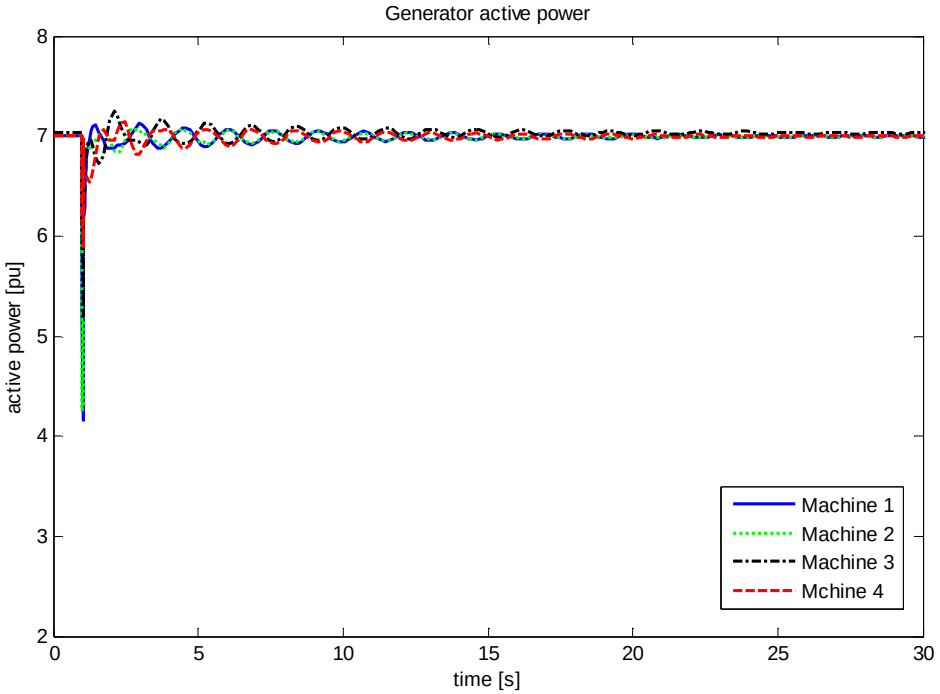

Figure D.18: PSAT active power

Appendix E

E-mail Communications with software technical support

E1 Communication with DigSILENT

Email communication about HVDC generic equations:

From: "DIgSILENT Support" <support@digsilent.de> Thursday - November 25, 2010 12:53 PM

To: "'Albino UBISSE'" <ALBINO.UBISSE@uct.ac.za>

Subject: RE: HVDC generic equations

Attachments: Mime.822 (6 KB) **[View]** **[Save As]**

Hello Albino

More, or different) equations are possible, since the DSL language provides the user with a lot of flexibility in terms of defining the controllers. For the converters the equations are as stated in the manual.

Regards

Peter Lilje (support@digsilent.de)

DIgSILENT GmbH
Heinrich-Hertz-Str. 9 Tel : (+49) 7072 - 9168 50
72810 Gomaringen Fax : (+49) 7072 - 9168 88
Germany **http://www.digsilent.de**

-----Original Message-----
From: Albino UBISSE [mailto:ALBINO.UBISSE@uct.ac.za]
Sent: Montag, 22. November 2010 10:39
To: support@digsilent.de
Subject: RE: HVDC generic equations

Hi Peter,
Thanks for your reply. I do know that more extensive modelling of controllers can be done using DSL, however, the license that we have does not include DSL. Hence I would like to know if the equations for the modelling of the HVDC system available from the library are the ones available on the 6 pulse converter manual or more equations can be obtained.

Kind Regards,

Albino Ubisse

>>> "DIgSILENT Support" 11/22/10 9:28 AM >>>
Hello Albino

It is the user who decides how the controllers are modelled. These are defined in DSL, through block diagrams and equations, and include state variables. You need to study the controllers to see how they are modelled.

The mathematical model is the combination of the models of the individual
components. The models of the power components (lines, transformers, converters) are described in the manual.

For details on the models I recommend that you study the manual as well as
the controllers. The eigenvalue analysis uses the same equations as the RMS
time-domain simulation. The EMT time-domain simulation uses the more detailed models - including switching of individual thyristors.

Kind regards

Peter Lilje (support@digsilent.de)

DIgSILENT GmbH
Heinrich-Hertz-Str. 9 Tel : (+49) 7072 - 9168 50
72810 Gomaringen Fax : (+49) 7072 - 9168 88
Germany **http://www.digsilent.de**

-----Original Message-----
From: Albino UBISSE [mailto:ALBINO.UBISSE@uct.ac.za]
Sent: Donnerstag, 18. November 2010 15:56
To: undisclosed-recipients:
Subject: HVDC generic equations

Good day,

I am investigating the modelling of HVDC systems (in terms of the mathematical equations), however the manual is not very explicit on this regard.

I would like to know how the controllers are modeled with regards to their state variables and how it affects the small signal stability of a system. I read in literature that it affects the torsional modes of a generator, but little is said as to how it affects the electromechanical modes (inter-area and local modes).

Can I also get the mathematical modeling of the HVDC system, including converters and lines.

Are there any assumptions or any modifications on the HVDC system when performing small signal stability and transient analysis?

Email communication about component modelling:

From: **DIgSILENT Support** (support@digsilent.de)
Sent: 24 August 2010 10:36:11 AM
To: 'ALBINO UBISSE' (avubisse@hotmail.com)

Dear Albino Ubisse,

Thank you for your request!

Please use for further questions you official registered email address otherwise support is not possible.

The external grid uses internally a generator model with high inertia and high power. The model is slightly different from the standard synchronous generator therefore it has one more state variables than the synchronous generator (sat_filt). See also the screenshot below:

The rectifier/inverter model is a internally handled like a current source. The dynamic comes from the HVDC controller (modeled in DSL) and not from the rectifier/inverter model itself.

Please don't hesitate to contact us again for further questions or comments.

Kind regards / Mit freundlichen Grüßen,

DIgSILENT Support
Dipl.-Ing. Stefan Weigel
DIgSILENT GmbH E-Mail : **support@digsilent.de**
Heinrich-Hertz-Strasse 9 Tel : (+49) 7072 9168 50
72810 Gomaringen Fax : (+49) 7072 9168 88
Germany Website : **http://www.digsilent.de**

USER REGISTRATION. IMPORTANT NOTE:

From: ALBINO UBISSE [mailto:avubisse@hotmail.com]
Sent: Dienstag, 24. August 2010 01:06
To: support@digsilent.de
Subject: Component modelling

Good day,

My name is Albino Ubisse. I am using DigSILENT to perform small signal stability on a HVAC-HVDC system and would like to get some clarification on a few points I found out when using this software.

When modelling HVDC, what states are present in the modelling?

I ask this because I found in literature that when modelling HVDC the following states are used (X_dcr, X_dci, I_dcr, I_dci, Vdc) or (Xccc, I_dcr, Idci). And when i perform small-signal stability analysis, i see that the HVDC system does not have any states present on the eigenvalue results.

When modelling the external grid, what assumptions are made?

I as this because I saw that the external grid have 7 states associated to it. What states are these?

Hope to hear from you soon.

Regards/ Cumprimentos

Albino Ubisse

E2 Communication with Graham Rogers (PST)

From: "Graham Rogers" <cherry@eagle.ca> Sunday - September 12, 2010 4:45 PM

To: "'Albino UBISSE'" <ALBINO.UBISSE@uct.ac.za>

Subject: RE: Small Disturbance on PST with HVDC

Attachments: Mime.822 (3 KB)

No, but it has the ability for you to use a user defined model for a feedback controller in an HVDC system. There is an Example in Chapter 10 of my book, 'Power System Oscillations'.

-----Original Message-----
From: Albino UBISSE [mailto:ALBINO.UBISSE@uct.ac.za]
Sent: Friday, September 10, 2010 7:59 PM
To: cherry@eagle.ca
Subject: Small Disturbance on PST with HVDC

Good day,
I would like to know if the HVDC system in PST is equipped with supplementary control to improve the damping of the electromechanical modes of ac oscillations?

If yes, how do I make use of this property?

If no, can I models such in PST? how would I do it?

Best Regards,

Albino Ubisse

From: "Graham Rogers" <cherry@eagle.ca> Thursday - June 4, 2009 3:40 PM
To: "'Kehinde Awodele'" <kehinde.awodele@uct.ac.za>
Subject: RE: Assistance on HVDC power flow simulation Attachments: dtestdc.m (10 KB)

These programs are set up to model interconnected ac systems with imbedded HVDC links. It is not possible to model isolated dc links. To model these I would suggest that you r student uses MATLAB's Simulink.

You may be able to get away, in PST and the MATNET programs by setting up a small ac systen in which the dc line is embedded by modifying dtestdc which is supplied. However, even for this small system, the system does not recover form a three phase fault.

Graham Rogers
RR#5 Colborne, Ontario
Canada K0K 1S0
phone: (905)349-2485
http://www.eagle.ca/~cherry

-----Original Message-----
From: Kehinde Awodele [mailto:kehinde.awodele@uct.ac.za]
Sent: Thursday, June 04, 2009 6:03 AM
To: cherry@eagle.ca
Subject: Assistance on HVDC power flow simulation

Dear Mr Graham,

The forwarded mail was sent by Mr Albino Ubisse, one of our postgrads.

He has difficulty in performing power-flow simulations with DC line only in PST and MatNetEig.

H
e has succeeded with AC lines and hybrids.

We will appreciate your assistance as to how he should proceed.

Expecting your response.

Thank you.
Kind regards,

Mrs Kehinde Awodele.
Lecturer
Electrical Engineering Dept,
University of Cape Town.

E3 Communication From Federico Milano (PSAT)

To psatforum@yahoogroups.com
From:**Federico Milano** (Federico.Milano@uclm.es)
Sent: 07 October 2010 10:54:54 AM
To: psatforum@yahoogroups.com
Dear All,

HVDC systems have been little tested in PSAT. When I set up the HVDC mdoel I was able to make it work but all parameters have to be carefully chosen. It is also possible that putting a PV generator and an HVDC terminal at the same bus creates problems.

I have also heard that there is some bug showing up when using two or more HVDC. This is possibly a bug but I have not had time to chase it so far.

Best regards,

Federico

Dr. Federico Milano

Associate Professor

Electrical Engineering Department,
Univ. Castilla - La Mancha,
Campus Universitario, s/n,
13071 Ciudad Real, Spain

Email Federico.Milano@uclm.es
Tel. +34 - 926 - 295219
Fax +34 - 926 - 295361
Web Site http://www.uclm.es/area/gsee/Web/Federico/
